CODEN:LUTEDX/(TEIE-5404)/1-95/(2018)

Industrial Electrical Engineering and Automation

Grid impact study of frequency regulation with EVs

Emma Blomgren

Division of Industrial Electrical Engineering and Automation
Faculty of Engineering, Lund University

Master Thesis

Grid impact study of frequency regulation with EVs

Emma Margareta Viktoria Blomgren

Faculty of Engineering LTH at Lund University
Division of Industrial Electrical Engineering and Automation

Technical University of Denmark - DTU
Department of Electrical Engineering

supervised by
LTH: Olof Samuelsson
DTU: Seyedmostafa Hashemi Toghroljerdi
Peter Bach Anderssen

June 19, 2018

Acknowledgements

I would firstly like to express my gratitude to the main supervisor for this thesis, Professor Olof Samuelsson at LTH, the Division of Industrial Electrical Engineering and Automation. Thank you for contributing with your expertise, good advice and keeping me enthusiastic about the subject throughout the project. It was very much appreciated.

I would also like to thank Seyedmostafa Hashemi Toghroljerdi and Peter Bach Anderssen for giving me the opportunity to perform the project in this thesis at DTU, Electrical Engineering. A special thanks goes to Seyedmostafa Hashemi Toghroljerdi for always taking the time to discussing the project and contributing with your knowledge.

Lastly, I would like to show my appreciation to the Parker Project, without which the thesis would not have been possible. The Parker Project and the EV fleet at Frederiksberg Forsyning have supported this thesis with the required data which was very appreciated.

Abstract

The ongoing grid paradigm shift has resulted in synchronous generators currently being phased out. As the generators have been providing ancillary services, such as frequency control regulation, this means that new technologies to perform ancillary services need to be developed and evaluated. Electric vehicles (EVs) is an energy source that today is being underutilized. Therefore, research has been investigating the possibility to provide ancillary services trough vehicle-to-grid technology (V2G) and especially utilizing EVs as frequency containment reserves (FCR). [1–6]. However, real world data to evaluate this technology is lacking today.

The study in this thesis utilizes real world data from one of the world's first commercial EV fleets providing FCR-N (Frequency Containment Reserve - Normal Operation) [7], with the aim to evaluate grid impacts from the V2G technology. Initially, the grid impacts in the studied system is analyzed. Thereafter, a simulation model is created in Matlab Simulink. Through varying the cable length (0.02 km to 1.6 km) and the installed power of the EV chargers (100 kW to 800 kW) different scenarios are created and simulated, using the model. Thereby, it is evaluated if and when problems will occur for the grid operation in the studied system. Additionally, it is investigated if grid impacts in terms of voltage can be minimized through reactive power compensation. The main focus of the analysis concerns voltage issues but load profiles are also analyzed.

For the studied system no voltage limit violations or thermal limit issues were found. However, the FCR-N provision changes the shape of the load profile for the building, to which the EV fleet belongs. For the reactive power compensation it was found that the suggested minimum power factor (PF) for battery plants suggested by the transmission system operator (TSO) [8] was enough to improve voltage profiles up to 0.2 km, however for longer cable lengths the suggested PF was not enough. Instead a proportional Q(P) controller is suggested which improves voltage profiles up to 0.4 km as well as for lower installed power levels for 0.8 km. For 0.8 km cable length and longer it is not possible to minimize grid impacts through reactive power compensation. Instead grid upgrades would be required if the V2G technology is adapted in systems requiring cable lengths and installed power levels of these sizes.

In the load profile analysis it was seen that the peak load in the morning increased severely as a result of upscaling the installed power in the EV fleet. Additionally, the afternoon peak load increased in magnitude and time for the higher installed power levels. Strategies to minimize the peak loads such as smart scheduling are discussed but not tested for.

It is concluded that the V2G technology is a possible strategy to perform FCR-N in an under-utilized grid. However, if utilized to such extent that grid updates are required, the cost of grid updates needs to be weighted against the gains from FCR-N provision and cost of EV batteries for further evaluation.

Keywords: Electric vehicles (EVs), grid impact, ancillary services, frequency regulation, FCR-N, vehicle-to-grid (V2G), voltage, reactive power, load profile.

Abbreviations and Nomenclature

BEV - Battery Electric Vehicle
DSO - Distribution System Operator
EV - Electric Vehicle
EVI - Electric Vehicle Initiative
FCR - Frequency Control Regulation
FCR-N - Frequency-Controlled Normal Operation Reserve
FF - Frederiksberg Forsyning
ISO - Independent System Operator
LL - Line to Line
LN - Line to Neutral
P - Active power
PEV - Plug-in Electric Vehicle
PF - Power Factor
PHEV - Plug-in Hybrid Electric Vehicle
Q - Reactive power
R - Resistance
RMS - Root Mean Square
S_{SC} - Short Circuit Capacity
SOC - State Of Charge
TSO - Transmission System Operator
V - Voltage
V2G - Vehicle to Grid
Z - Impedance
X - Reactance

Contents

1. Introduction

This initial chapter gives an introduction to the subject of this thesis. It formulates the problem statement accompanied by the scope and limitations.

1.1. Background and Motivation

It cannot be denied that the planet and its climate is affected by human actives. The consequences for our climate are especially severe as they become more and more noticeable due to our unsustainable exploitation of energy resources. The situation is problematic since energy services often are indications of the quality of life at the same time as the welfare of future generations will be threatened if no radical changes are made now [9]. Today, 80 % of the global energy provision comes from fossil fuels such as oil, coal and gas [10], whereas for the transport sector oil accounts for 96 % of the energy usage [11]. The oil reserves are predicted to last another 50 years with the current exploitation [12]. Thereby, the fossil fuel dependency threatens the global growth. Furthermore, with an increasing population and global living standards developing for the better this calls for changes in our technical development to proceed in a sustainable way that does not risk the future generations welfare neither economically, environmentally nor socially.

As the global leaders are becoming more and more aware of the situation during the last decades several goals have been set to maintain a sustainable climate. Within the European Union the states have agreed to, until the year of 2020 with respect to the values of 1990, decrease greenhouse gas emissions by 20 %, decrease the energy usage by 20 %, that 20 % of the energy usage will be from renewable energy sources and within the transportation sector the fraction of renewable energy should be at least 10 %. In addition to the 20-20-20 goals, the union has also proposed that the greenhouse gas emissions should be reduced by 30 % by 2030, the energy efficiency should increase by 30 % until 2030 and the renewable energy should account for 27 % of the energy usage by 2030. [10,13] Furthermore, countries in Scandinavia have been pushing on setting stricter climate goals. The government of Sweden has stated that Sweden should have no net emissions in 2045 and the government in Denmark has decided that the country should be independent of fossil fuels by 2050. [13, 14] With the goals being set this calls for research that enables renewables and cleaner technologies and secures the future for the coming generations.

As previously mentioned the transportation sector is heavily dependent on fossil fuels, and in order to achieve our sustainability goals radical changes are required within and around this sector. One strategy to mitigate the fossil fuel dependency is electrification of transportation through the introduction of electric vehicles (EVs). However, it should be clarified that the EVs and the electricity production in total should require lower net emission than the total emissions of the conventional cars and the corresponding electricity production for this to be a successful strategy. The electrification would supposedly result in less total energy consumption per distance but increased electricity consumption. Furthermore, we now see a paradigm shift for the power grid as the power flows are changing. Traditionally, the power flows in the grid has been going from centralized production units, through transmission and distribution, to costumers unidirectionally [15]. However,

because of the challenge to find new ways of producing clean and environmental friendly electricity, the electricity production is becoming more and more decentralized, which changes the power flows. Additionally, strategies to minimize the total energy consumption are being developed. Electricity consumers have for a long time been considered as uncontrollable units but now techniques of optimized production and consumption are being researched, envisioning the consumers as variable and controllable units.

As a result of the mentioned changes the traditional synchronized electricity production is being phased out in Denmark. This might evolve in different complications for grid operation as the synchronous generators are one of the main providers of ancillary services due to their suitability for the task. Thus, ancillary services need to be provided from other components in the future grid. As understood from the reasoning above, controllable units that are integrated into the grid could contribute to the operation of the grid, especially if the power flow can be bidirectional. EVs are energy sources that most of the day are not being utilized. They can be integrated into the grid and they also have the opportunity of bidirectional charging. Thereby, EVs could support the grid through providing frequency control by utilizing the batteries in EVs when they are connected to the grid. [1–6] This technology is known as Vehicle to Grid (V2G). Through electrifying the transportation and through the ancillary services that they can provide while connected to the grid, EVs could play an important role in our future infrastructure. This calls for research on electric vehicles and their interaction with the grid, which is the theme of this thesis.

1.2. The Parker Project

The work of this thesis is associated with the Parker Project. The project is a collaboration between Mitsubishi Corporation, Mitsubishi Motors, Nissan, NUVVE, PSA Groupe, PowerLab DK, Enel, Frederiksberg Forsyning, Insero and DTU Institute for Electrical Engineering. The Parker Project aims to evaluate series-produced EVs as a vertically integrated resources to support the power grid both locally and system-wide. The project involves topics such as market, technology and users applications. Furthermore, the project builds on three pillars - grid applications, grid readiness certificate as well as replicability and scalability. More information about the project can be found in [7] .

Additionally, the Parker Project is supported by one of the world's first commercial pilot of series produced V2G cars providing system services. The pilot provides this thesis with data.

1.3. Thesis Objectives

The aim of the thesis is to do an impact study on how charging and discharging of EVs affects the grid when providing frequency-controlled normal operation reserve (FCR-N). The thesis will mainly focus on impacts in terms of voltage levels, but also discuss feeder load profiles in parallel. Utilizing results from the impact study, the thesis will also investigate strategies to decrease the impacts on the grid. The objectives of this thesis are further defined through the following questions:

How does the FCR-N provision through EVs affect the studied system today?
To answer this question the voltage and load profiles will be analyzed to evaluate if there are any problems regarding the grid operation at Frederiksberg Forsyning today.

If and when will there be issues for the grid operation?
This question involves creating a simulation model. With the model different scenarios will be simulated through varying the installed power and the cable length in order to determine when problems in the studied system will arise. Issues regarding voltage and load (and thereby thermal impacts) will be taken into account.

Can reactive power compensation be utilized to minimize grid impact?
Here, it will be investigated if reactive power compensation can be utilized as a solution strategy to mitigate voltage impacts. Thermal impact solutions will be evaluated in a subsequent discussion.

1.4. Methodology

Initially, a literature study will be provided to give the required background knowledge needed for this project. Furthermore, data will be imported and filtered to take away time periods with non usable data. Thereafter, an analysis of the studied case, referred to as base case, in terms of grid impact will be conducted. The studied system will be modeled and simulated in Matlab Simulink, where the variables will be determined through a theoretic model, the previous analysis and simulation calibration. From the simulation model different possible scenarios will be simulated through varying the installed power and cable length. Two different reactive power compensation methods will be evaluated throughout the simulations. In parallel to the simulations the limitations of the EV frequency control technology with respect to grid impacts will be investigated and discussed. Furthermore, the load profiles for the different simulations will be evaluated in the analysis. The work flow for the thesis (excluding the literature study) is visualized in Fig. 1.

1.5. Scope and Limitations

Due to the available data the work in this thesis will be limited in different directions. One of them is for which time spectra that the data is available. The resolution of the data is given in one second time steps and is available over a time period of three months (December 2017, January 2018 and February 2018). Within these three months, the analysis will apply to the weeks that have usable data.

Another aspect through which the work is limited is with respect to the type of EV user. The data comes from an EV fleet belonging to a company and hence the following analysis will be valid for suchlike users. A thorough analysis for household users is therefore not possible. Furthermore, the study involves one point of connection and one consumer (Frederiksberg Forsyning). Additionally, the study looks at battery electric vehicles (BEVs) charging through charging posts and therefore electric roads are not taken into account in the analysis.

There are many different ways of providing reactive power compensation. In this thesis the aim is to evaluate whether it can be utilized as a solution strategy or not and therefore a functioning controller will not be developed and not all possible solution strategies could be evaluated. Other options could be possible, but this control strategy is considered sufficient to determine if and when problems will occur in the studied system.

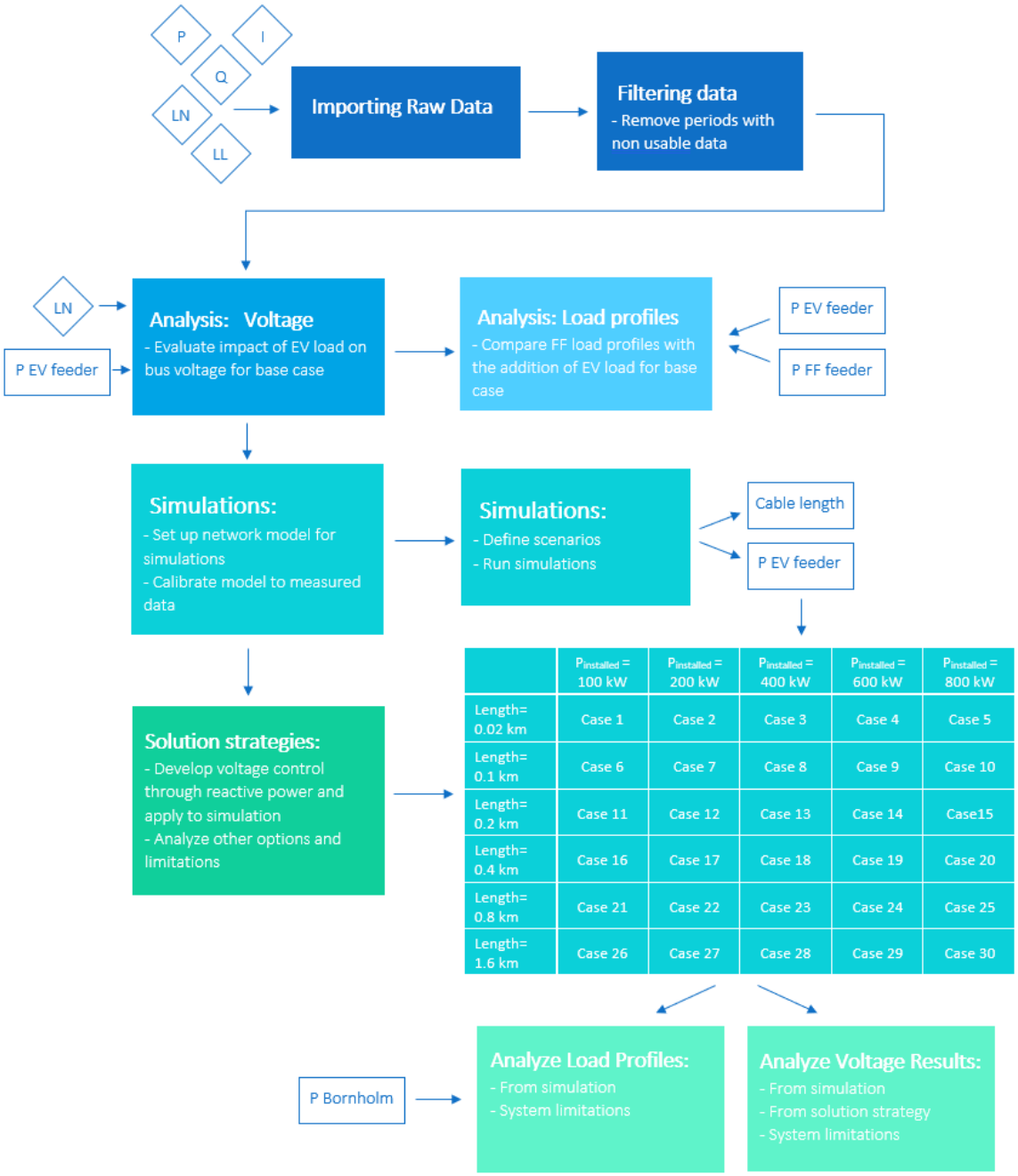

Figure 1: *Work flow to determine grid impacts from the frequency regulating EVs at Frederiks bergs Forsyning (FF). Abbreviations: LN - line to neutral voltage, LL - line to line voltage, P - active power, Q - reactive power, I - current, P EV feeder - active power in EV feeder (see Fig. 15), P FF feeder - active power in feeder to Frederiksberg Forsyning (see Fig. 15), P Bornholm - active power in feeders from an electric system in Bornholm (see chapter 4).*

1.6. Outline

In chapter 2 the required theory and background knowledge will be found together with a literature review on the state of the art regarding frequency regulation and voltage control with EVs. Chapter 3 presents the data from the EV fleet. The data analysis for the base case regarding voltage and load profiles is found in chapter 4. The procedure for developing the simulation model and the scenarios is presented in chapter 5 and the results and analysis for voltage, load and system limitations are presented in chapter 6. Finally, chapter 7 presents a discussion. Chapter 8 presents the conclusions and chapter 9 future work.

2. Theory and Background

This chapter will provide the theory and background knowledge laying the ground for this project. Initially, the required theory on power grids, frequency and voltage regulation are presented. Furthermore, the chapter continues with the state of the art regarding EVs and grid integration as well as technical regulations for battery plants.

2.1. Power grid

In a traditional power system the electricity is produced in centralized production facilities such as hydro power plants, nuclear power plants or thermal power plants. From the power plants the electricity travels through AC high voltage transmission lines known as the transmission grid, where the voltage normally is 400 kV [16]. Through substations the voltage is first leveled down to 150 kV in the subtransmission grid (in Denmark and in Sweden 130 kV). The voltage is further leveled down to medium voltage (MV), 10 - 70 kV, and then to low voltage (LV) 0.4 kV. The distribution grid consists of both MV and LV grids. [16] The normal electricity consumer is connected to the LV grid, whereas larger industries are connected to the MV grid or even the subtransmission grid. The Transmission System Operator (TSO) in each country is responsible for the operation and maintenance of the transmission line system and in smaller countries there is normally only one TSO as this is a natural monopoly. In Sweden the TSO is Svenska Kraftnät and in Denmark the TSO is Energinet.dk. When it comes to the distribution grid there are more actors on the market and in Denmark there are 50 Distribution System Operators (DSOs) [17]. In parallel to the physical transportation of the electricity, the electricity is traded with through long-term bilateral contracts and on electricity markets. In Scandinavia the electricity market is built up by three markets. On a day-ahead market, Elspot (governed by Nord Pool), where electricity is bought and sold on an hourly ahead basis. As a complement there is also a market where electricity can be sold and bought during the day of delivery. This market is known as Elbas (governed by Nord Pool) and works as a bidding market where the electricity can be bought up to one hour before the time of delivery. Additionally, there is a financial market Nasdaq OMX Commodities Europe. [10]

2.1.1. Frequency regulation

In Europe there are several synchronous areas and within each area the frequency of the grid is the same. As seen in Fig. 2 for example Germany has the same frequency as Greece [18]. Within each synchronous area the power production has to equal the demand at every point of time. The entire system can be described by one balance equation (eq. 1) and one can think of all generators operating as one. [15] Denmark is divided in to two different areas DK1 and DK2 which are part of two different synchronous areas. Jutland and Fyn belongs to DK1 and Zealand belongs to DK2. [19]

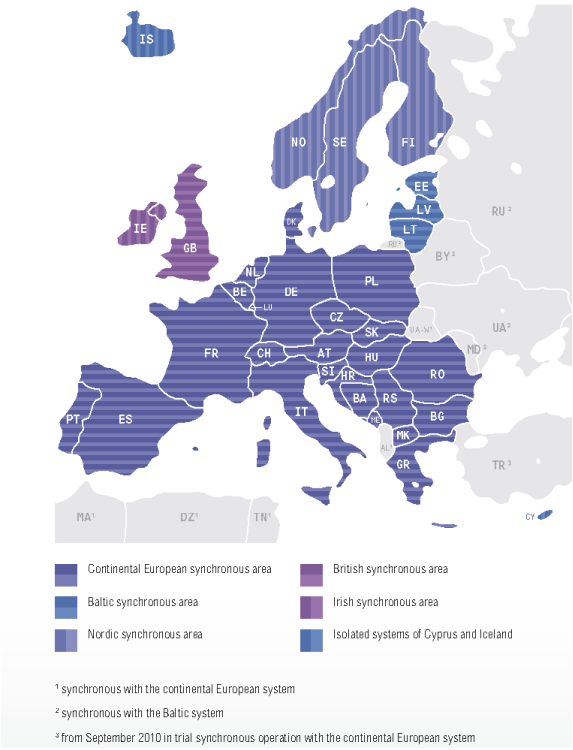

Figure 2: *Synchronous areas of Europe, where each marked area holds the same frequency in the the entire grid. [18]*

To maintain a frequency around 50 Hz, which is the commonly utilized system frequency in Europe, frequency control regulation is required. There are both primary and secondary frequency control techniques, where the primary control usually is fast but normally gives a stationary error that is reset by secondary control, which is automatic but slower. A general strategy for primary frequency control is to let generators respond to the change in frequency with respect to their size. This is known as droop control and is described through the following formulas:

$$\omega_{nom} J_{total} 2\pi \frac{df_{system}}{dt} = P_{m,total} - P_{e,total} \tag{1}$$

$$\frac{df_{system}}{dt} = \Delta f = f_{system} - f_{nom} \tag{2}$$

$$\Delta P_m = -\frac{\Delta f}{R} \tag{3}$$

where $P_{m,total}$ and $P_{e,total}$ denotes power production and demand respectively. f_{nom} denotes the nominal frequency (i.e. the setpoint 50 Hz), f_{system} the actual frequency in the system, R denotes the droop in Hz/MW or p.u/p.u and ΔP_m the change in power for the generator [15]. To let the machines contribute according to their size the R is determined in p.u. In the Nordic countries the total 1/R is required to be at least 6000 MW/Hz and the allowed Δf is 0.1 Hz. Frequency control reserves are traded on a market by Energinet.dk in Denmark (in Sweden this governed by Svenska Kraftnät) [19]. If ΔP_m is positive, i.e. power is injected to the grid to raise the frequency. It is called *upregulation*. If instead ΔP_m is negative, i.e. power is drawn from the grid to lower the

frequency. This is known as *downregulation*

Synchronous generators have been very suitable for frequency regulation control as their active power is controllable. Additionally, the synchronous generators keep the frequency more robust towards changes due to their inertia. With more and more renewable power production there will be less synchronous generators and thus less inertia in the electrical system. Thereby, the frequency will be more sensitive to changes in power production and demand. Thus, we need to both find new units in the grid that can provide frequency regulation and units that respond faster. One strategy to do this is to let the power demand follow the production, i.e. in eq. 1 to control the demand ($P_{e,total}$) to follow the production ($P_{m,total}$), instead of vice versa which is the traditional strategy to keep difference between the variables close to zero (and thereby minimizing the changes in the frequency, f_{system}). This have recently been investigated for smart grids applications [20]. It is however debated whether it can be fully conducted as the only solution since some facilities in society needs to operate regardless of the current power production, such as hospital, schools etc.. Other strategies are to install large batteries that can operate as a power reserve or to follow the traditional solution and install more power production than required in a system. By installing more power than required wind power plants and PVs can provide frequency upregulation. Another solution is to let the batteries of electric vehicles (EVs) jointly operate as one large battery providing frequency regulation and this will be further explained later on in this chapter (2.2.4).

Frequency concepts
Frequency Containment Reserves (FCR) are active power reserves utilized for the primary frequency control with the aim to dampen changes in the frequency. There are two types of FCR:

- *Frequency Containment Reserve - Normal operation (FCR-N)*, which is FCR utilized for frequency deviations within a ±0.1 Hz span. The work in this thesis concerns this type of frequency regulation.
- *Frequency Containment Reserve - Disturbance (FCR-D)*, which is activated for frequencies below 49.9 Hz and over 50.1 Hz.

Fast Frequency Response (FFR) aims to manage faster deviations in the system frequency, but is not available on the Nordic market today.

Frequency Restoration Reserves (FRR) is active power reserves utilized for the secondary frequency control aiming to reset the frequency to nominal value. [21]

2.1.2. Voltage control and line loadability

It is of the TSOs and DSOs concern to keep balanced voltage levels in the grid. With a stable voltage the grid is stronger and more robust. The transfer capacity of a line is improved and losses are reduced if the voltage is higher. On the other hand too high voltages can lead to faults and damage the insulation. Additionally, if the current is too high, the components of the system could get overheated causing damage and thus, thermal limits are also set to not exceed the limitations of the lines. Normally the thermal limit has a higher impact for the loadability at lower voltage lines. Hence, the DSOs normally set limits within which the voltage is allowed to vary at the connection to costumers in order to maintain a stable grid and to improve line loadability. [15] In Denmark the voltage variation limits are ±10 % of the nominal voltage, whereas in Sweden the limits are often set to ±3-5 % of nominal voltage. Thus for a line to neutral voltage of 230 V the limits are 207 to 253 V. [8] Within the grid the TSOs and DSOs have internal rules to maintain the voltage level.

The importance of keeping voltage stable for the stability of the grid can also be explained through plotting the maximum power that can be extracted from a line versus the voltage. Fig. 3 below shows the relation between the two variables. Here it can be seen that certain voltages will cause the power to drop drastically.

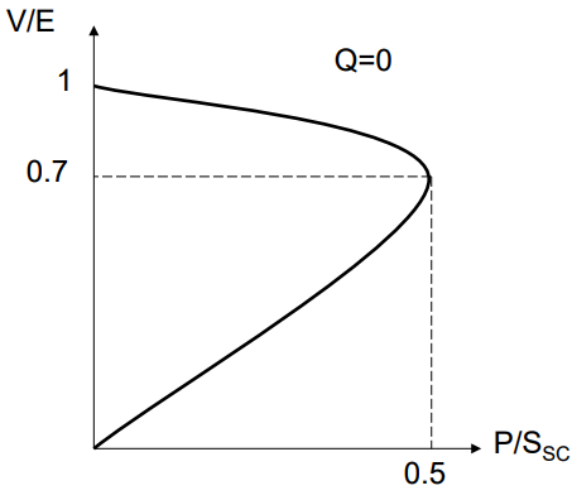

Figure 3: *The relation between the voltage at the receiving end of a line over sending end voltage (V/E) and the maximum power at the receiving end over the short circuit capacity (P/S_{SC}). Known as nose curve because of the shape. (The power factor in the curve is 1 and thus reactive power is 0) [22]*

There are of course different ways of modeling electrical systems, but a common way to do so is through Thevenin equivalents. Illustrating a line with a load at the end would result in the Thevinin equivalent below (Fig 4).

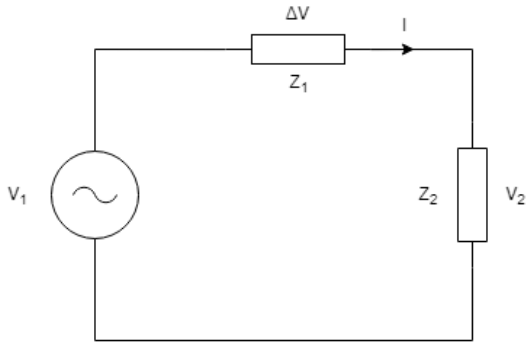

Figure 4: *The above Thevenin equivalent represents a load at the end of a line, where V_1 is the sending end voltage. V_2 denotes the receiving end voltage at load while Z_1 represents the impedance of the system 'upstream' and Z_2 the impedance of the load.*

According to Fig. 4 the voltage at the receiving end can be described through:

$$V_1 = V_2 + \Delta V = V_2 + Z_1 I \tag{4}$$

$$V_1 = (1 + \frac{Z_1}{Z_2})V_2 \tag{5}$$

The voltage at two ends of a line can also be described through the line diagram in Fig. 5

Figure 5: *The line diagram between a sending bus and a receiving bus.*

In accordance with the figures above the voltage can be described through the equation.

$$V_2 = V_1 + \frac{PR + QX}{V_1} \tag{6}$$

where R and X are the resistance and the reactance of the line, respectively, and P and Q are the active and the reactive power loads at the receiving bus.

The voltage profile for a low voltage line with no load is usually flat, i.e. the sending end voltage equals the receiving end voltage. When active power is withdrawn at the end of the line the voltage at the receiving end will be lower compared to the sending end voltage. For high generation at the receiving end the voltage will instead be higher compared to the sending end. Since impedance increases with the length of the line, the voltage profile steepness depends on the impedance per length and the resulting voltage at the end thereby depends on the length of the line. [15] This behavior is seen in Fig. 6.

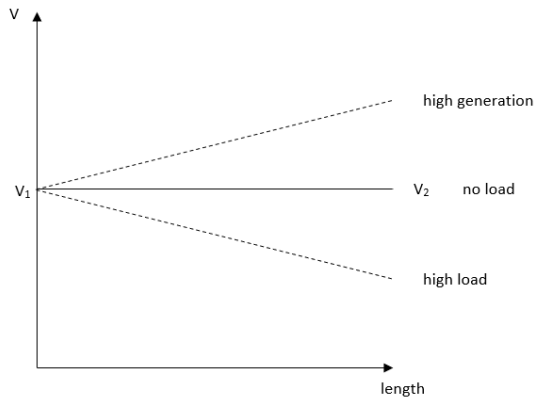

Figure 6: *Voltage profile illustrating the receiving end voltage.*

As previously stated and further realized through equations 4 and 6, the voltage at the receiving end depends on R and X (i.e. P and Q) at the load or R and X in the cable. The effect that the adjustment of P and Q at the load has on the voltage depends on the X/R ratio of the line. If the line is inductive, i.e. X/R ratio is high, adjusting X (or Q) has a larger impact. On the other hand, if the line is mostly resistive, i.e. X/R ratio is low, adjusting R (or P) has a larger impact. Generally, overhead lines are inductive and cables are resistive. [15]

With more and more renewable energy integrated in the grid power flows will fluctuate more, which makes voltage control a matter of concern. With higher penetration of PVs and wind power plants in distribution networks voltage profiles will increase at remote parts of the network. On the other hand with a higher penetration of EVs with unidirectional charging the voltage will drop at receiving ends. Thus, the concern emerged that increased measures of control are required in electricity grids and calls for new methods and strategies to solve this problem. This will be further discussed throughout the report.

2.2. EV development and grid integration

This section will give an overview of the current development of the EV technology regarding charging strategies and grid integration with a special focus on frequency regulation and voltage control.

The number of new electric car registrations are continuously increasing since the transition of electrifying the cars began about a decade ago. The global stock of electric cars is currently over two million and the countries with the largest stocks are the US and China, where China increased its stock from 100 thousand in 2014 to 650 thousand vehicles in two years and now holds 40 % of the total amount of sold electric cars in the world. The largest market penetration is however achieved by Norway with a market share of 29 % followed by the Netherlands with 6.4 % and Sweden with 3.4 % (these numbers are from 2016). The market penetration in Denmark is 0.6 %, whereas Copenhagen has had bigger success introducing electric vehicles with a market share of 3.6 %. Even though the mentioned numbers show a positive development, the global market penetration is still low and electric cars only account for 0.2 % of all passenger light-duty vehicles and the growth rate has been declining. However, in the EV3030 campaign the Electric Vehicle Initiative (EVI) countries have set a goal to reach 30 % market share by 2030. [23]

Clearly, there is still a long way to full adoption of the electric car technology. In the Global EV Outlook 2017 [23] the EVI states that policy support is the major driver for adoption. Within policy support the EVI highlights the following keystones for electric car deployment - support for research and development of innovative technologies; targets, mandates and regulations; and financial incentives. Among these research support is indispensable for cost improvements that could further allow for scale-up production. Within this discussion the battery cost is of major concern and in general seen as an obstacle for scaling up the electric car production. [23]

2.2.1. Charging strategies

There is not yet a universal standard for charging, but different standards have been defined regarding *level, type* and *mode*. *Level* refers to the power output of a charger outlet, whereas *type* defines the socket and connector of the charger. In conventional EV charging cables, connectors and communication technology between the vehicle and the charger is required, whereas communication between the charger and the grid is optional. The communication protocol between vehicle and charger is described by the *mode*. There are commonly three levels - level 1, for charging below 3.7

kW, level 2, for charging between 3.7 and 22 kW and level 3 for charging above 22 kW and up to 150 kW. Level 2 chargers are known as slow chargers and level 3 as fast chargers and for the latter DC charging is also possible as opposed the the more common AC charging. Regarding connectors, i.e. type, there are many different solutions on the market as the actors have not agreed on a standard yet. There are however initiatives to create a standard solution, such as CharIN promoting a combined charging system. [23]

Charging strategy is something that also differs extensively between different solutions. This area of research has gained a lot of attention and development. The most traditional strategy is known as dumb charging, where the electric car users simply connect their vehicle to the charger and the battery is charged until maximum state of charge (SOC) is reached. The key motivations for this strategy is that it is simple and easy to use. With another strategy, smart charging, the motivation on the other hand is to charge in a more optimized way. A common optimization is to minimize the cost and through this the charger requires a lot more in terms of communication as a signal from the market and the electricity price is required. The optimization problem could also aim to even out the power demand in the grid. Smart charging strategy usually requires more time and can be more demanding for the electric car user, but on the other hand it can be both cheaper for the EV user and cause less stress on the grid. [23, 24]

In terms of power flow, most chargers today are unidirectional. This means that the battery can only be 'filled up' through the charger and the power always flows from the grid to the battery. However, bidirectional chargers are currently being developed, allowing for power flowing both ways between battery and grid. Today, NUVVE, is branding their company as the only company providing an electric vehicle battery technology that is bidirectional and gives the user the opportunity to generate, store and resell unused energy in the local grid. This is a technology that allows EVs not only to do smart charging, but also to be integrated into the grid and perform frequency regulation control, for which bidirectional power flow is a prerequisite. [25]

2.2.2. Effects of EVs on power grid and energy usage curves

It is especially interesting to analyze the impacts of EV loads on the grid since it differs from traditional loads. As opposed to traditional stationary loads, as a fridge for example, the EV load is movable, i.e. it could be charged at a home once and the next time at a public charging facility. EV load is also less predictable in comparison to many other kinds of loads since it depends on the user which can change its behavior from one day to another. How EV charging will affect the power grid and the societal energy consumption depends on many different factors. One obvious factor is to which extent EVs will penetrate the market. According to the IEA the additional demand caused by EV adoption will only be 1.5 % of the total electricity demand 2030. However, the adoption of EVs could vary on a local basis and effects on the grid as well as energy usage should not be ignored but taken carefully into account. [23] A Finnish study showed that with an integration of 5 million EVs in Finland the power demand would increase by 6 % at the most [26].

Impacts on the grid will also depend on which charging strategy or mode that is utilized as well as where charging takes place. In other words, impacts will depend on whether dumb or smart charging is most commonly used, unidirectional or bidirectional and if the charging takes place in homes, businesses or public charging facilities. In the case of adoption to electric roads the driving patterns could also have an impact, however this is not the focus of this study. Additionally, the charging behavior depends heavily on the user, for example if the EV owner is a household or a company, and thus the owner type also has a major impact on the grid. The IEA foresees that

the EV charging will initially have a large impact on the local low-voltage grids in residential or commercial areas. In a future scenario of high electricity demand and low production, additional EV charging could lead to increasing prices on a wholesale market level. In addition, the IEA expects consequences during peak times for system operators in terms of systems services such as frequency control, which requires a careful maintenance of reserve power capacity. At distribution level overloading of power lines and transformers as well as voltage drops could be a risk. [23]

Different strategies have been and are being developed to mitigate the impact that EVs, but also other components, have on the grid. Very commonly discussed is to minimize the impact on the grid through reducing the peak demand, which occurs in the morning and in the evening. One strategy, highlighted in the Global EV Outlook, is to combine EV and PV technology and let the EV charging coincide with the PV production. For this the IEA have created a possible scenario with and without combined EV and PV technology for 2030 as seen in Fig. 7.

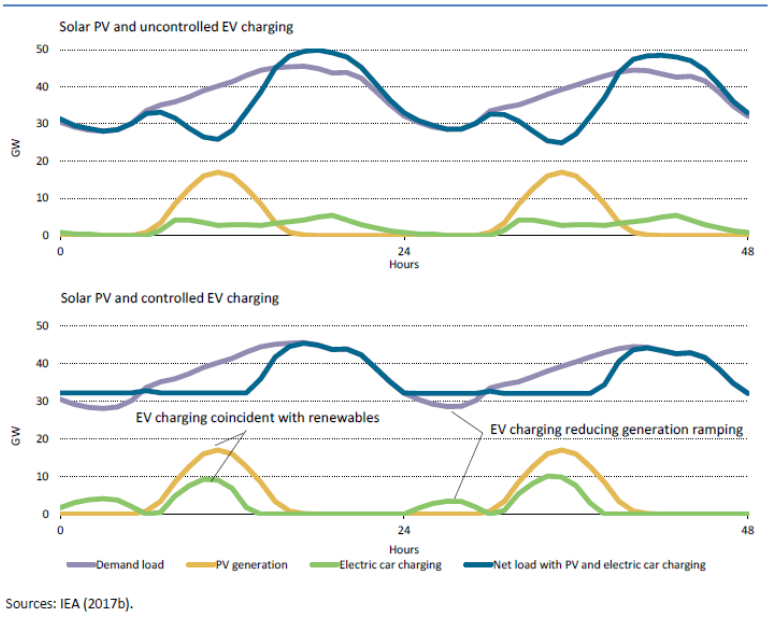

Figure 7: *Demand profile for year 2030 with EV charging. In the upper graph EV charging is not combined with PV production, whereas it is combined in the lower graph, i.e. EV charging is controlled according to the PV production. [23]*

In [27] the author investigates the grid readiness for EVs in terms of capacity or highest load per costumer. This was done for two areas, Vallkärra and Stångby in southern Sweden, with real measured data. Previously, the grid in Sweden has been overdimensioned, since direct electric heating was commonly utilized and caused an uncertainty of the load. Now, direct electric heating have been replaced by heat pumps in many places. Thus, the author conclude that because of the previous over dimensioning the grid is ready for introduction of EVs. However, the DSO needs to be informed if more EVs are connected to the grid since it might lead to changes in the accuracy of formulas utilized by the operator and additionally it might be a problem for certain transformers in the grid.

In [28] a case study is done for E.ON on a stressed grid with high penetration of EVs in Järfälla, southern Sweden. Additionally, the study investigates the impact of solar cells. Furthermore, the authors evaluate the impact on substation transformers, cable loadings and voltage drops. They conclude that even on a day with a more stressed grid the impact is generally within E.ONs guidelines and they should not be worried in terms of grid readiness for a high penetration of EVs.

2.2.3. Vehicle-to-grid enabled EVs

The vehicle-to-grid (V2G) technology allows vehicles to be integrated with the grid, meaning that the vehicle can both receive and provide electricity to the grid. This technology makes it possible to utilize electric vehicles as power resources or reserves and thus the vehicles can support the grid with load leveling and other ancillary services. Vehicles that are compatible with the V2G technology and can be integrated are defined as Grid Integrated Vehicles (GIV). [7] Today there is no certificate or common requirements for a vehicle to gain a GIV status. It is however understood through the definition of V2G that bidirectional charging is a necessity for the technology as well as a GIV software to give commands of charging or discharging in real time [1]. The V2G concept was developed by NUVVE and its founder Prof. Willett Kempton about 20 years ago and as previously mentioned this company is to my knowledge the only provider of bidirectional battery charging for GIVs. [7,29]

Up to this point it is clear that the grid is undergoing a paradigm shift. Thus, we need to develop new technologies to produce electricity but also to provide grid support services, that traditionally were provided by conventional power plants. [2]. This is why the V2G technology is interesting. It is only a minor period of time that the car is actually utilized and most of the time electric vehicles are parked somewhere and not utilized [2]. During the majority of time the EV is thus an energy storage resource that is not being utilized [1]. When society now has realized that energy resources needs to be utilized in smarter, more efficient and optimized ways V2G has become an interesting topic of research.

The Parker project holds the first commercial V2G EV fleet [7], but more V2G projects and initiatives are being developed and implemented. GIVs utilized as energy sources are often referred to as virtual power plants, which could be described as cloud-based distributed power plants (or distributed energy resources). For example, NUVVE and University of California San Diego will demonstrate how electric vehicles can be utilized as virtual power plants in a project based in San Diego [30]. Additionally, NUVVE has been proceeding in other countries such as the Netherlands where TenneT (the TSO in the Netherlands and one out of four TSOs in Germany) has approved for the company to participate in the frequency regulation market. [1] Furthermore, in Japan Nissan and TEPCO (Tokyo Electric Power Company) will collaborate to perform a study on how electric vehicles can serve to support the power grid as virtual power plants. [31]

2.2.4. EVs and frequency regulation

As previously sated, the grid paradigm shift calls for new ways of supporting grid operation [2]. EVs are energy storage units that are not passive loads and the majority of the day the EVs could be available for the grid. Hence, several research initiatives are trying to evaluate the ability for EVs to perform frequency regulation control [3]. It is also stated through [4] that traditional frequency regulation is slow and not satisfying and that new technologies could provide the service with faster response.

However, to implement the V2G technology to provide frequency regulation develops into a range

of questions on how this distributed energy resource technology should be managed. Several articles propose an aggregator that would manage and efficiently utilize the distributed power of the EVs and thereby also be the trading middle-hand between EV owners and the grid operator [4, 32]. Supposedly, conflicts of interests would arise between the TSO, the aggregator and the EV owner (in the article: PHEV owner) [4]. How the aggregator should operate has been discussed and solved differently in research today. In [32] the authors suggests a mathematical formula through which revenue is maximized. In their optimization problem they considered the energy capacity of the battery important and designed their weight function to reflect the energy constraints. Furthermore, they claimed to have developed an optimal charging control using dynamic programming. The authors also address the relative importance between final state of charge (SOC) and revenue. They state that their control strategy increases revenue, but that this can be further increased through seeing the final SOC, i.e. when the EV should be ready to use for the owner, as an interval instead of a fixed point of SOC. The users are more interested in that their car can drive a certain distance rather than that the battery is charged up to a certain point of SOC and through this revenue could be increased.

The authors of [4] instead suggest a hierarchical game-theoretic approach for the aggregator to optimize the frequency regulation. The authors state that their load frequency regulation manages to coordinate the charging of the EVs (PHEVs) while participating in the frequency regulation. At the same time they claim to have managed benefits between EV owners, aggregators and the TSO through balancing the hierarchical game approach at different levels. Through this approach they have also reduced the RMS frequency deviation from 0.028 Hz to 0.009 Hz and also reduced the peak load through their intelligent charging.

The predictability of the availability of EVs for the market is clearly a matter of concern and is addressed in the Parker Project through [33]. Additionally, EV owners might be concerned about battery degradation and how this affects the overall economical picture of the EV. Reference [24] stresses this topic and proposes that unidirectional charging is the overall best charging strategy for market participation when accounting for battery degradation today. In [2] the cost of battery degradation in relation to gains from frequency regulation is addressed. It is suggested that lowering the SOC set-point gives better outcome in revenue even though that this would give less income through frequency regulation. This is due to the negative impact on revenue that the frequency regulation causes in terms of battery degradation. However, research proposes benefits such as increased revenue and an improved grid operation without the requirement of grid reinforcement. [2, 5, 32]

2.2.5. EVs and voltage control

As previously mentioned, a well maintained voltage level in power lines increases the active power transfer capacity [6]. Certain research articles point out that voltage regulation (with reactive power regulation) close to loads would give especially efficient results compared to voltage control at centralized synchronous machines and capacitor banks [34]. Since, voltage regulation can be designed in ways in which the active power flow is not distinctly affected EVs could be a suitable resource to provide voltage control. [35] Among other changes that the grid is now facing, an increase in penetration of PV installation and connected EVs, the voltage regulation of the grid will be more complex and demanding [3, 36]. Historically, the DSOs have usually dealt with congestion and voltage limitations through grid reinforcements. New technology however, allows the limitations to be met through active demand management strategies [20]. If implementing voltage control for the EV chargers, the EV technology will not only solve their own created problem in terms of voltage

level but also be able to support the grid with voltage regulation when required due to other reasons.

The possible future case of high EV and PV penetration is especially interesting for voltage analysis. EVs and PV installations are usually integrated in low voltage (LV) grids. Since power injection to the grid increases the voltage level in the distribution grid (where R is larger than X) [15], PV installations usually cause higher voltage levels whereas the effect of EV charging is the opposite. With bidirectional charging of EVs that is utilized for frequency regulation the situation differs. This enables the EVs to inject power to the grid. Thus, a worst case scenario for such grids is when PVs are producing power at the same time as EVs are injecting power to the grid. This scenario is highlighted in [3] as well as in [36]. Another factor that will make the voltage situation more crucial is longer power lines, since this makes the grid weaker and less robust for load changes.

How to implement the voltage control with EV charging has been solved differently in research. In reference [37], the authors suggest reactive power compensation through a three-phase ac-dc converter that is able to operate in all 4 P-Q quadrants. Thus, this charger would also be able to provide frequency regulation since the charger is bidirectional. Both power factor correction and capacitive and inductive reactive power operation are investigated. Through their offboard charging strategy the EV (PEV) owner requests a SOC until departure and the charger responds to utility commands for reactive power. The authors highlight the importance of quick response from the charger and designed their charger to respond within 3 grid cycles. Through their study they conclude that smart charging with V2G applications such as reactive power compensation is more advantageous in terms of grid operation than only smart charging. Other methods utilize single-phase chargers, but through this concerns about unbalanced phases arise [3,34]. Reference [3] suggests a reactive power injection between ± 0.5 p.u.. In [38] the authors state that their investigated charging strategy decreases voltage violations using duty-cycle charging. In [39] a capacitive charger is implemented instead which reduces the voltage deviations through a capacitive power factor of 1 to 0.95. The author claims that a power factor in this range does not cause any disadvantage in terms of residential peak load or grid losses.

To be able to provide both frequency regulation and voltage regulation, the charger needs to be able to operate in all four quadrants. This results in 9 operating modes as seen in Fig 8 [40]. Such chargers are designed and evaluated both in [40] and [41]. In the design of these chargers offboard chargers are desirable [40], since chargers with extended functions could be heavier due to power electronics. Offboard charging increases the time and distance that the vehicle could manage which is of major concern for EV owners. [40] Providing voltage regulation control through reactive power compensation is beneficial since it does not require any active power flow and thus leave the battery charged [35]. Additionally, several studies have claimed that reactive power compensation does not have an impact on the battery degradation which is positive for the EV owner [6]. At the same time it gives an opportunity to increase revenue if participating in reactive power markets. Reference [42] states that it will be cheaper for the ISO (independent system operator) when EV owners are included in market, whereas in [6] the authors suggest a theoretical monthly income of 5 USD for the EV owners when providing reactive power compensation and frequency regulation as opposed to only providing frequency regulation. This is further reinforced through reference [43] that has studied the benefits of voltage regulation in a parking lot and concludes that the revenue of the parking lot is increased by 19 %.

Even though concluded by [36] that the benefits of voltage regulation are greater than the disadvantages, there are some concerns regarding this technology that require attention. When performing voltage regulation cable loading is increased and might lead to violations of current limita-

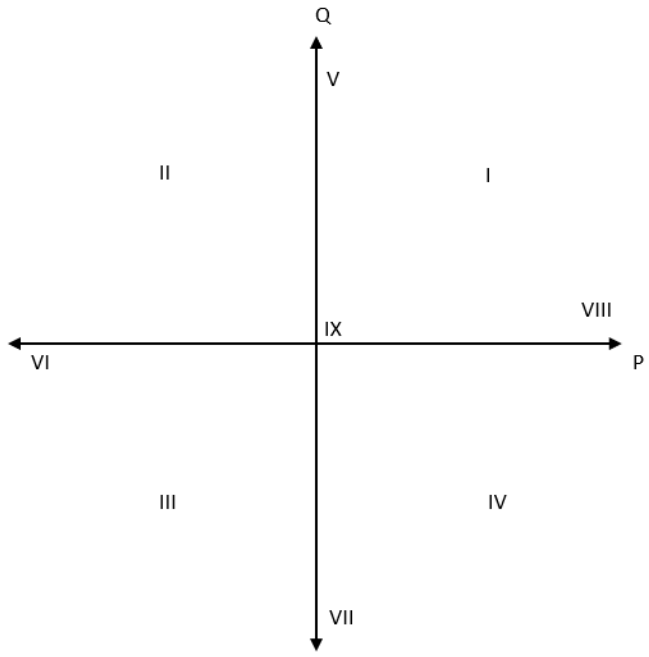

Figure 8: *Operating modes for combined frequency regulation and voltage control with reactive power. I-IV represents the area of the quadrants without the axes, V-VIII represent the modes along the axes and IX represents the origin.*

tions [3, 36]. Thus, it is important to be aware of this when designing voltage control strategies for EV chargers. If utilizing single-phase chargers phase unbalances is a concern which requires further research [3, 36]. Additionally, market models need to be developed to be able to make a profit out of the technology. In [6] the authors suggest optimization through both a day-ahead command-based and a day-ahead price based problem statement for both frequency and voltage regulation. The authors also highlight the constraints in terms of maximal apparent power, charging deadlines and battery capacity. Furthermore, the X/R ratio should be considered when designing voltage control through reactive power compensation. For MV and especially LV grids the X/R ratio is lower and thus reactive power compensation has less effect compared to high voltage transmission lines [39].

As stated in several references there is a lack of experimental verification of the V2G technologies in terms of frequency regulation and voltage control [6, 37, 38]. Studies involving real data is crucial for the implementation of the technologies. To my best of knowledge there is yet no study that has been investigating the impact on the grid in terms of voltage and thermal limits from EVs performing frequency regulation using real world data.

2.3. Battery plant regulations in Denmark

Here, technical regulations for battery plants in Denmark will be addressed as this concerns the EV fleet. Not all countries have battery plant regulations yet, and Sweden for example does not have this type of regulations. According to the Technical Regulations for battery plants, provided by

the Danish TSO Energinet.dk, a battery plant is a plant that is able to store and deliver electrical energy according to at least one of their definitions [8]. One of which being to *'absorbing electrical energy from the public electricity supply grid and, at a given time, delivering it back in the Point of Connection'* [8]. This definition would suit the pilot EV fleet at Frederiksberg Forsyning as the aim here is to perform frequency regulation and the definition is thus a requirement for this purpose [7]. Furthermore, the definition by Energinet.dk *'covers both permanently and temporarily connected battery plants'* [8]. Thereby, V2G electric vehicle charging stations are included and regarded as battery plants for which the defined regulations apply.

The regulations define different categories of battery plants with respect to their size. The pilot fleet at Frederiksbergs Forsyning consists of 10 EVs charging 10 kW each (more information regarding the EV fleet can be found in chapter 3). Hence, the battery plants size is 100 kW and falls in to category B which includes battery plants above 50 kW up to and including 1.5 MW.

Battery plants of category B must, according to the regulations be designed in such manner that they are able to operate within the active and reactive power range defined in Fig. 9 below. If nothing else is given the battery plant should operate with a power factor of 1.00, but at any time it should be able to operate the plant within the defined span if requested. Since, the battery plant falls within the category B it is required to have Q control and power factor (PF) control according to the TSOs regulations. Voltage control and automatic power factor control could be implemented but is not required.

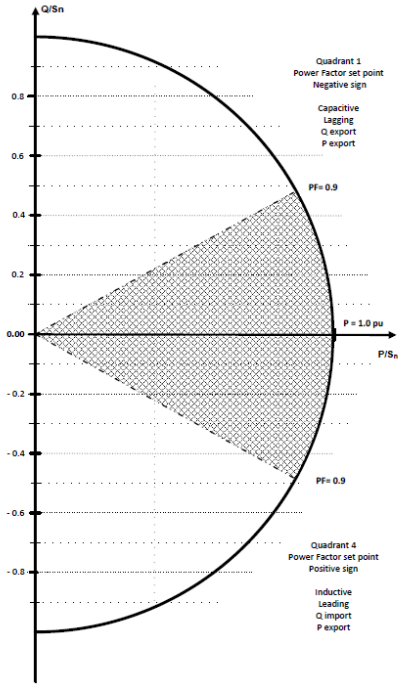

Figure 9: *Requirements from Energinet.dk on operating point in the active and reactive power plane [8].*

Q control, according to Energinet.dk, is the control of reactive power independent of active power

and grid voltage at the point of connection. The Q control should operate with respect to a certain set point (the red line in Fig. 10) and should respond within 2 seconds and be completed within 10 seconds when a change of the set point is given. The accuracy of the set point is not allowed to deviate more than 1 % within a 1 minute time span. The Q control is illustrated in Fig. 10.

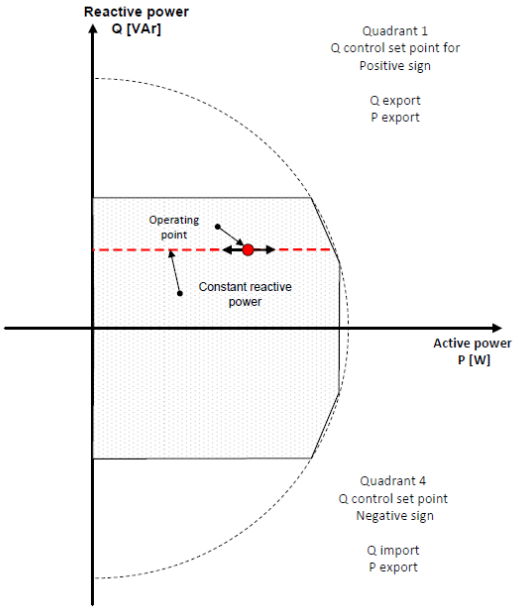

Figure 10: *Q control (reactive power control) as defined by Energinet.dk [8]*

.

'*Power factor control function controls the reactive power proportionately to the active power in the point of connection*' [8], as seen in Fig. 11. Thus, the power factor control is determined using a droop. The required accuracy and resolution of the power factor set point is 0.01. The required response time is the same as for Q control but the deviation is allowed to be 1 % over 0.01 minute only.

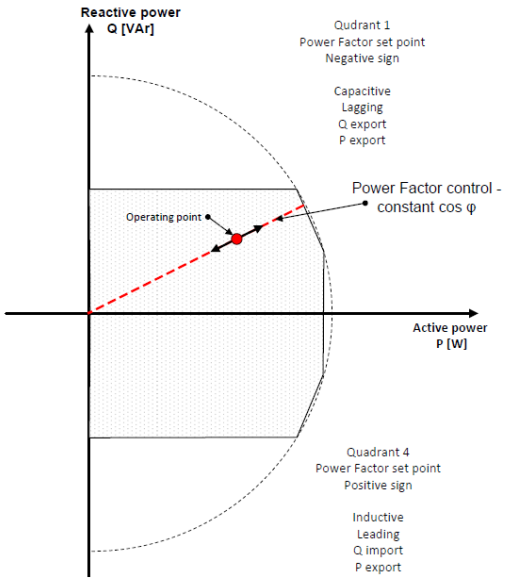

Figure 11: *Power factor control as defined by Energinet.dk [8].*

Automatic voltage control controls the voltage according to a voltage reference set point automatically, but is not required for the battery plant in this case study. The response time requirements are the same as stated above, but is not allowed to deviate more than 0.5 % over a 1 minute time period. The function of the automatic voltage control is seen below in Fig. 12.

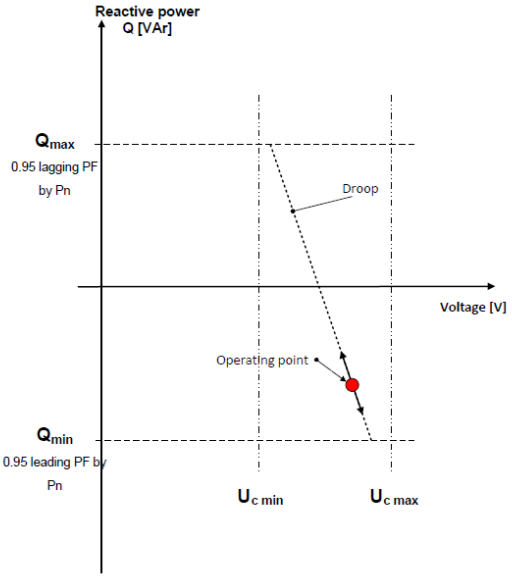

Figure 12: *Automatic control as defined by Energinet.dk. [8]*

Automatic power factor control operates through automatically activating and deactivating to keep the voltage at a certain level in the voltage reference point. This is illustrated by Energinet.dk below (Fig. 13). Comparing Fig. 13 to Fig. 11 it appears that automatic power factor control is similar to power factor control but here a dead band is introduced, i.e. for lower active power levels no power factor control is applied. Thus, this option could be a strategy to decrease the total reactive power input.

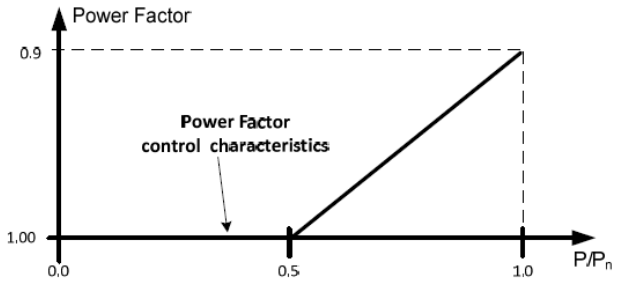

Figure 13: *Automatic power factor control as defined by Energinet.dk, where P/P_n is the normalized ratio for rated power. (P_n is the delivered or absorbed rated power). [8].*

3. The Measurement Data and the EV fleet

This chapter will give an overview of where the data was collected from followed by a presentation of the raw data.

3.1. Frederiksberg Forsyning

Frederiksberg Forsyning (FF) is a utility company providing gas, tap water, district heating and cooling and sewage to about 100 000 residents. Additionally, they provide wind energy. FF is situated in the municipality Frederiksberg in Copenhagen, Denmark. They serve both households and larger industries with maintaining utility pipes as well as expanding the pipe grid, customer support, installations and repair of technical devices. The company has approximately 180 employees. [44]

3.2. The EV fleet

The EV fleet consists of 10 BEVs vans (battery electric vehicle vans) that are utilized by Frederiksberg Forsyning in their daily work. The vehicles are of the brand Nissan e-NV200. Each car has a battery size of 24 kWh and is connected to a 10 kW charger which in total gives a charging capacity of 100 kW (see Fig. 14). When parked at the utility, the cars are connected to the grid through a bidirectional charger for both charging and providing frequency control regulation for normal operation (FCR-N). The V2G technology is provided by NUVVE. The EV fleet is the world's first fully commercialized V2G hub, where the providers of the fleet define commercial as the project being based on 'components and technology that can be purchased by consumers'. [45]

With the NUVVE V2G technology the EV user connects the vehicle, which then is charged to 50 %. When 50 % SOC is reached the charger switches mode to provide frequency regulation in communication with an aggregation platform that gives commands of charging and discharging. Through the aggregation platform (a cloud connected application) it is ensured that the vehicle has enough SOC for the next trip at a certain time. The technology predicts revenue, travel distance and time. [25]

The cars leave FF at 7 am at the earliest and return at 7 pm at the latest [33]. This means that they are available for FCR provision at least from 7 pm to their charging deadline in the morning. However, the cars might return during the day and be connected and thus occasionally providing FCR during the day. [33] With the current EV fleet the charging deadline is around 7 am and the chargers are connected with one phase AC charging.

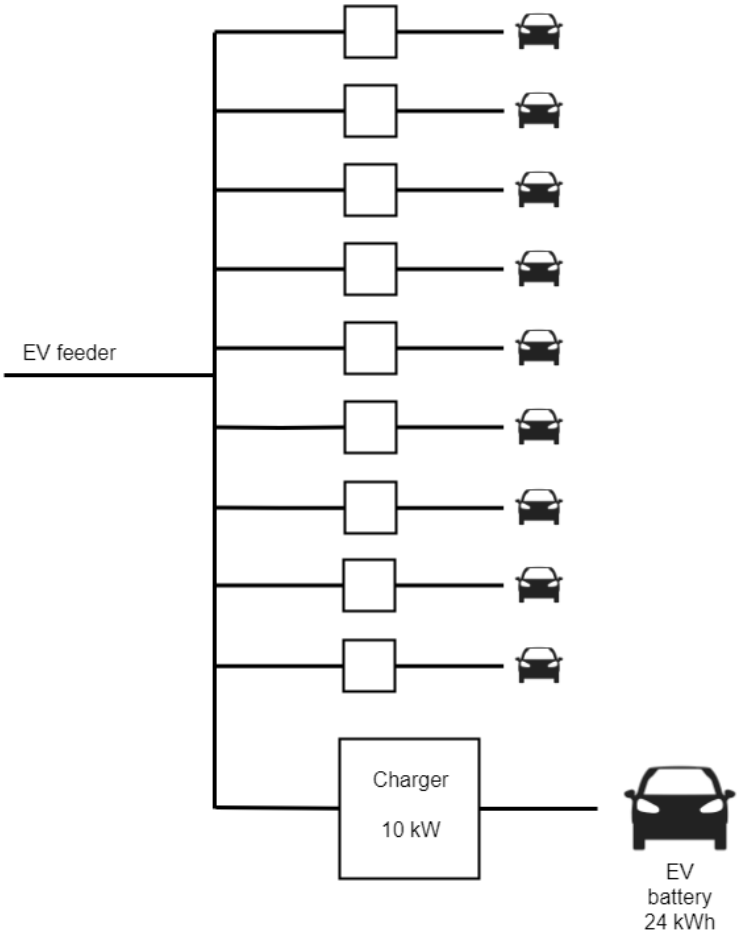

Figure 14: *The line diagram illustrates how the EVs are connected to the 'EV feeder'. All 10 EVs have a battery size of 24 kWh and are connected through a 10 kW bidirectional charger to the feeder.*

3.3. Network and network model

The measured data is collected at three points in the network, which is illustrated as a single line diagram in Fig. 15 below. Observe that this is a simplified line diagram where only the components that are of concern for this project are included. There are two cables connected to FF. Out of these only one phase of one cable is measured in 'Cable Outlet 2' and it is assumed that for different variables the measured value can be multiplied by 6 in order to get the total quantity of the two three-phase cables. The measuring point 'Cable Outlet 1' is the cable of the EV feeder (the line at which all 10 cars are being charged) and here all three phases are measured. Voltages for all phases are measured at 'Bus 1', to which all feeders in the FF building are connected. 'Bus 1' will be utilized in the rest of the report when referring to this specific bus.

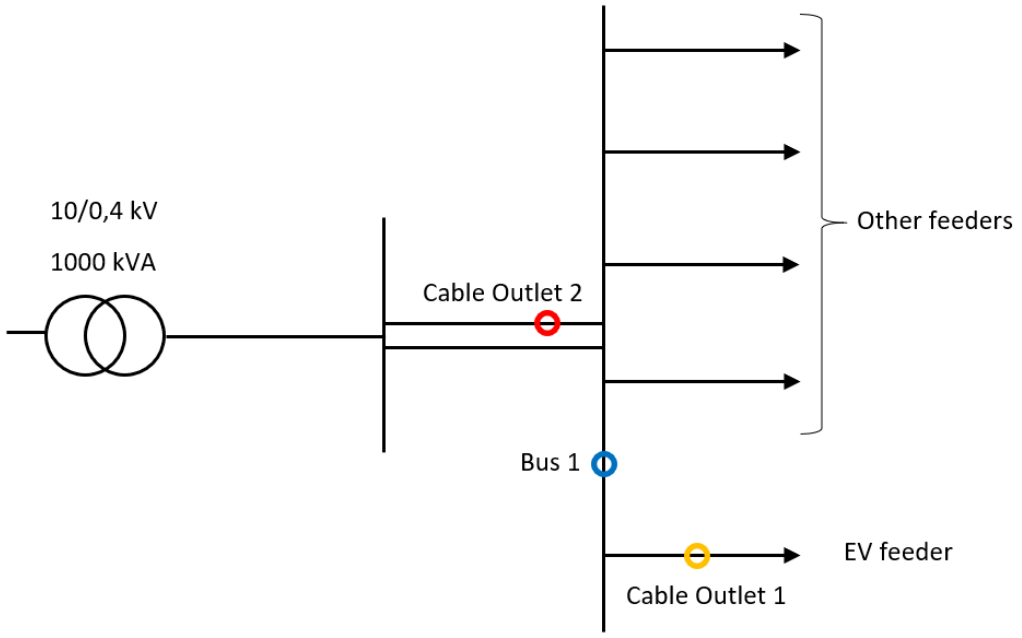

Figure 15: *Simplified line diagram for the analyzed system. In the red measuring point (Cable Outlet 2) only one phase out of six (there are two cables) is measured. At the blue measuring point (Bus 1) voltages are measured. At the yellow measuring point (Cable Outlet 1) all three phases in the EV feeder cable are measured.*

Theoretical Model

From the theory presented in 2.1.2 it is understood that an electrical system can be approximated as a Thevenin equivalent. This is of course a simplification of a complex system, but could be utilized to roughly determine properties of the system and additionally the accuracy of simulated results. The Thevenin equivalent in Fig. 16 represents the studied system where the upstream

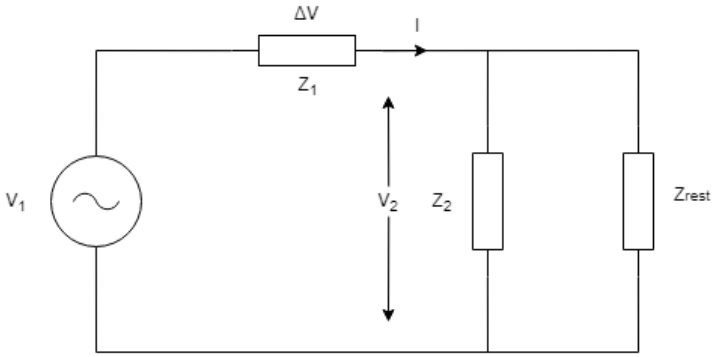

Figure 16: *Thevenin model/approximation of the system in Fig. 16*

network is included in V_1 and Z_1 (i.e. cables, transformers etc.). V_2 represents the voltage at bus 1. Z_2 is the load at the EV feeder and Z_{rest} is the combined load of the remaining feeders at bus 1. With this Thevenin model implementing eq. 4 gives the following formula:

$$V_1 = (1 + \frac{Z_1}{\frac{Z_2 Z_{rest}}{Z_2 + Z_{rest}}})V_2 \tag{7}$$

3.4. Raw data

The measured data is collected with one second time resolution and a measurement is only collected if the sensor detects a change of the variable. The data comes in a csv-file that does not contain measurement for every second and also includes all approximately 50 variables unsorted. The data was collected for three months (December 2017, January 2018 and February 2018). There are however 'gaps' in the data, possibly due to communication problems in the measuring devices. Scripts were written in Matlab to sort out the variables of interest as well as extending the variable vectors to contain measured values for 'all seconds' within the data collection time frame. In Table 1 the collected variables are found.

Measured variable	Variable name
RMS voltage L1-N	LN1
RMS voltage L2-N	LN2
RMS voltage L3-N	LN3
RMS voltage L1-L2	L1L2
RMS voltage L2-L3	L2L3
RMS voltage L3-L1	L3L1
Average active power L1 cable outlet 1	Pow1_1
Average active power L2 cable outlet 1	Pow2_1
Average active power L3 cable outlet 1	Pow3_1
Average reactive power L1 cable outlet 1	Rea1_1
Average reactive power L2 cable outlet 1	Rea2_1
Average reactive power L3 cable outlet 1	Rea3_1
Average RMS current L1 cable outlet 1	I1_1
Average RMS current L2 cable outlet 1	I2_1
Average RMS current L3 cable outlet 1	I3_1
Average active power cable outlet 2	Pow1_2
Average reactive power cable outlet 2	Rea1_2
Average RMS current cable outlet 2	I1_2
Time in date format	t_date
Time in numerical format	t

Table 1: *Table of collected variables and utilized abbreviations/variable names.*

To illustrate the data availability the raw data for the load in cable outlet 2 for all three phases from all three months is seen in Fig. 17. More data along with procedures for filtering are presented in the next chapter.

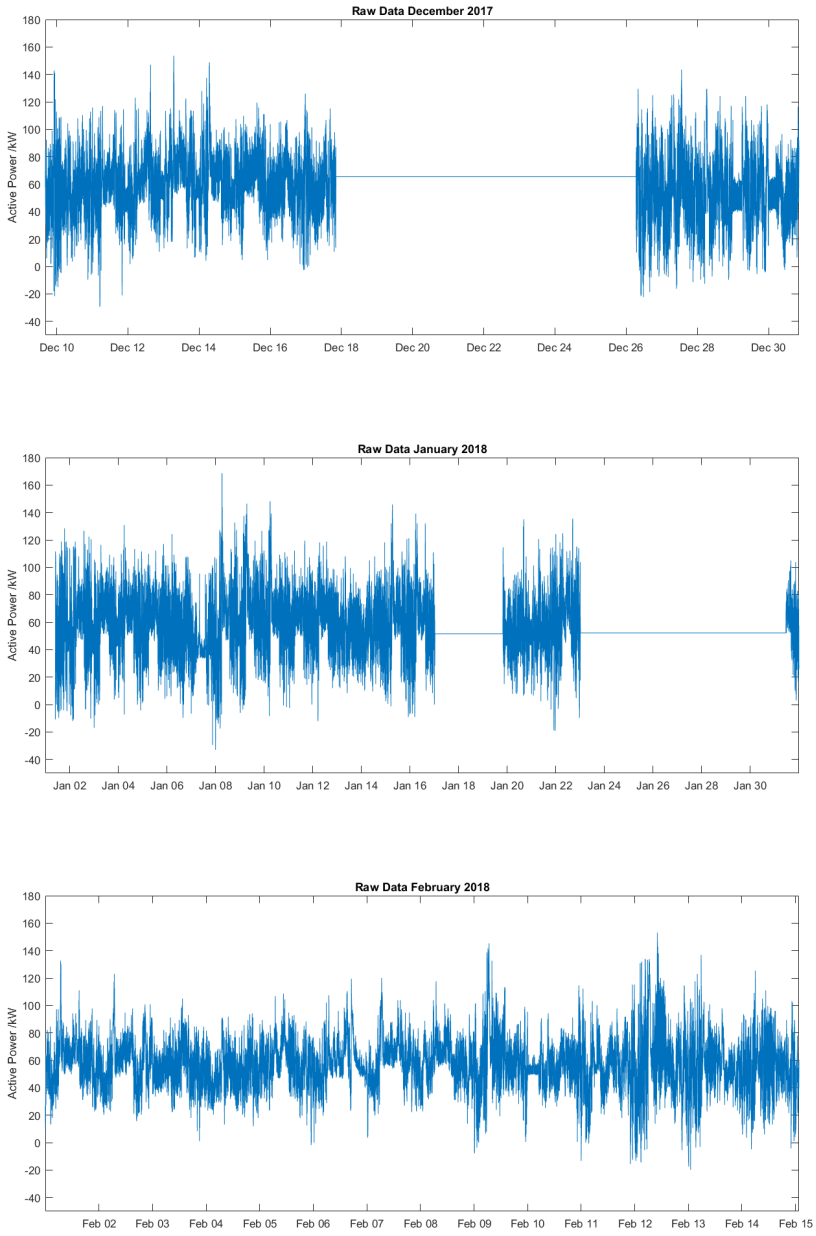

Figure 17: *Raw data for the load in cable outlet 2, i.e. for entire FF building for December, January and February (top to bottom). The gaps in the data are due to that no data collection occurred during these times, possibly due to a communication problems in the measuring devices.*

4. Measurement Data Analysis

This chapter initially presents how data was 'filtered' followed by a voltage analysis. Thereafter load profiles are presented and analyzed. The analysis considers the studied system, i.e. the base case where no variation of variables are introduced, and aims to answer the initial question 'How does the FCR-N provision through EVs affect the studied system today?'

4.1. Data selection

To compare the behavior of the variables and to be able to pick out reasonable periods of data for further analysis the time frame to visualize the data is chosen to be one week. One week is chosen because it is hard to evaluate if the behavior of one day is representative, since the behavior might depend on which day of the week that is being analyzed. To compare on a weekly basis thus makes more sense. Hence, data periods of one week need to be extracted from the raw data. Since the raw data contains 'gaps', i.e. periods were no data was collected, this needs to be taken into account and limits the selection (see Fig. 17). Additionally, whole weeks were preferred which introduced further limitations for the selection. The chosen weeks are shown in Table 2 and will be referred to as specified in the table for the rest of the thesis.

Time period of week	Referred to as
11-Dec-2017 00:00:00 - 17-Dec-2017 23:59:59	Week 1
01-Jan-2018 09:50:09 - 07-Jan-2018 23:59:59	Week 2
08-Jan-2018 00:00:00 - 14-Jan-2018 23:59:59	Week 3
05-Feb-2018 00:00:00 - 11-Feb-2018 23:59:59	Week 4

Table 2: *Table of weeks that the following analysis concern.*

Observe that the data for week 2 begins at around 10 am. This is due to a gap in the data collection up to this time, but the absent data for the period was considered too small to disregard the data for the entire week.

4.2. Voltage analysis

This section will present the data analysis regarding voltage along with the methodology of the analysis.

4.2.1. Voltage limitations/violations

An initial natural question regarding voltage impact analysis is whether the voltage limitations are violated at any point already in the base case. As stated in 2.1.2 the voltage limits for a 230 V line is 207 V to 253 V (a $\pm 10\%$ variation range). In Fig. 18 it is seen that the voltage does not reach these limits at any time during the four analyzed weeks. Another observation is however that

all three phases frequently change quite radically. This is most probably due to tap changes in an upstream transformer.

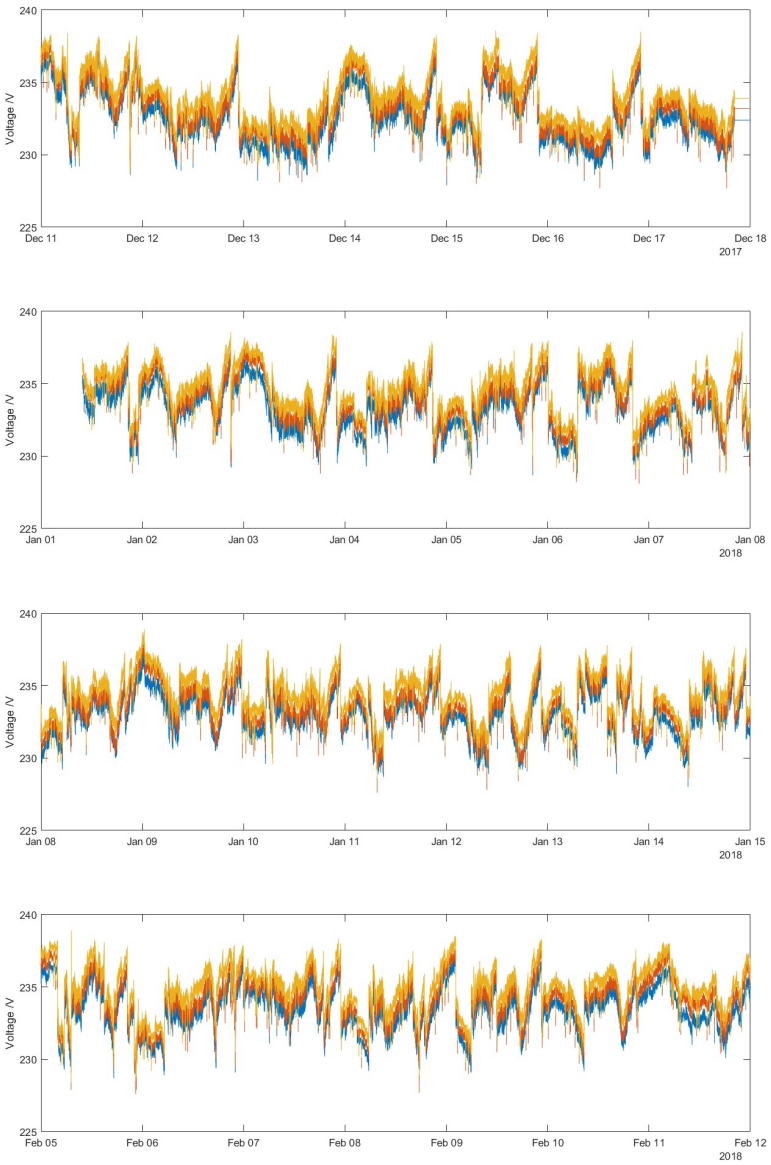

Figure 18: *The three line to neutral voltages for week 1, 2, 3 and 4 (top to bottom). (blue - phase 1, red - phase 2 and yellow - phase 3)*

4.2.2. Power - voltage relation

This analysis aims to evaluate how the load of the EV feeder affects the voltage at bus 1 and thereby determine the impedance Z_1 in Fig. 16. To be able to conduct this analysis and to plot power against voltage, shorter time periods need to be extracted for evaluation. In order to find periods where the EV load correlates with the voltage at bus 1, the following conditions are searched for:

- Periods where FF load and EV load follow the same behavior. This indicates that EV feeder could have an impact on the total system.
- Periods where impact from other feeders are suspected to be low.
- Periods that do not contain tap changes for the voltage.
- Periods that contain large fluctuations in EV feeder load, i.e. that contain power levels close to 100 kW or -100 kW, as this could possibly lead to crucial voltage conditions.

To have a reference for how the EV load might not relate explicitly well with the voltage at bus 1, periods with the following conditions are searched for:

- Periods where FF load and EV load do not follow the same behavior.
- Periods where the impact from other feeders are suspected to be high or intermediate.
- Periods that do contain tap changes for the voltage.

Initially the EV feeder load was plotted against the FF load (EV load excluded) to roughly pick out days where an analysis could be interesting. Thereafter the voltage profile was looked at to avoid tap changes and the load profiles were analyzed further to evaluate the impact from other feeders with respect to the EV feeder. For further reading on the method and graphs utilized to extract periods of data with the above stated conditions are found in Appendix A.

In the graphs in Fig. 19 below a period with very low correlation between the EV and FF feeder load can be seen. The impact from other feeders is expected to be high. As seen in the graph the active power in the EV feeder and the voltage do not correlate.

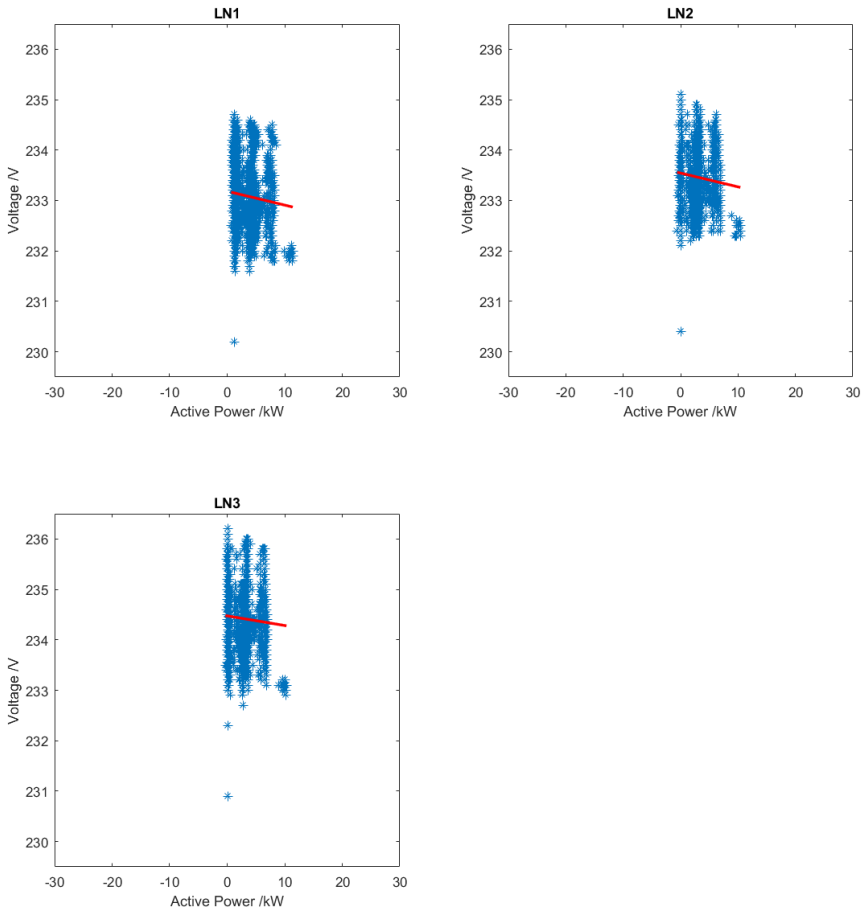

Figure 19: *Values of active power for each phase plotted against line to neutral voltage for time 01:58:00 to 04:15:00. The red line represents a linear regression respectively. The linear regressions were calculated to be LN1=233.1843 – 0.0275* P1, LN2=233.5441 – 0.0273*P2, LN3=234.4753 – 0.0191* P3 where P1, P2 and P3 are in kW. Correlation coefficients are -0.074, -0.074, -0.049.*

For the graphs in Fig. 20 and 21 below data are presented from periods where EV load and FF load follow the same behavior and the impact from other feeders are suspected to be low.

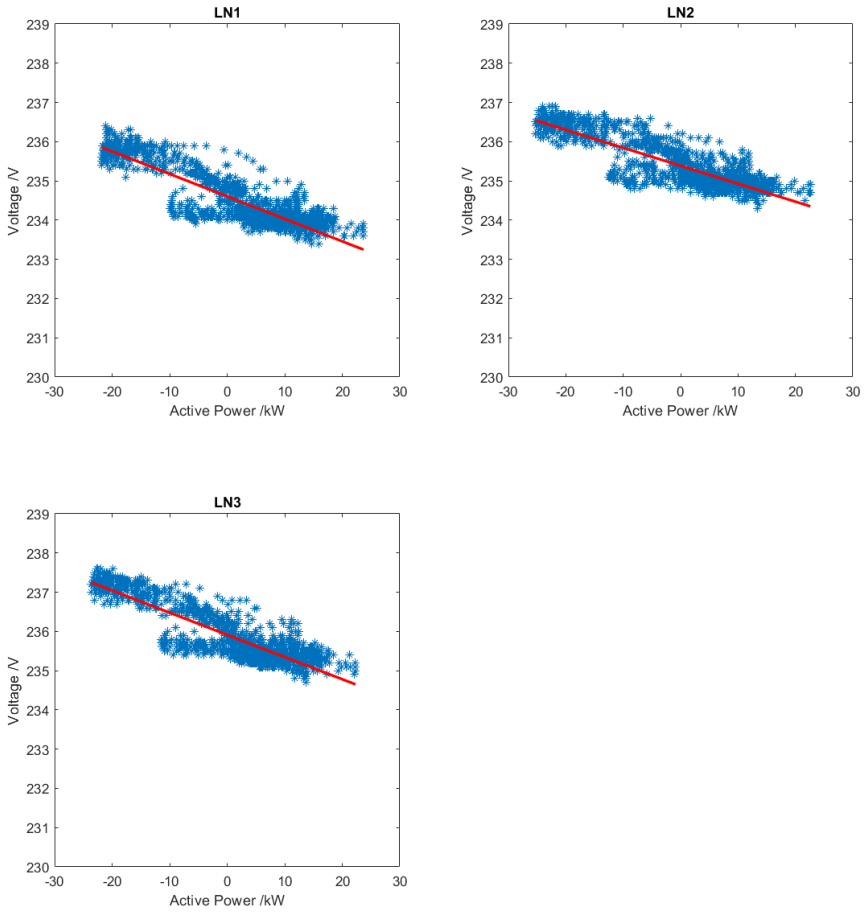

Figure 20: *Values of active power for each phase plotted against line to phase voltage for time 04:15:00 to 05:15:00. The red line represents a linear regression respectively. The linear regressions were calculated to be LN1=234.6051 - 0.0573 P1, LN2=235.3866 – 0.0458 P2, LN3=235.9130 – 0.0566 P3, where P1, P2 and P3 are in kW. Correlation coefficients are -0.88, -0.85 and - 0.88 respectively.*

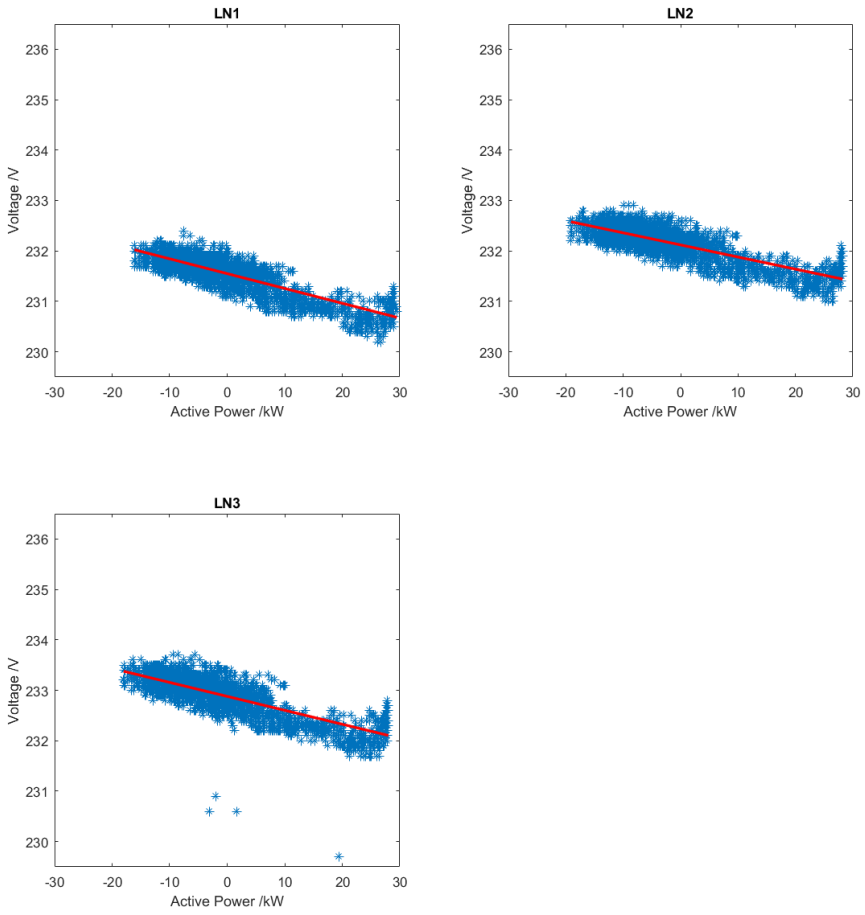

Figure 21: *Values of active power for each phase plotted against line to phase voltage for time 01:58:00 to 04:15:00. The red line represents a linear regression respectively. The linear regressions were calculated to be LN1=231.5505 – 0.0294* P1, LN2=232.1196 – 0.0240*P2, LN3=232.8794 – 0.0277* P3, where P1, P2 and P3 are in kW. Correlation coefficients are -0.85, -0.81, -0.80.*

The graphs above are examples from the collected data on how well the voltage and the EV load can relate, but does of course not give the entire picture on how they relate. They can however, be utilized to conclude that the EV load sporadically has a major impact on the voltage at bus 1. Additionally, they can be used to roughly approximate Z_1 at the EV feeder.

4.3. Load profile analysis

As a measure to analyze the thermal impact of the FCR providing EVs, this section presents an analysis of load profiles for week 3 (January 8th to January 14th 2018). In Fig. 22 load curves for weekdays are shown and in Fig. 23 load profiles for the days of the weekend are shown. From these graphs it can be concluded that the highest load for the FF building (EV feeder excluded) is

around 90 kW and for just maintaining the building with no workday activities the building requires approximately 50 kW.

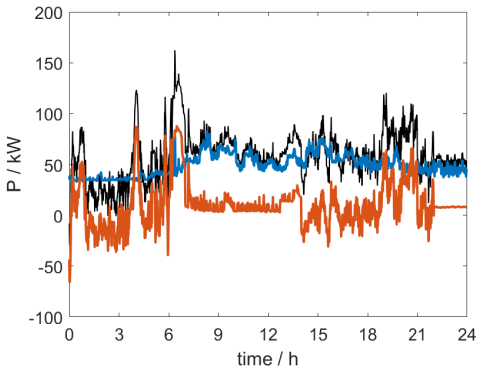

(a) *Load curves for Monday (Jan 8th 2018)*

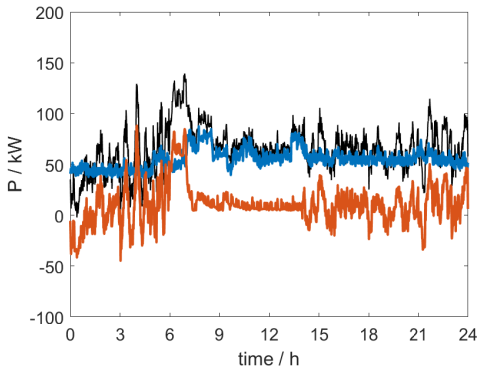

(b) *Load curves for Tuesday (Jan 9th 2018)*

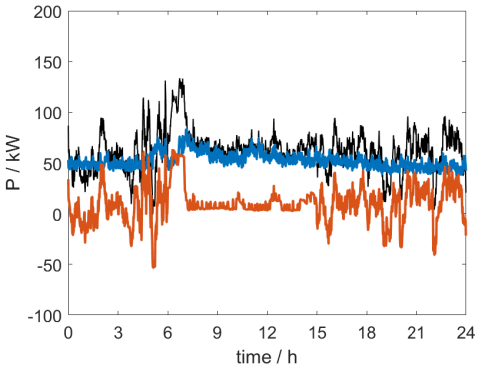

(c) *Load curves for Wednesday (Jan 10th 2018)*

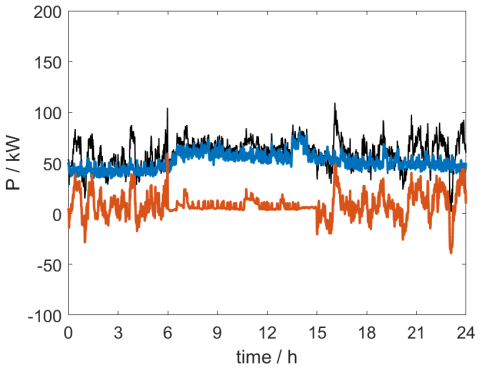

(d) *Load curves for Thursday (Jan 11th 2018)*

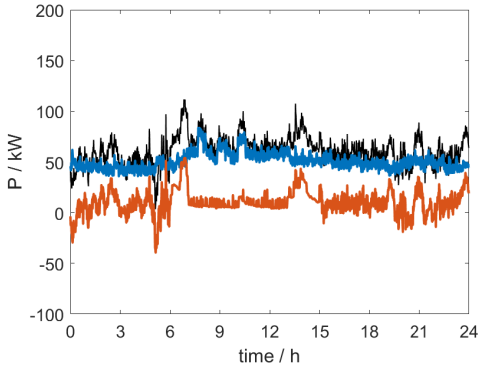

(e) *Load curves for Friday (Jan 12th 2018)*

Figure 22: *Load curves for the weekdays of week 3 (January 8th to 14th 2019) Black - FF and EV load combined, Blue - FF load (EV load excluded), Red - EV load.*

Regarding the EV feeder load, it can be observed that they are scheduled to have 'full tank' around 7 am (also observe that 'full tank' does not mean fully charged battery, but charged to the set SOC).

This causes a morning peak around this time as the EVs changes from 'FCR providing mode' to 'charging mode' at the same time as the workday activity starts. Monday and Tuesday appears to be the busiest days load wise and during these days the maximum EV load reaches values of the maximum FF load, i.e. approximately 90 kW in the morning.

For the days during the weekend no clear peak can be observed. However, the EVs are available for FCR provision during the entire day which leads to the load profile reaching fairly high values sporadically.

Thus, it can be concluded that the most critical hours during weekdays occur in the morning, since the start of the workday and the EV charging occurs at the same time. Sporadic peaks can occur during the afternoon of weekdays as well as weekends, but these peaks depends on the FCR demand and do not always have a clear pattern. The morning peak during weekdays could possibly lead to thermal impact problems when scaling up the EV feeder load.

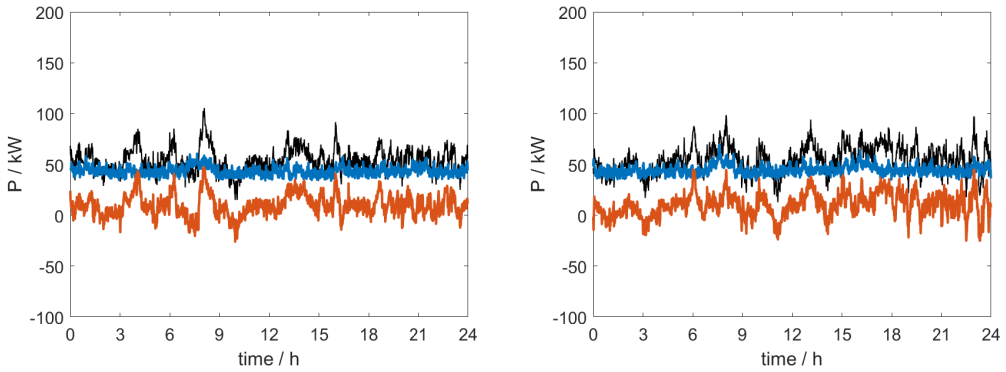

(a) *Load curves for Saturday (Jan 13th 2018)* (b) *Load curves for Sunday (Jan 14th 2018)*

Figure 23: *Load curves for the weekend of week 3 (January 8th to 14th 2019) Black - FF and EV load combined, Blue - FF load, Red - EV load.*

5. Simulation and Control Strategies

The aim of this part of the project is to first model the studied system and from this model simulate possible variations of the existing case possibly being future scenarios. This is done in order to evaluate if a voltage problem will occur for the different scenarios. This is followed by applying different solution strategies (or control strategies) as well as analyzing the stability of the system and different load curves.

5.1. Simulation model

A simulation model was built in Matlab Simulink to represent the studied network (Fig. 24). For the input variables to the simulation, only measurements from week 3 were chosen, since choosing all four weeks would result in too long simulation times that did not fit within the time frame of this project. Here the properties for the transformer was applied according the actual transformer in the studied network (10/0.4 kV 1000 kVA), whereas the properties for cables and upstream network were not available and thus taken from another but similar low voltage network.

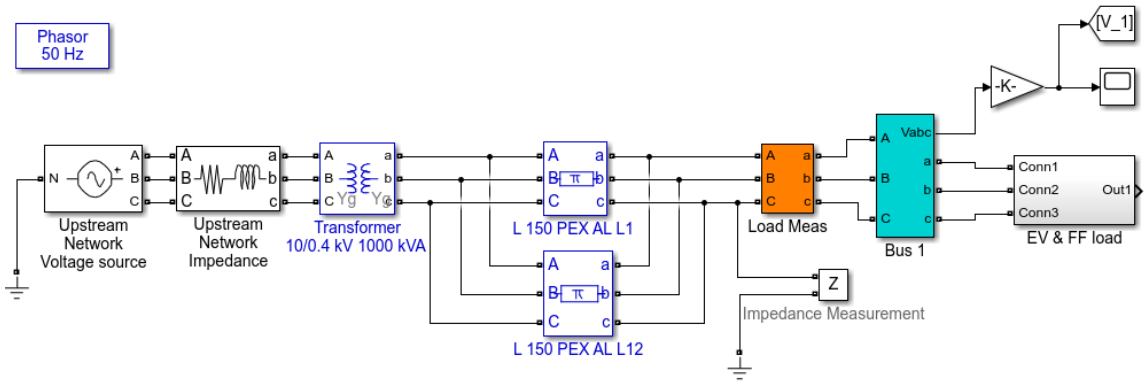

Figure 24: *Network as simulated in Matlab Simulink*

The initial hurdle in order to build different simulation scenarios is that the known properties of the electrical systems are at the 'end of the system' (at the right end of the system in Fig. 24). In order to be able to simulate different scenarios with different properties at the end of the electrical system (to vary for example the load of the feeders) known properties at the upstream network are required, such as a voltage source vector. Thus, the initial step in the simulation process was to find out the voltage and impedance of the upstream network. From Fig. 21 and 20 it is seen that the inclinations are around 0.02 to 0.05. Hence, it was assumed that the impedance of the network, Z_1 in Fig. 16, would be in the range of 0.02 to 0.05 ohms. It should be noted that for the analysis in chapter 4 the reactive power and the reactance was assumed negligible. However, looking at the

graphs it appears that Fig. 21 is a 'better fit' and the impedance might be closer to 0.02 ohms. In the model above (Fig. 24) it can be seen that the system impedance was divided into 'upstream impedance', 'transformer impedance' and 'cable impedance', illustrated in Fig. 27 as $Z_{upstream}$, $Z_{transformer}$ and Z_{line}. The impedance for the transformer was, as stated, applied according to the actual transformer and the impedances for the cables were taken from supposedly similar cables to the ones in the system. The X/R ratio of the upstream network was set to 7 and the impedance was then computed through the short circuit capacity of a similar network (from which the cable properties were taken). An initial guess of the impedance was set between 0.02 and 0.05 ohms to compute a voltage vector for the upstream network. The upstream voltage vector was utilized to compute a new voltage vector for bus 1 through the simulation to compare the accuracy of the model. From the simulation the impedance for the assumed model could be measured to 0.02 ohms with a 73 degree angle. Since this was in the range suggested by the analysis in chapter 4 this was considered acceptable and a new voltage vector for the upstream network was computed (Fig. 25). The simulated voltage and the measured voltage at bus 1 can be seen in Fig. 26. As seen in the figure the simulated voltage is close to the measured voltage and the approximated model is considered satisfactory.

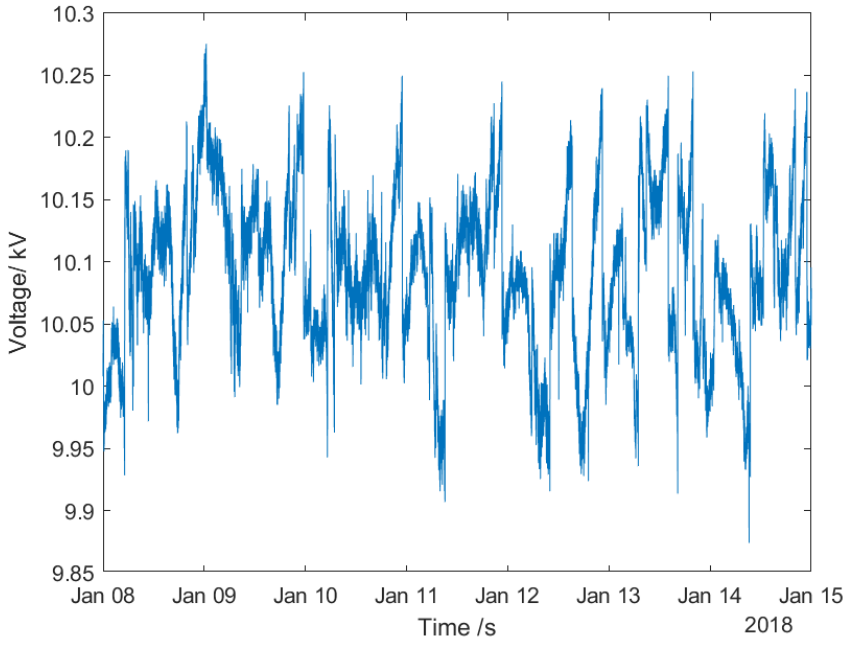

Figure 25: *Computed voltage for the upstream network for week 3.*

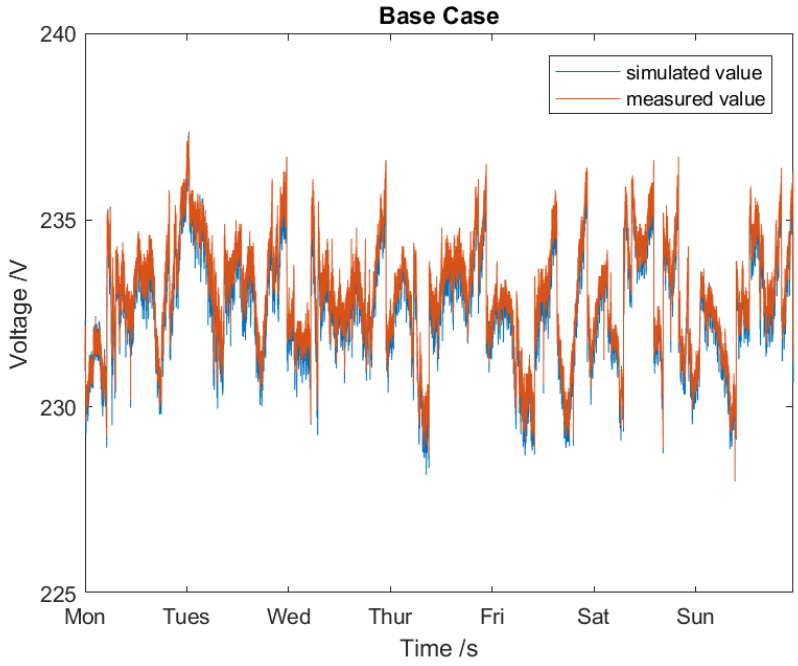

Figure 26: *Measured voltage for week 3 (red) and simulated voltage (blue) according to the approximated model.*

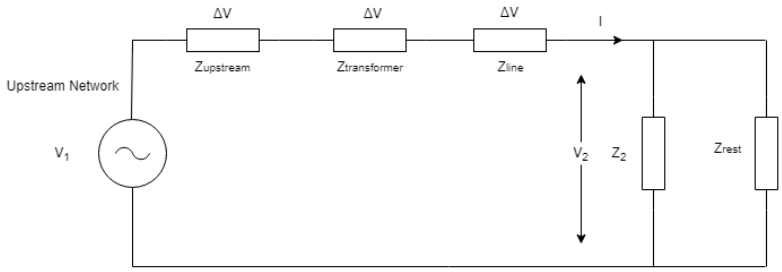

Figure 27: *Assumed model for the network.*

5.2. Simulation scenarios

For the different simulated scenarios mainly two variables are considered - installed power and the cable length. These variables were chosen in order to represent a variety of possible future scenarios. Installed power was chosen because it could both represent an increase in cars but also larger charging capacity for each car. Both are possible future scenarios as the total vehicle fleet at FF is 40 cars and the EV fleet could be extended to include all cars. One could also prospect that the batteries and chargers could be upgraded to respectively storing and charging more power. It might also be of interest for other companies to evaluate the replicability of the technology and thus also evaluate which number of EVs or size of batteries resulting in a specific installed power that would suit their specific case. Five installed power levels for the simulations are chosen to

be 100 (base case), 200, 400, 600 and 800 kW. As previously stated, the size of the transformer is 1000 kVA and the last installed power level 800 kW might result in a too high power flows for the transformer. However, this installed power level is included in the analysis since the aim is to find the limitations of the system. It is assumed that the frequency control regulation will be the same as in the studied case and thus the EV chargers would respond in the same way, but stronger since there is more installed power available.

Variations of the cable length from the transformer to FF are introduced to the simulations to represent stronger or weaker grids. When the cable length increases the X/R ratio will be smaller and thus the grid will be weaker in the sense that the voltage will be more sensitive to changes in the active power (since R is larger than X). Different lengths for the cable from the transformer to FF are chosen to be 0.02 (base case), 0.1, 0.2, 0.4, 0.8 and 1.6 km. It is assumed that the lengths will represent different realistic 'cable length scenarios' within an urban or suburban area. This is done to evaluate the applicability of the technology and the need for voltage adjusting technologies. The different cases (scenarios) that are evaluated are seen in Fig. 28 below.

	$P_{installed}$ = 100 kW	$P_{installed}$ = 200 kW	$P_{installed}$ = 400 kW	$P_{installed}$ = 600 kW	$P_{installed}$ = 800 kW
Length= 0.02 km	Case 1	Case 2	Case 3	Case 4	Case 5
Length= 0.1 km	Case 6	Case 7	Case 8	Case 9	Case 10
Length= 0.2 km	Case 11	Case 12	Case 13	Case 14	Case15
Length= 0.4 km	Case 16	Case 17	Case 18	Case 19	Case 20
Length= 0.8 km	Case 21	Case 22	Case 23	Case 24	Case 25
Length= 1.6 km	Case 26	Case 27	Case 28	Case 29	Case 30

Figure 28: *Simulated cases/scenarios, where case 1 is the 'base case' and cases 2 to 30 are scenarios created through varying the cable length in the electrical system and the installed power level of th EV fleet.*

5.3. Control strategies

As will be seen later on in the results some of the simulated cases will result in violated voltage limits. This calls for measures to control the voltage at the feeder. Even for the highest installed power evaluated (800 kW) the EV fleet would still fall within category B for the battery plants regulations from the Danish TSO [17]. According to these regulations such battery plants are required to have PF control and Q control. Additionally, it needs to be able to provide any, both positive and negative, PF between 1 and 0.9 when assigned to do so. In this project PF control will be evaluated as a measure to investigate if voltage can be controlled with reactive power compensation for the studied scenarios.

The controller of reactive power can be designed to have active power or voltage as input (Q(P) or Q(V) respectively). Since Q(P) is a feedforward controller, this is usually an easier solution than Q(V), which is a feedback controller. Thus, it is important to evaluate Q(P) for practical reasons. The Q(P) control strategy additionally is a good starting point for analyzing possible limits for reactive power input for the controller. If stability issues are experienced for this controller it might be difficult to design a controller of the Q(V) type that does not cause the same stability issues. As a Q(V) controller could be more accurate and the voltage is already being measured at bus 1 this option will be discussed. In the following section the evaluated Q(P) control strategies are described.

5.3.1. Q(P) Control

Here the control strategies utilizing active power as input signal are described. First a PF controller is described followed by a proportional Q(P) controller.

PF control
This function is designed similarly as the power factor controller proposed by Energinet.dk seen in Fig. 11. However, here only one PF level is evaluated and set to ±0.9. For power flows this is a common utilized PF level and is also the required minimum PF by Energinet.dk as seen in Fig 9. Thus, PF= ±0.9 is chosen to evaluate the capability of this method. The equation for the controller is seen in eq. 8 below where P is the total active power of the FF building including the EV feeder. The control function is illustrated in Fig. 29 below.

$$\begin{aligned} Q_c &= -Ssin(\alpha) = -Ptan(\alpha) \\ &where: \\ \alpha &= arccos(PF) \end{aligned} \tag{8}$$

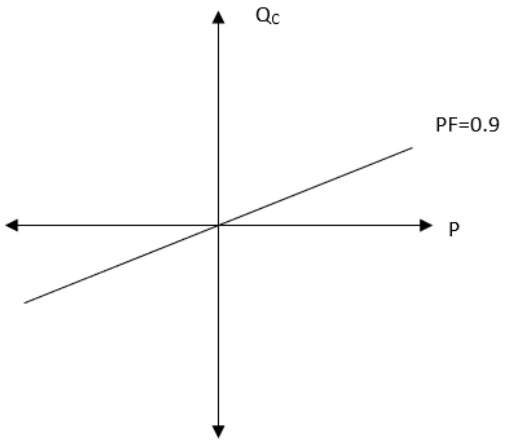

Figure 29: *Illustration of the PF control function.*

Proportional Q(P) control
The PF control above might not be able to provide enough reactive power to keep the voltage level

stable for the more crucial scenarios. This is due to the fact that the X/R ratio is smaller than one for the studied case and thereby, a change in reactive power will result in less proportional change in voltage as it would for example for a case including overhead lines. That is - more reactive power is required to achieve a change in the voltage behavior. If rearranging eq. 6 and assuming that ΔV should be kept zero the following equation is achieved:

$$\begin{gathered} Q_c = -kP \\ where: \\ k \approx \frac{R}{X} \end{gathered} \tag{9}$$

This equation is utilized to control the reactive power output and will have the same behavior as in the previous method (Fig. 29). The R/X ratio was determined through measuring the impedance of the network in the Simulink simulation.

To both methods a dead band, such as in Fig. 13, could be introduced to minimize the total reactive power input. However, the aim is to evaluate if the voltage can be controlled with reactive power without violating the system limitations. Thus, this option is not included in the simulations.

5.4. Limitations of the studied system

When evaluating the results both from the simulation of the scenarios but also for the possibility to implement control strategies, the limitations of the system needs to be discussed and analyzed. In this project the limitation analysis will be motivated through PV-curves, Thevenin models and the short circuit capacity (S_{SC}). As the length of the cable increases the impedance will increase which in turn results in a decreasing short circuit capacity. Thus this will both limit the active power transfer at the feeder but also the possibility to control the voltage through reactive power as it might result in an apparent power (S) that exceeds the short circuit capacity. Additionally, the reactive power compensation will give different PF factors which leads to changes in the PV-curve and thereby changes for the voltage limits, for which the system is no longer stable. This analysis will be presented in parallel with the other results and analysis.

5.5. Load curves

For the simulated scenarios a load curve analysis will be carried through. Here, the changes for the FF load profiles as well as the changes for a transformer load profile will be analyzed. Through this analysis the thermal impacts and the impacts on the peak load will be discussed.

6. Results and Analysis

This chapter presents the results from the simulated scenarios as well as the accompanying control strategies. The chapter is divided into the simulation scenarios and the control strategies. Together with the next chapter it aims to answer the questions 'If and when will there be issues for the grid operation?', as well as 'Can reactive power compensation be utilized to minimize grid impact?'.

6.1. Simulated scenarios

For all of the simulated scenarios the results are summarized in Fig. 30. The results are divided into three categories - cases for which the voltage was kept within the limits, cases for which the voltage limitations were violated and cases that could not be simulated. As seen in the figure for cases 1-14 and 16-17 the voltage is kept within the limits, but for cases 15, 18-23 as well as 26 the voltage limits are violated. The voltage limits are also violated for cases 24-25 and 27-30, but here it is to such extent that the system becomes unstable and therefore the cases are not possible to simulate. This will be further discussed in the following section.

	$P_{installed}$ = 100 kW	$P_{installed}$ = 200 kW	$P_{installed}$ = 400 kW	$P_{installed}$ = 600 kW	$P_{installed}$ = 800 kW
Length= 0.02 km	Case 1	Case 2	Case 3	Case 4	Case 5
Length= 0.1 km	Case 6	Case 7	Case 8	Case 9	Case 10
Length= 0.2 km	Case 11	Case 12	Case 13	Case 14	Case15
Length= 0.4 km	Case 16	Case 17	Case 18	Case 19	Case 20
Length= 0.8 km	Case 21	Case 22	Case 23	Case 24	Case 25
Length= 1.6 km	Case 26	Case 27	Case 28	Case 29	Case 30

Figure 30: *Results for the simulated scenarios, where green represents cases where voltage are kept within the limits (207 - 253 V), red represents the cases that violate the voltage limits and black represents cases that could not be simulated.*

6.1.1. Electrical system limitations

In the following analysis the limitations of the electrical system will be evaluated to motivate the outcome of the results in Fig. 30. Additionally, the aim of the control strategies in the next section is to make the red and black cases green with reactive power compensation, but whether this is possible or not can be further explained through this analysis. Here, relevant questions are if the short circuit capacity is exceeded, how PV-curves for each cable length look like and how this relates to the power and voltage levels for the different cases. Starting with the PV-curves the underlying formulas are the described through the following equations:

$$P(R) = V(R)I(R) \tag{10}$$

$$Q(P) = Ptan(\phi) \tag{11}$$

Recalling Fig. 3 from chapter 2 the PV-curve has the shape of a 'nose curve' and the maximum P is reached at the 'tip' after which the system faces a blackout, i.e. the power drops to zero. In the case of a resistive load the maximum active power is reached when it equals the source reactance (R=X) [46]. Thus, when load is added and the resistance goes from large to small, before the 'tip' the resistance is larger than the source reactance (R>X) and after the resistance is smaller than the source reactance (R<X). For 'weaker' grids a change in active power has more effect on the voltage compared to a change in reactive power, due to a small X/R ratio, and hence the curve is steeper and reaches maximum P 'quicker'.

The PV-curves for each cable length that is evaluated can be seen in Fig. 31. Note that the PV-curves depend on the short circuit capacity, thus also on the impedance of the system, and thereby they are different for each cable length. The graphs in Fig. 31 were created through the simulation in Simulink and by ramping up P with a load of $P+jtan(\phi)P$. Recalling Fig. 3 it is realized that only the top of the PV-curves are represented in Fig. 31. After the 'tip' of the curve the maximum power has been passed and there is a blackout in the system.

'Zoomed in' versions of the PV-curves are found in Fig. 32. With the help of the lines for the maximum 'measured' active power for each installed power it can be visually evaluated for which cases the voltage limits will not be violated. The minimum and maximum active power when having the five different levels of installed power are found in Table 4. In Table 3 the maximum power without violating the the voltage limits are found for tan(ϕ)=0 (no reactive power compensation) and for tan(ϕ)=-1.

For the result in Fig. 30 no reactive power compensation is applied and thus tan(ϕ) could be assumed to be approximately zero. Looking at the graphs for tan(ϕ)=0 in Fig. 32 it is seen that for cable lengths 0.02 km and 0.1 km all levels of installed power will be kept within the voltage limits. For a cable length of 0.2 km the highest power level will not be kept within the voltage limits. Furthermore, for 0.4 km cable length the voltage limits will be violated for 400 to 800 kW installed power, for 0.8 km this is further extended to 200 to 800 kW and for 1.6 km all of the installed power levels will cause voltage limit violations. This is well in line with the results in Fig. 30.

The PV-curves can also explain the appearance of 'black cases' and why they are not possible to simulate. Through a visual inspection of Fig. 31e and 31f it can be seen that for cable lengths 0.8 and 1.6 km voltages lower than approximately 140 V causes a blackout in the system. For case 23 the lowest voltage is 141 V and it can be suspected that the voltage for cases 24 and 25 would drop further violating the voltage stability limits. Therefore, cases 24 and 25 are not possible to simulate since the system blacks out. For case 26 the lowest voltage is 173 V. It is not entirely

clear if the voltage would drop this low for the following case 27 when looking at Fig. 31. However, when looking at maximum active power for which the system is still stable in Table 3 it is seen that the limit for 0.8 km is 440 kW and for 1.6 km the limit is 227 kW. Comparing these values to the maximum active power levels in Table 4 it is understood that case 24 and 25 for cable length 0.8 km and case 27 to 30 for cable length 1.6 km will violate the system limitations and thus cause a blackout in the system. Thus, they cannot be simulated.

As stated, the aim for the control strategies in this chapter is to make the 'red' and 'black' cases green through reactive power compensation. However, it can already be seen in Fig. 31 as well as Fig. 32 that for cable lengths 0.4 km and longer, increasing the reactive power ($\tan(\phi)<0$) does not increase the voltage enough. This can be further realized through Fig. 33. Furthermore, looking at Fig. 32 it can be seen that for cable lengths 0.02 km to 0.2 km it is possible to adjust the reactive power input ($\tan(\phi)$) in order to keep the voltage within the limits for the maximum power for all installed power levels. For cable length 0.4 km it will be possible to keep all except for the last case within the voltage limits with the suggested values of $\tan(\phi)$. For 0.8 km only 2 cases will be possible to solve with reactive power compensation and for 1.6 km none will be possible to solve. The following section will present the results and the evaluated reactive power control strategies to demonstrate this.

Cable length	P_{max} for $\tan(\phi) = 0$ (system limits)	P_{max} for $\tan(\phi) = 0$ (voltage limits)	P_{max} for $\tan(\phi) = -1$ (voltage limits)
0.02 km	3 568 kW	2 300 kW	1 302 kW
0.1 km	2 188 kW	1 082 kW	3 102 kW
0.2 km	1 426 kW	625 kW	1 513 kW
0.4 km	822 kW	335 kW	640 kW
0.8 km	440 kW	173 kW	279 kW
1.6 km	227 kW	88 kW	129 kW

Table 3: *Maximum active power without violating the stability limits for tan(ϕ)=0, followed by maximum active power without violating the voltage limits (207 to 253 V) for tan(ϕ)=0 and tan(ϕ)=-1 for each cable length respectively.*

$P_{installed}$	P_{min}	P_{max}
100 kW	- 33 kW	169 kW
200 kW	-102 kW	252 kW
400 kW	-239 kW	420 kW
600 kW	-377 kW	589 kW
800 kW	-514 kW	770 kW

Table 4: *Minimum and maximum active power for each installed power respectively when providing FCR-N through the EV fleet. The values are from week 3.*

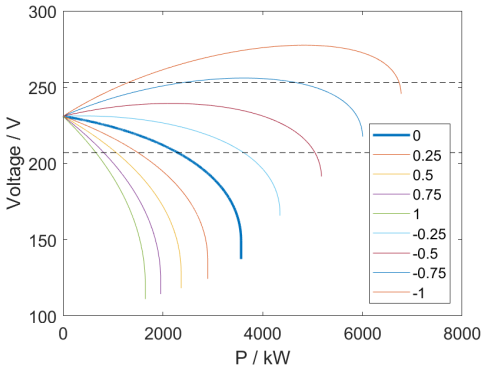

(a) *PV-curve for cable length of 0.02 km.*

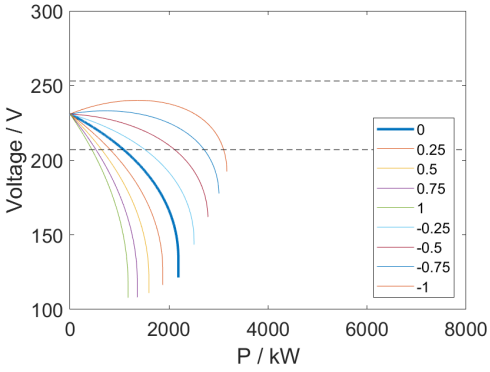

(b) *PV-curve for cable length of 0.1 km.*

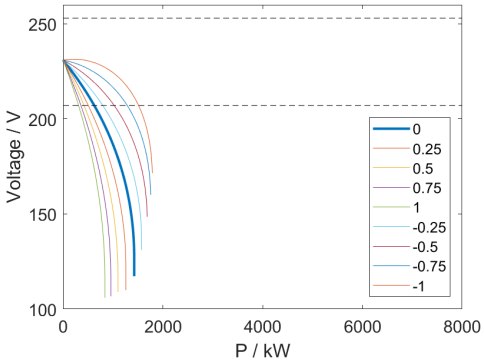

(c) *PV-curve for cable length of 0.2 km.*

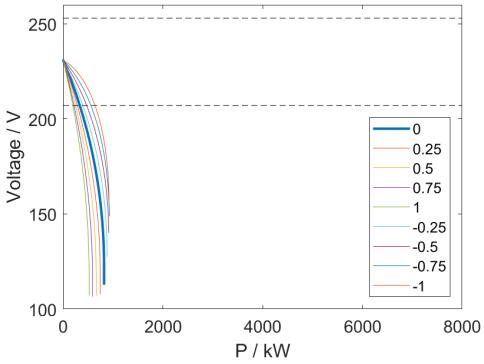

(d) *PV-curve for cable length of 0.4 km.*

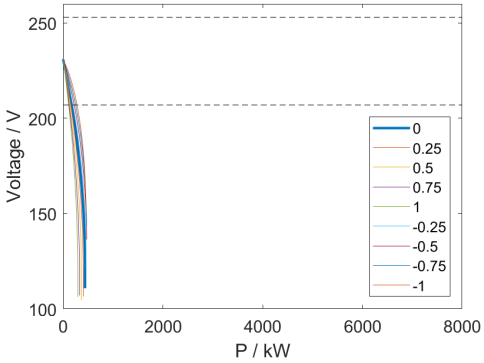

(e) *PV-curve for cable length of 0.8 km.*

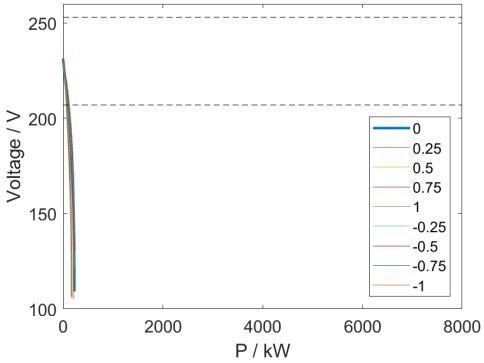

(f) *PV-curve for cable length of 1.6 km.*

Figure 31: *PV-curves for the investigated cable lengths. PV-curves are plotted for tan(ϕ) = 0, 0.25, 0.5, 0.75, 1 , -0.25, -0.5, -0.75 and -1 for lengths 0.02, 0.1, 0.2, 0.4, 0.8 and 1.6 km.*

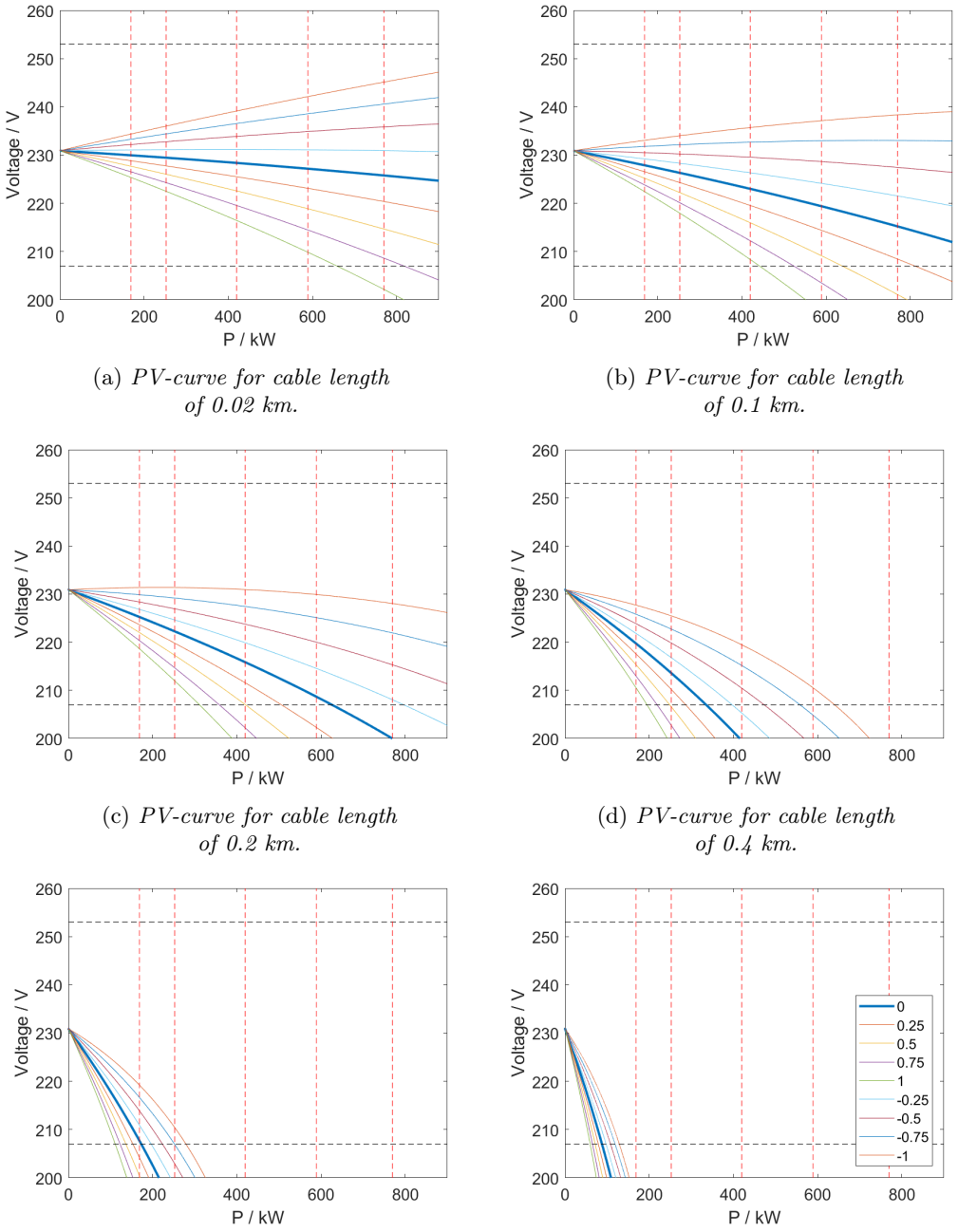

(a) *PV-curve for cable length of 0.02 km.*

(b) *PV-curve for cable length of 0.1 km.*

(c) *PV-curve for cable length of 0.2 km.*

(d) *PV-curve for cable length of 0.4 km.*

(e) *PV-curve for cable length of 0.8 km.*

(f) *PV-curve for cable length of 1.6 km.*

Figure 32: *PV-curves from Fig. 31. The vertical lines represent the maximum 'measured' power for each installed power; 100 kW, 200 kW, 400 kW, 600 kW and 800 kW from left to right.*

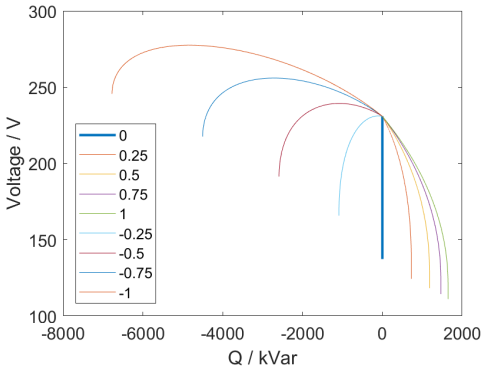

(a) *QV-curve for cable length of 0.02 km.*

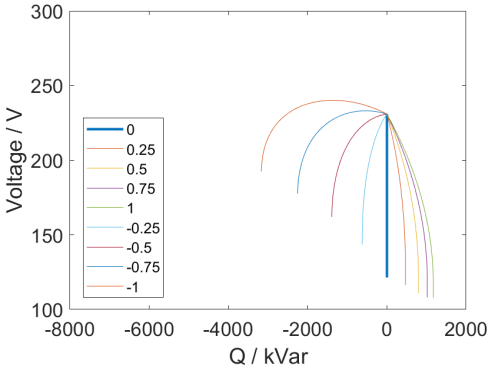

(b) *QV-curve for cable length of 0.1 km.*

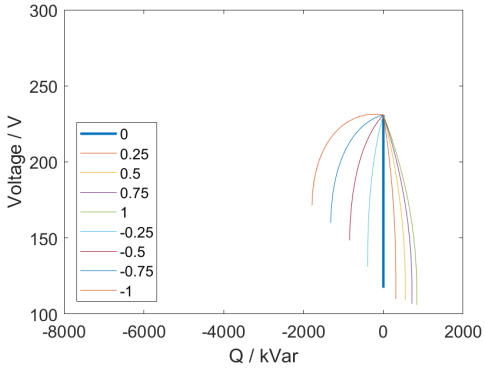

(c) *QV-curve for cable length of 0.2 km.*

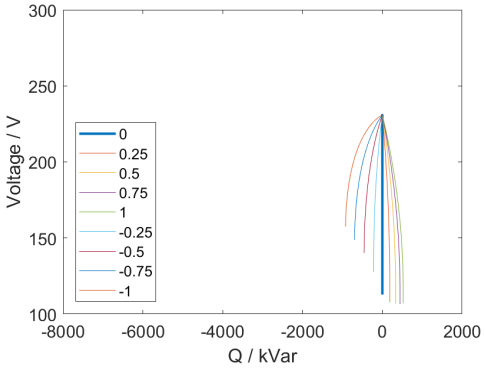

(d) *QV-curve for cable length of 0.4 km.*

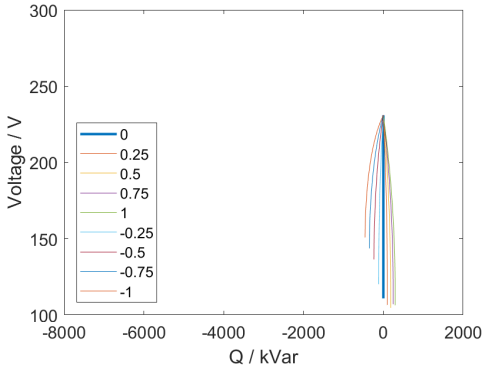

(e) *QV-curve for cable length of 0.8 km.*

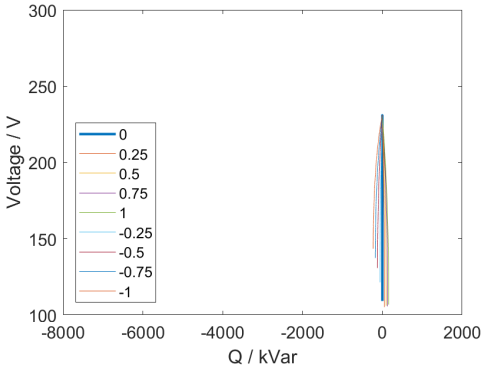

(f) *QV-curve for cable length of 1.6 km.*

Figure 33: *PQV-curves for the investigated cable lengths. PV-curves are plotted for tan ϕ = 0, 0.25, 0.5, 0.75, 1 , -0.25, -0.5, -0.75 and -1 for lengths 0.02, 0.1, 0.2, 0.4, 0.8 and 1.6 km.*

6.2. Control strategies - Q(P)

PF control

For this strategy a constant PF of 0.9 ($\tan(\phi) \approx 0.5$) was chosen with a negative sign when active power is positive and vice versa. Thus the reactive power input will be the same for each cable length, but vary with installed power since it only depends on active power input. This control was tested for to evaluate if the suggested PQ-operation minimum requirements from Energinet.dk (in Fig. 9) would be enough to adjust the voltage. The line to neutral voltage for the original simulation and with the PF control strategy applied are seen for cases 10 and 20 respectively in Fig. 34. Here, improvements for the voltage are seen for case 10, whereas there are slight improvements for case 20 however, clearly not enough. The results are summarized in Fig. 36. As predicted, it is here seen that this control strategy does not provide enough reactive power to adjust the voltage for the longer cable lengths, but does make a change for cases 15 and 18 which with this control strategy becomes green (Fig. 36).

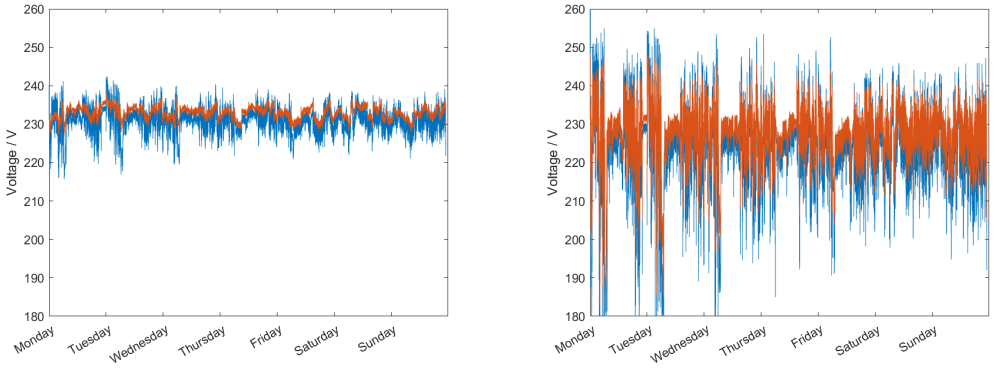

(a) *Results for case 10.* (b) *Results for case 20*

Figure 34: *Results for case 10 and 20 for the PF control strategy, where the blue line represents the line to neutral voltage for week 3 for the original simulation and the red line represents the line to neutral voltage with the PF control strategy applied.*

	$P_{installed}$ = 100 kW	$P_{installed}$ = 200 kW	$P_{installed}$ = 400 kW	$P_{installed}$ = 600 kW	$P_{installed}$ = 800 kW
Q max (Var)	15 983	49 256	115 800	182 350	248 890
Q min (Var)	- 81 657	- 122 190	- 203 270	- 285 220	- 372 690

Figure 35: *Results for the reactive power - minimum and maximum reactive power during a week for each installed power respectively (and valid for all cable lengths).*

In Fig. 35 the maximum respective the total amount of reactive power compensation can be seen. The values are for all cable lengths, since this strategy only depends on active power input.

	$P_{installed}$ = 100 kW	$P_{installed}$ = 200 kW	$P_{installed}$ = 400 kW	$P_{installed}$ = 600 kW	$P_{installed}$ = 800 kW
Length= 0.02 km	Case 1	Case 2	Case 3	Case 4	Case 5
Length= 0.1 km	Case 6	Case 7	Case 8	Case 9	Case 10
Length= 0.2 km	Case 11	Case 12	Case 13	Case 14	Case15
Length= 0.4 km	Case 16	Case 17	Case 18	Case 19	Case 20
Length= 0.8 km	Case 21	Case 22	Case 23	Case 24	Case 25
Length= 1.6 km	Case 26	Case 27	Case 28	Case 29	Case 30

Figure 36: *Results for PF control strategy. where green represents cases where voltage are kept within the limits (207 - 253 V), red represents the cases that violate the voltage limits and black represents cases that could not be simulated.*

Proportional Q(P) control
For this method eq. 9 in chapter 5 suggests a proportional reactive power input of approximately k=R/X, as this could 'even out' the resistance and the reactance of the system and increase the loadability of the cable. In Table 5 below the impedance for each cable length together with the corresponding R/X is shown. Looking at Fig. 31 the most suitable k could be approximated through determining for which tan(ϕ) that the voltage is kept within the limits when the active power increases from zero to the maximum load. Here, the maximum load from the FF building is approximately 90 kW and with the addition of the EV load the total maximum with the measured values from week 3 can be found in Table 4. For each cable length the maximum load of the highest installed power (800 kW) was utilized when approximating most suitable tan(ϕ) from Fig. 32. The maximum tan(ϕ) that could be analyzed from the figures was ± 1 and thus for cable lengths 0.4 km, 0.8 km and 1.6 km the reactive power compensation will not be enough (see Table. 5 for maximum active power limits). Since, the tan(ϕ) was approximated through a visual inspection the R/X values are probably more suitable as k-values for the Q(P) control and thus set accordingly. For cable lengths 0.4 km, 0.8 km and 1.6 km a higher tan(ϕ) than ± 1 might not be enough to increase the maximum active power further, but was tested for to evaluate the option.

Cable length	Z_1 (magnitude in ohms, angle)	R/X	tan(ϕ)
0.02 km	0.020, 73°	0.31	-0.25
0.1 km	0.034, 49°	0.87	-0.75
0.2 km	0.054, 38°	1.3	-1
0.4 km	0.098, 30°	1.7	-1*
0.8 km	0.19, 26°	2.1	-1*
1.6 km	0.36, 23°	2.4	-1*

Table 5: *Impedances Z_1 for each cable length respectively, together with the corresponding R/X ratio and approximated most suitable tan(ϕ).*
** For this tan(ϕ) the voltage limits are violated (see Table 3 and 4).*

The results for the line to neutral voltage for case 10 and 20 are seen in Fig. 37. Here, it is seen that the voltage profile for case 10 is improved. The voltage profile is also improved for case 20, but here voltage violations still occur. It should however be noted that the voltage violations only occur during the first 4 minutes of the simulation, but to be conservative this is marked red in the results. The results for all cases are summarized in Fig. 38. Here, case 15, 18, 19, 21 and 22 has become green as predicted by the analysis in 6.1.1. While the results became better for the mentioned cases it became worse for case 23. This is further discussed in the following section.

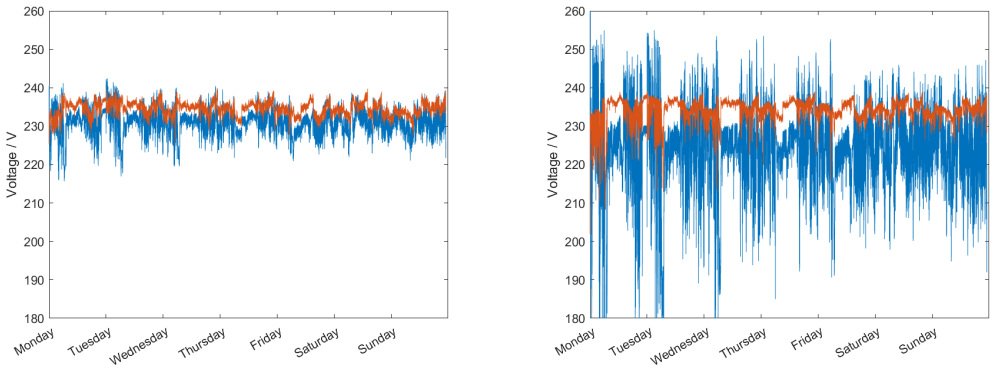

(a) *Results for case 10.*

(b) *Results for case 20*

Figure 37: *Results for case 10 and 20 for the proportional Q(P) control strategy, where the blue line represents the line to neutral voltage for week 3 for the original simulation and the red line represents the line to neutral voltage with the PF control strategy applied.*

	$P_{installed}$ = 100 kW	$P_{installed}$ = 200 kW	$P_{installed}$ = 400 kW	$P_{installed}$ = 600 kW	$P_{installed}$ = 800 kW
Length= 0.02 km	Case 1	Case 2	Case 3	Case 4	Case 5
Length= 0.1 km	Case 6	Case 7	Case 8	Case 9	Case 10
Length= 0.2 km	Case 11	Case 12	Case 13	Case 14	Case15
Length= 0.4 km	Case 16	Case 17	Case 18	Case 19	Case 20
Length= 0.8 km	Case 21	Case 22	Case 23	Case 24	Case 25
Length= 1.6 km	Case 26	Case 27	Case 28	Case 29	Case 30

Figure 38: *Results for the proportional Q(P) control strategy, where green represents cases where voltage are kept within the limits (207 - 253 V), red represents the cases that violate the voltage limits and black represents cases that could not be simulated.*

6.2.1. System limitations

For the control strategies in this section the only variable that is added to the system compared to the simulation cases is controlled reactive power (Q_C). Adding reactive power with the right sign (positive or negative) should improve the voltage conditions. However, when adding more reactive power to case 23 the system situation became worse. This section will explain why this happens.

Fig. 39 represents a circuit model for the Q controller. Looking at this circuit it can be inferred that for very high reactive power inputs the apparent power will be high and thus also the current. With a high Z_1 and increasing current the ΔV will increase as well, leaving a small range within the V_2 could vary according to Kirchhoffs voltage law. Thus, for high $\tan(\phi)$ the reactive power input might decrease V_2 instead of increasing V_2. In Fig. 40 the voltage phasors for V_1, V_2 and ΔV representing the same load in active power (835 kW) for cable length 0.8 km can be seen. With $\tan(\phi)$=0 the magnitude of the voltage is 160 V. Increasing the $\tan(\phi)$ to -1 also increases the voltage to 188 V. However, increasing $\tan(\phi)$ further to -2 decreases the voltage to 182 V. It is also seen that ΔV for $\tan(\phi)$=-2 is larger than for $\tan(\phi)$=-1, which ascertains the theory of that a higher Q_C will decrease V_2 because of an increased ΔV. It appears that a limit has been reached for the system for which the addition of reactive power does not increase the voltage, but decreases the voltage instead. For cable length 0.8 km $\tan(\phi)$ is set to -2.1 which would explain why the condition for case 23 became worse.

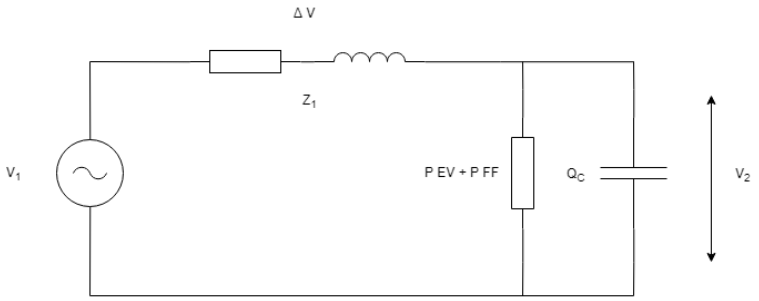

Figure 39: *Circuit model for the reactive power controller, where V_1 is the source voltage, V_2 is the voltage at the load, Z_1 is the system impedance (transformers, cables etc.), ΔV is the voltage drop over Z_1 and Q_C is the reactive power input from the controller.*

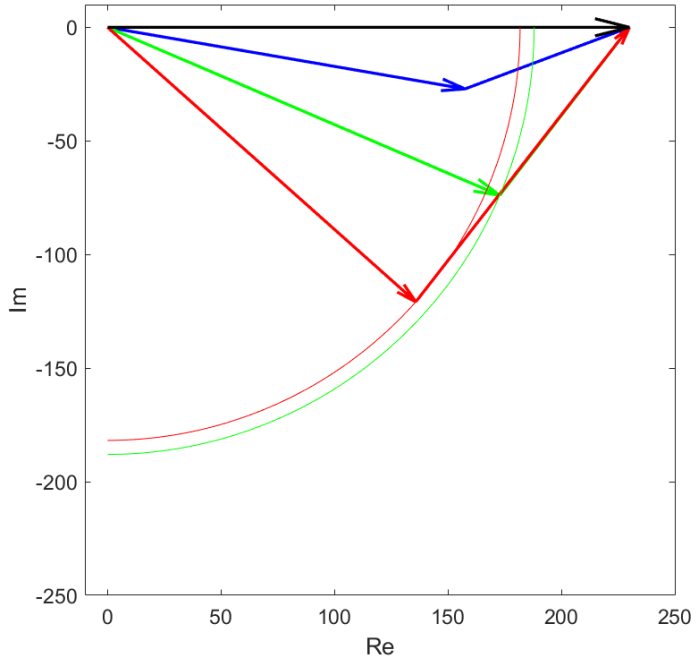

Figure 40: *Complex voltages for cable length 0.8 km where the black line represents V_1 and the blue line represents V_2 and ΔV for tan(ϕ)=0 according to Fig. 39 for maximum power. The green phasors represent V_2 and ΔV for tan(ϕ)=-1 and the red phasors represent V_2 and ΔV for tan(ϕ)=-2. All phasors are for the same active power level, 835 kW. The magnitude for V_2 is 160 V, 188 V and 182 V respectively.*

Additionally, another aspect is that increasing the reactive power input will increase the apparent power. Increasing the length of the cables and thereby increasing the impedance of the electrical system will decrease the short circuit capacity. At the 'tip' of the PV-curve, where Z_1 equals the reactance of the system and tan(ϕ)=0 this corresponds to $S_{SC}/2$. Thus, after $S_{SC}/2$ the system would exceed the system limitations. Thus the blackouts for case 23-25 and 27-30 could be further

realized through Fig. 41 and 42. The apparent power with the proportional Q(P) controller for case 21-25 is found in Fig. 41. Here, it is seen that case 23 would exceed the short circuit capacity and thus would cause the system to blackout. In Fig. 42 the apparent power for case 26-30 with the proportional Q(P) controller is visualized. From these graphs it is seen that case 27-30 would exceed the short circuit capacity and thus they are neither possible to simulate nor possible solutions for the voltage limit problem.

It can thus be concluded that the 'red' and 'black' cases in Fig. 38 cannot be solved through reactive power compensation. Therefore, different strategies are required such as changing the cable or adding another transformer.

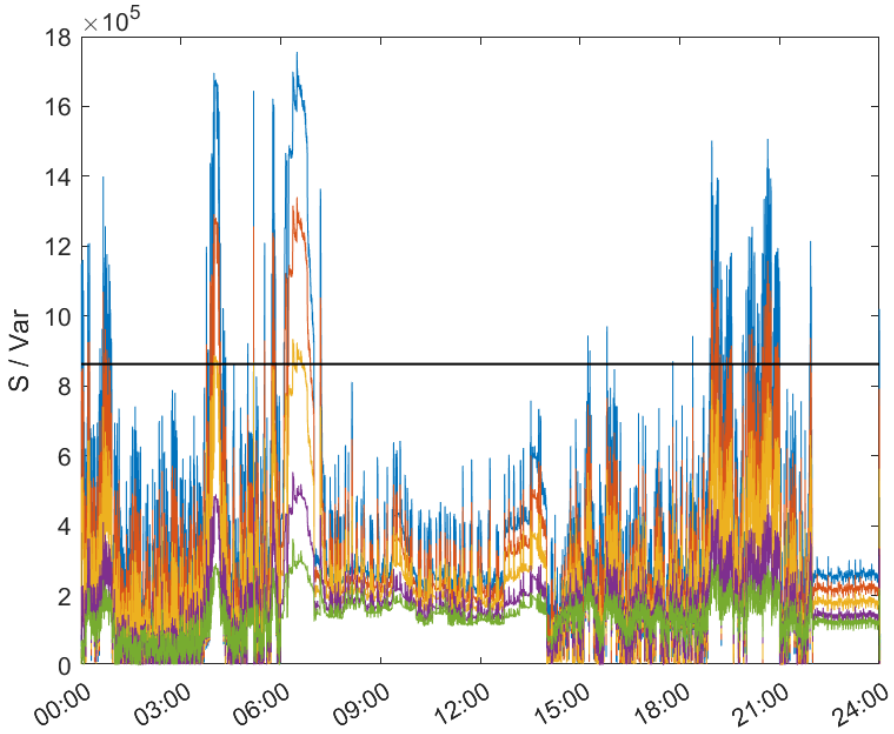

Figure 41: *Here the apparent power (S) for the day with the most critical hour (Monday) is plotted for the proportional Q(P) control for cable length 0.8 km. In the apparent power the active and reactive power from the simulated cases are included as well as the added reactive power (Q_C). The horizontal black line represents the short circuit capacity for the evaluated cable length. Green - installed P=100 kW (case 21), purple - installed P=200 kW (case 22), yellow - installed P=400 kW (case 23), red - installed P=600 kW (case 24), blue - installed P=800 kW (case 25).*

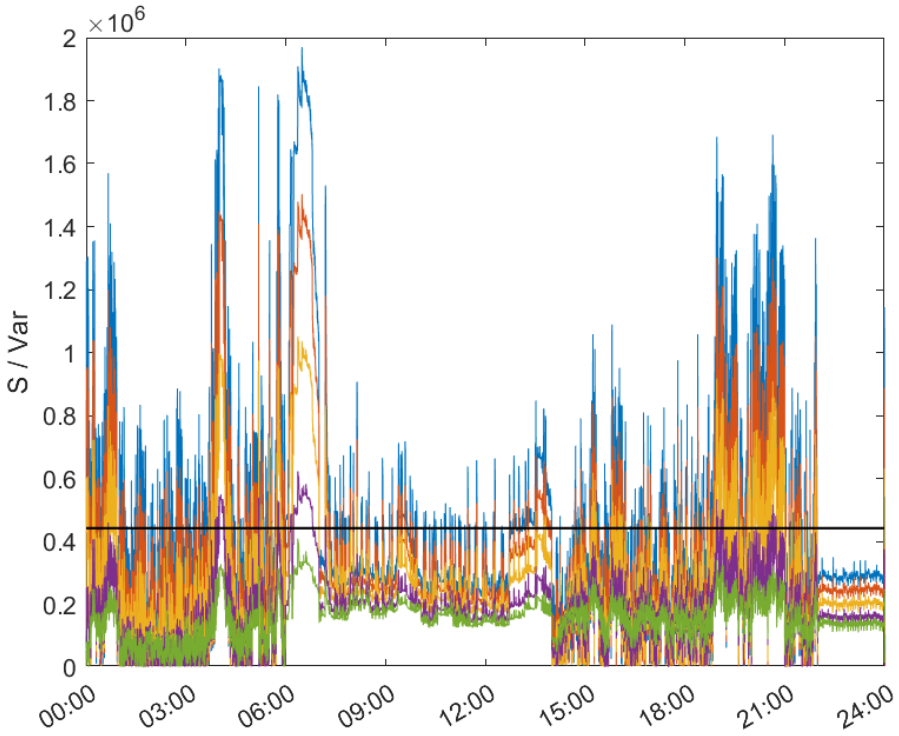

Figure 42: *Here the apparent power (S) for the day with the most critical hour (Monday) is plotted for the proportional Q(P) control for cable length 1.6 km. In the apparent power the active and reactive power from the simulated cases are included as well as the added reactive power (Q_C). The horizontal black line represents the short circuit capacity for the evaluated cable length. Green - installed P=100 kW (case 26), purple - installed P=200 kW (case 27), yellow - installed P=400 kW (case 28), red - installed P=600 kW (case 29), blue - installed P=800 kW (case 30).*

6.3. Load profile analysis

This section presents a load profile analysis for the simulated scenarios. Initially, it compares the FF load with and without EV feeder load for the different scenarios and thereafter it compares the load profile for a transformer with and without adding FCR providing EVs to the system. As there are five different levels of installed power these will be analyzed. This means that the analysis is valid for each column in Fig. 30 that represent each installed power respectively.

In Fig. 43 to Fig. 47 below the FF load curve with and with out EV feeder load for the different installed power levels are presented respectively. Here, it can be noted that the frequency regulation gives the load profile an unusual shape even for lower the lower installed power levels. As predicted in chapter 4, the EV charging deadline at 7 am leads to a peak load in the morning. For installed power of 400 kW and higher (Fig. 45 to 47) the EV load profile appears to be dominating the profile behavior as it contributes to the majority of the load and the FF load is almost not noticeable. Additionally, for the highest installed power level (800 kW), the highest active power is around 700 - 800 kW which is not exceeding the transformer limit (1000 kVA) but might limit the range in which other feeders could vary in active power as well as the reactive power.

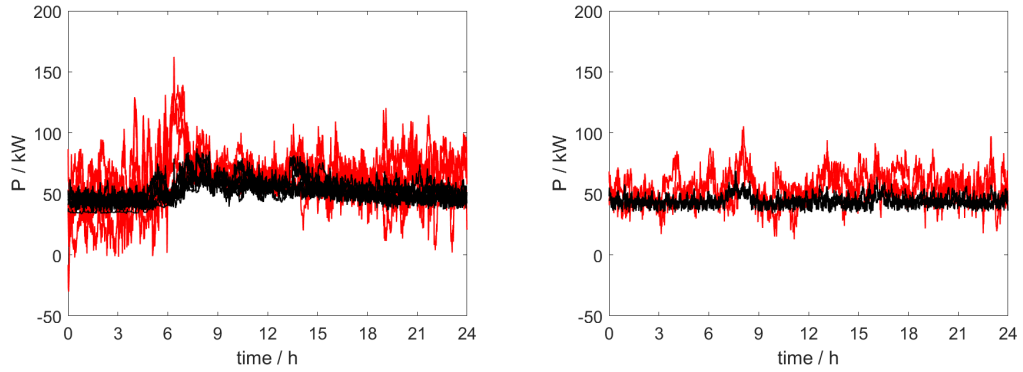

(a) *Results for weekdays (January 8th to 12th 2018).*

(b) *Results for weekend (January 13th to 14th 2018).*

Figure 43: *Load profiles for the FF load excluding EV feeder load (black) and FF load including EV feeder load with 100 kW installed power (red).*

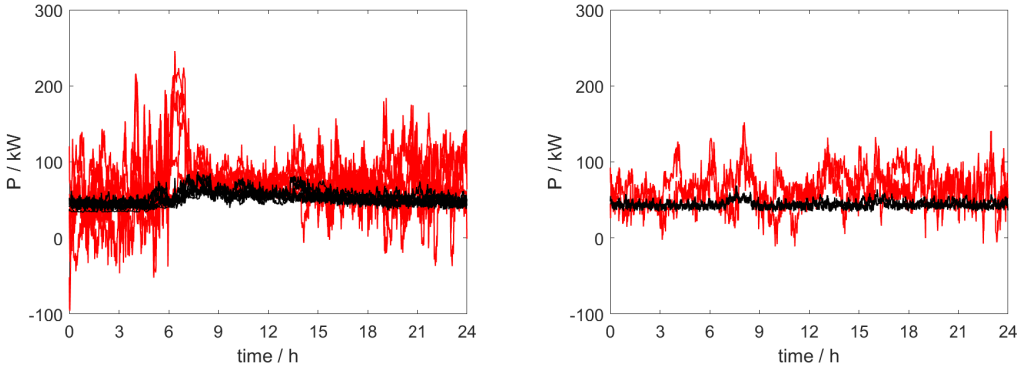

(a) *Results for weekdays (January 8th to 12th 2018).*

(b) *Results for weekend (January 13th to 14th 2018).*

Figure 44: *Load profiles for the FF load excluding EV feeder load (black) and FF load including EV feeder load with 200 kW installed power (red).*

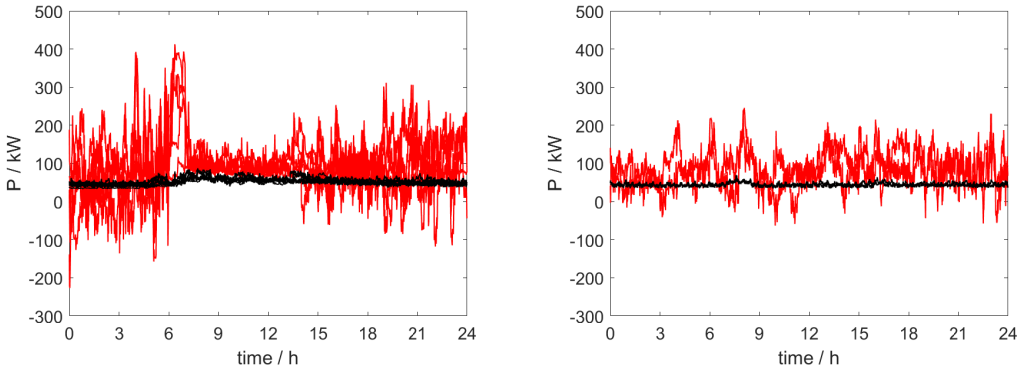

(a) *Results for weekdays (January 8th to 12th 2018).*

(b) *Results for weekend (January 13th to 14th 2018).*

Figure 45: *Load profiles for the FF load excluding EV feeder load (black) and FF load including EV feeder load with 400 kW installed power (red).*

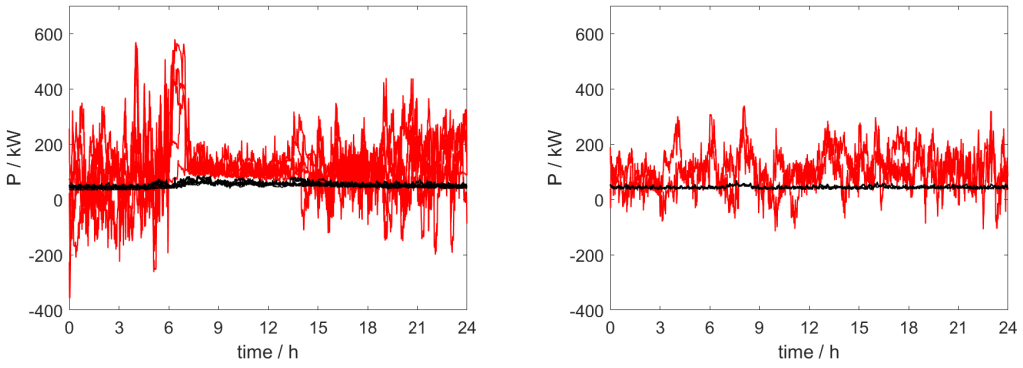

(a) *Results for weekdays (January 8th to 12th 2018).*

(b) *Results for weekend (January 13th to 14th 2018).*

Figure 46: *Load profiles for the FF load excluding EV feeder load (black) and FF load including EV feeder load with 600 kW installed power (red).*

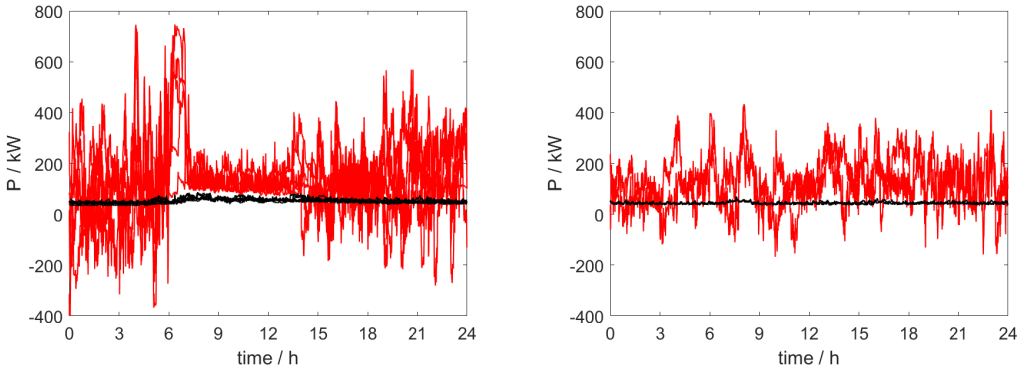

(a) *Results for weekdays (January 8th to 12th 2018).*

(b) *Results for weekend (January 13th to 14th 2018).*

Figure 47: *Load profiles for the FF load excluding EV feeder load (black) and FF load including EV feeder load with 800 kW installed power (red).*

An interesting aspect when it comes to performing FCR with EVs is whether this will affect the peak load for the transformers in the system or not. The data for the transformer in the studied system, in which the FF building is situated, is not available and thus the data from a transformer at Bornholm is analyzed instead. This transformer is rated 60/10 kV 10 MVA and is thereby 10 times larger than the transformer closest to FF, which is 1 MVA. When comparing the EV load with the transformer load the transformer data was scaled down by a factor of 0.1 (divided by 10) to represent the size of the transformer in the FF system. The data from the Bornholm transformer are from the first week of the year, January 1st to 7th 2013 (Tuesday to Monday). Since January 1st 2013, a Tuesday, was a holiday it is not comparable to the load profile of Tuesday, January 9th 2018, and hence the Tuesday load profiles were excluded from the analysis. Additionally, only apparent power values were available per minute and thus the apparent power for FF was computed and averaged per minute. (The feeder loads for the transformer can be seen in Appendix D.). The transformer load with and without the EV feeder load for weekdays and weekends respectively are seen in Fig. 48 to 52. In Fig. 48 and 49 representing the installed powers of 100 kW and 200 kW at the EV feeder it is seen that the overall shape of the load profile for the transformer does not change considerably.

In Fig. 50 to 52 power profiles representing installed powers of 400 kW, 600 kW and 800 kW are shown below. Here, it can be seen that the EV feeder load changes the shape of the load profile for the transformer. It is realized that two major problems occur - a peak load is added in the morning and the peak load in the afternoon becomes even higher and wider. Additionally, at non-peak-hours the system occasionally reaches loads larger than the original peak. The lastly mentioned change is especially noticeable for weekend days. Comparing the EV feeder load to this specific transformer it appears as if especially the morning peak load would be severely exceeded for 400 kW installed power and higher. This is of course dependent on the analyzed case and transformer. For 600 kW the morning peak reaches values of approximately 1000 kVA which is the limit for the transformer and thermal limits might be exceeded. For 800 kW installed power the maximum load has more than doubled compared to the transformer load without EVs and additionally, the peak exceeds the maximum capacity for the transformer. For this installed power level the thermal limits would probably be exceeded.

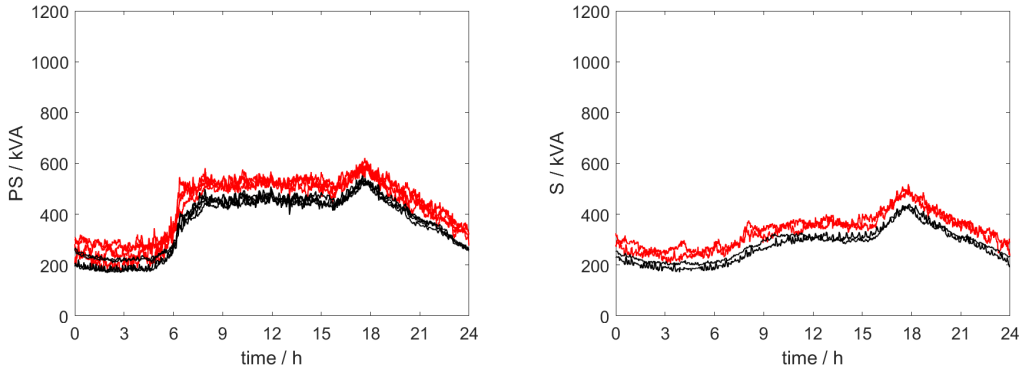

(a) *Results for weekdays (January 8th, 10th to 12th 2018 and January 7th, 2nd to 4th 2013).*

(b) *Results for weekend days (January 13th to 14th 2018 and January 5th to 6th 2013).*

Figure 48: *Load profiles for the transformer excluding EV feeder load (black) and the transformer including EV feeder load with 100 kW installed power (red).*

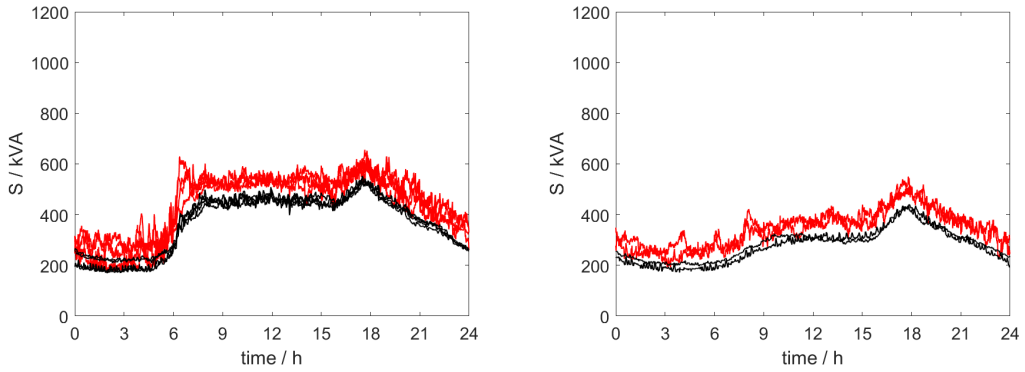

(a) *Results for weekdays (January 8th, 10th to 12th 2018 and January 7th, 2nd to 4th 2013).*

(b) *Results for weekend days (January 13th to 14th 2018 and January 5th to 6th 2013).*

Figure 49: *Load profiles for the transformer excluding EV feeder load (black) and the transformer including EV feeder load with 200 kW installed power (red).*

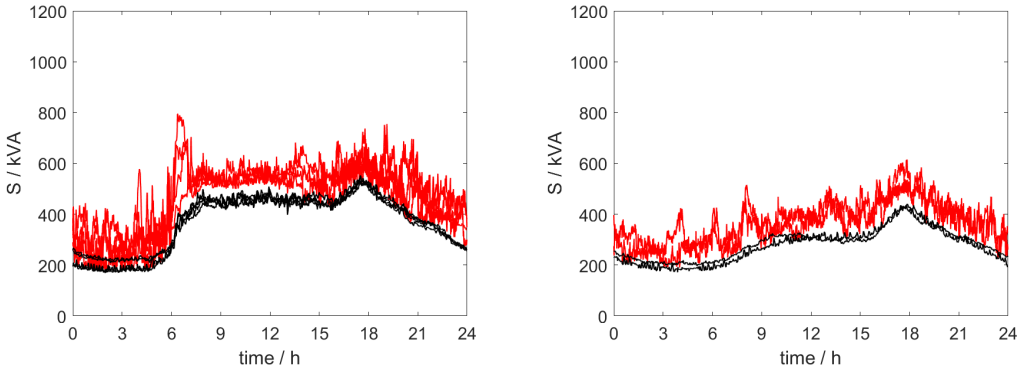

(a) *Results for weekdays (January 8th, 10th to 12th 2018 and January 7th, 2nd to 4th 2013).*

(b) *Results for weekend days (January 13th to 14th 2018 and January 5th to 6th 2013).*

Figure 50: *Load profiles for the transformer excluding EV feeder load (black) and the transformer including EV feeder load with 400 kW installed power (red).*

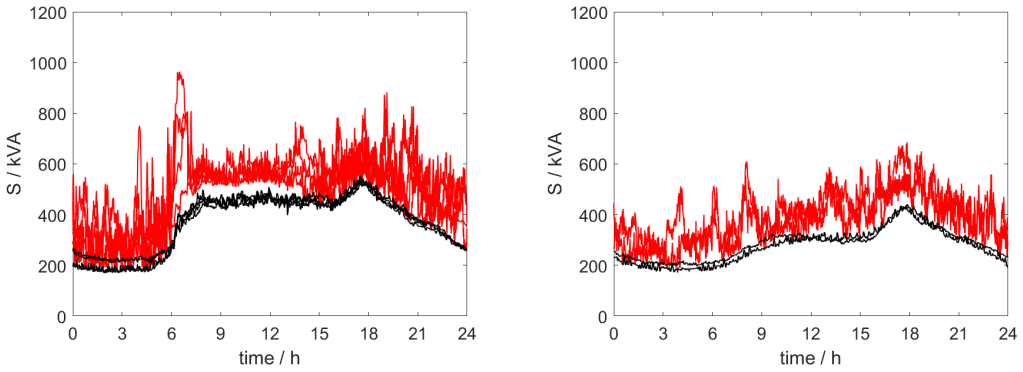

(a) *Results for weekdays (January 8th, 10th to 12th 2018 and January 7th, 2nd to 4th 2013).*

(b) *Results for weekend days (January 13th to 14th 2018 and January 5th to 6th 2013)*

Figure 51: *Load profiles for the transformer excluding EV feeder load (black) and the transformer including EV feeder load with 600 kW installed power (red).*

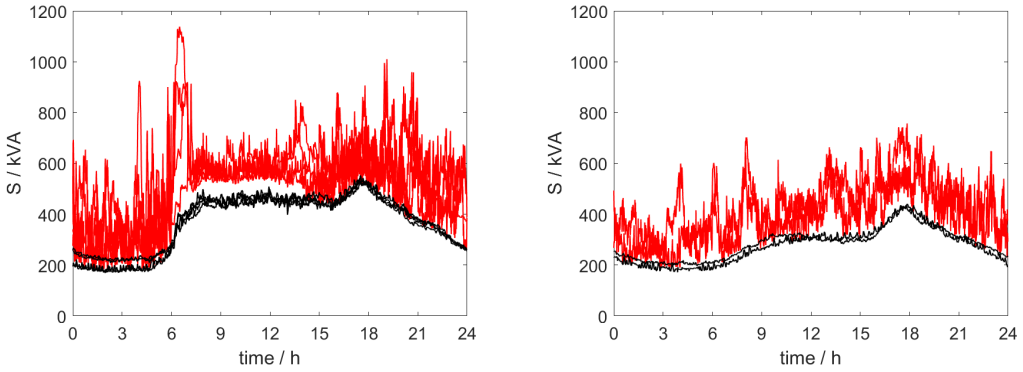

(a) *Results for weekdays (January 8th, 10th to 12th 2018 and January 7th, 2nd to 4th 2013).*

(b) *Results for weekend days (January 13th to 14th 2018 and January 5th to 6th 2013)*

Figure 52: *Load profiles for the transformer excluding EV feeder load (black) and the transformer including EV feeder load with 800 kW installed power (red).*

As previously stated, it is seen that the EV feeder load leads to a morning peak load at around 6 pm (18.00) and an afternoon peak at around 4 to 8 pm (16.00 to 20.00), where the morning peak is higher than the afternoon peak. During the morning peak the EVs change their mode from 'FCR provision' to 'charging' at the same time as the activity in the building starts. For the afternoon peak, where the peak is especially high for the transformer, residential load for the transformer is probably high and at the same time the EVs are performing FCR in both direction, i.e. both upregulation and downregulation. The downregulation adds power to the peak load since this means that the EVs are charging active power. This would add stress to a system that already is stressed due to the high load at this time. If performing downregulating FCR at peak load hours this could have a thermal impact as high load leads to higher current and thus higher temperatures in the cables and transformers. For the FF system there are probably less residential areas around which might ease the stress of the afternoon peak, but crucial power levels would still occur for the morning peak for 600 kW and 800 kW of installed power. A strategy to avoid affecting the thermal impact as well as adding to the peak load could be to only perform upregulating FCR at peak load hours, i.e. discharging the EVs. Often the EVs still have power left in their battery when they return to FF in the afternoon and this could thus be a possible strategy for decreasing both thermal impact and peak load.

7. Discussion

This chapter presents a discussion on the performed work in this thesis. Mainly, it focuses on load profiles, the simulations, control strategies and system limitations in the respective order. Together with the previous chapter it aims to answer the questions as stated in the objectives: 'If and when will there be issues for the grid operation?', 'Can reactive power compensation be utilized to minimize grid impact?'.

Frederiksberg Forsyning and their EV fleet is clearly an interesting case, being one of the first commercial EV fleets providing frequency control regulation. This allows for real data analysis on FCR provided by EVs such as the study performed in this thesis, which is lacking in the currently available literature as seen in chapter 2. The following sections will discuss the FCR provision through EVs and within which frames, set by the electrical system limitations, that the technology is applicable.

7.1. Load profiles

In the load curve analysis in chapter 6 the following impacts on the FF load profile were noted:

- The frequency regulation is clearly noticeable in the load profile shape at all power levels.
- A morning peak is added around 7 am, as the charging deadline for the EVs occurs at the same time as the workday activities in the building starts.
- For installed power levels of 400 kW and higher, the EV load profile is dominating and the FF load profile is barely noticeable.
- The active power alone does not reach the capacity limit of the transformer (1000 kVA).

Additionally the following impacts on the transformer load profile in Bornholm were observed:

- Installed power levels of 400 kW and higher, changes the shape of the transformer load profile.
- The highest peak load occur in the morning around 7 am for 400 kW and higher.
- The afternoon peak load increases and becomes wider.
- Higher loads outside peak hours are observed, especially during weekends.
- For 600 kW installed EV power the morning peak reaches values around 1000 kVA, which is the rated capacity of the transformer.
- For 800 kW installed EV power the morning peak exceeds the rated capacity of the transformer, and the afternoon peak reaches values around rated capacity (1000 kVA).

The observed impacts that occur around 400 kW installed EV power is that the peak loads are noticeably changed. Generally, this might have an impact of the total installed power required in the grid if the technology is heavily adopted, since the installed power required in a grid is determined by the peak load. The observed impacts that occur at 600 kW installed power and higher

will probably lead to stressed thermal conditions and exceeded thermal limits for 800 kW and higher.

There are however different solutions that could be implemented to solve the aforementioned problems. The morning peak could be avoided, or at least decreased, through not scheduling the EVs to all charge at the same time. When the installed capacity of EVs increases and all EVs are scheduled to charge to 'full tank' at the exact same time this will of course result in an added peak to the system. If this technology would be heavily adopted in a region this type of charging scheduling will not be sustainable. If instead charging the cars to full load at different times the peak could be decreased. However, the initial idea for performing FCR through EVs is to utilize the energy source in an optimal way to minimize the time that the available energy source is being underutilized. After charging to 'full tank' in the morning the EV will not preform FCR as the EV user would like the EV charged to the set SOC in the morning. Thus, the time that the EVs could perform FCR would decrease, leaving the energy storage underutilized. Thus, in the future, the problems concerning the morning peak needs to be balanced against the problems regarding underutilized energy sources. Possibly, the morning peak problem could partly be solved through only providing downregulating FCR, i.e. charging the EVs in the morning. The aspects of optimized charging scheduling and downregulating FCR in the morning requires further research.

It was also recognized that the peak load in the afternoon was increased. This occurs due to the fact that the EVs are performing FCR at the same time as the 'original' peak load of the transformer. If increasing the peak load would be a problem for the grid operation, this could be solved either through not performing FCR during peak hours or through only performing upregulating FCR. In fact, the latter could even decrease the peak load as active power would be injected to the grid. With this solution strategy, it could be of general concern that the battery would be empty in the afternoon when the driver might need the vehicle later. For FF this should however not be a problem since the cars are for the utility Frederiksberg Forsyning and not used outside working hours. The EVs at FF often have energy left in their batteries when returning to FF in the afternoon and this could be a realistic and possible solution. If private EV users would make their vehicles available for FCR provision in the future, discharging the battery in the afternoon is probably of major concern. Thus, further research concerning private users is required.

7.2. Simulation, control strategies and system limitations

Simulation
In chapter 6 several scenarios were simulated to test for the limitations of the studied system. It was seen that with the cables and transformers that are utilized today it would be possible to increase the installed power to 800 kW and the length of the cable could be extended to 0.1 km without any violation of the voltage limits. If extended to 0.2 km voltage violations occur at 800 kW, but it should be noted that this is only for two short time periods for case 15 as seen in the voltage profiles in Appendix B. For cable lengths 0.4 km and longer voltage stability issues are noticeable for 400 kW installed power and higher. Studying the electrical system limitations in chapter 6 the system becomes unstable at cable length 0.8 km with 400 kW and 1.6 km with 200 kW or higher. Thus, these are the absolute limitations of the current system and of course limitations should be set more conservative. This means that in Denmark, where the voltage limitations are ±10 % of 230 V, the voltage should be kept well within this range and in other countries such as Sweden, where the voltage limits are ±3-5 %, this limits the possible variations of installed power and cable lengths further.

Comparing the results from the simulated scenarios and the corresponding load profile analysis for the studied system, if both voltage stability and thermal impacts should be taken into account,

the installed power should not be higher than 200 kW and the cable length should not be longer than 0.2 km. With these values it should not be necessary with a reactive power compensation for voltage control nor to change cables or transformers. However, this installed power might require rescheduling of charging in the morning and changed settings for the FCR in the afternoon to only provide upregulating FCR. The latter is a possible strategy since most of the vehicles have energy left in their batteries when returning to FF in the afternoon. The vehicles occasionally return to FF during the day and are then connected to the chargers. Additionally, it appears that the vehicles might not need the the whole capacity of the battery for the workday.

Q(P) Control
With a Q(P) controller with a PF set to ± 0.9 the voltage profiles are improved for cases with cable lengths up to 0.2 km. For cable length 0.4 the voltage profiles up to 400 kW are improved. However for other cases the reactive power input for this control strategy is not enough. Thus, the minimum PF set by Energinet.dk in their battery plant regulations will not be enough for the studied system with cable lengths of 0.4 km or longer. With an increased reactive power input in the proportional Q(P) controller all variations for the cases up to 0.4 km cable length and 600 kW installed power is possible. Even installed power levels of 100 kW and 200 kW for cable length 0.8 km will manage a voltage profile within the set voltage limits. However, if increasing the cable length or installed power level further the system limitations will be violated.

In the analysis for the system limitations in chapter 6 it was realized that it would not be possible to design a voltage controller with reactive power power provision with respect to the electrical system limitations for case 23-25 as well as 27-30 (i.e. cable length of 0.8 km with 400 kW installed power or more and cable length of 1.6 km with 200 kW installed power or more). The analysis was conducted for a Q(P) controller but similar conclusions can be made for a Q(V) controller. However, the latter would probably require less reactive power input than the Q(P) controller if the voltage is within reasonable values around the voltage limits. If on the other hand the voltage is far outside the voltage limits, which is the case for the longer cable lengths, the Q(V) will try to increase the reactive power until a voltage within the allowed limits is achieved. As seen in the PQV-curves for the longer cable lengths increasing the reactive power does not increase the voltage and the reactive power input for a Q(V) controller for the longer cable lengths would probably reach unreasonably high values. In order to make these cases work changes in the electrical system are required that would decrease the impedance and increase the short circuit capacity. Such changes could be to change the cable to one with a larger cross section or to connect another transformer in parallel. In the studied system there is a 1600 kVA transformer available and it could therefore be possible to evaluate this solution. This solution would mainly aim to increase the possible power flows of the system as well as to lower the total impedance. To increase the impact of a reactive power controller the resistance in the cables needs to be decreased, which could be realized through connecting another cable in parallel. However, these solutions did not fit within the time frame for this thesis and could not be evaluated. If this this option would be evaluated it would also be highly recommended to analyze the implementation of a Q(V) controller as this would be more accurate and a practically possible solution since the voltage is already measured at bus 1.

The analysis regarding the need for power grid updates in the case of FCR performing EVs differs slightly from analyses associated with 'normal' charging of EVs. In [27] and [28] the authors suggested that the power grid would not require any severe changes with the predicted amount of EV integration. For 'normal' unidirectional charging the process can be optimized with respect to other conditions of the grid. Since power grids in many cases are overdimensioned (especially in Sweden) there is capacity available that could be utilized for different ancillary services, for example

FCR provided by EVs. Hence, if synchronous generators are taken away from the grid, power grid updates in terms of ancillary services might be avoided through utilizing the EVs. However, this needs to be done carefully to not violate the limits of the electrical system. On the other hand, if a grid, possibly a microgrid, would be operated with FCR provided only by EVs in the future the system would probably need to be upgraded with respect to the grid operation studied in this project. The thermal impacts, increased peak load and voltage stability issues could probably be minimized with optimized bidirectional charging (FCR provision) with respect to the electrical system limitations. However, this could probably be done only to a certain extent and the grid will require updates if this technology is heavily adapted, especially in areas that require longer cable lengths. The firstly mentioned optimization should of course be preferred in order to minimize the environmental impacts of the grid, but when this method has reached its limits the grid might require an upgrade. The aforementioned solution, involving the available transformer however, would probably not require any advanced optimization or investments in new power electronics.

Additionally, it should be mentioned that no economical aspects have been regarded when analyzing the different values of $\tan(\phi)$. Thus, the tested reactive power input signals might be too high to economically motivate the upgrading of power electronics that would be required.

7.3. Other aspects

In this thesis the EVs of a utility building have been analyzed. This means that the applicability of the analysis for private EVs is limited. Private users could be an especially interesting topic to analyze since the possibility to perform FCR through EVs would increase significantly, due to the large number of vehicles that the private users posses. In order for private users to make their EV available for FCR this would probably require more thorough analyses of the economical aspects of FCR and how this affects the lifetime of the battery. The private user might be more economically vulnerable than a company investing in this technology and this type of research would be crucial for further adaptation of the technology.

The economical aspects of the lifetime of the battery is also related to the environmental aspects - the longer you can utilize the battery the more sustainable it is - and frequently charging and discharging the battery presumably have impacts on the battery lifetime. Additionally, topics such as life cycle analysis, CO_2 payback time and optimal charging with respect to CO_2 emissions for the electricity in the grid would be interesting to see more research from. Research regarding second life batteries for EVs and whether these can be utilized for FCR would also be necessary and interesting.

Additionally, the EV fleet only consists of 10 cars which somewhat limits the variety of for example different user behaviors. As the current EV feeder load is upscaled for the analyzed future scenarios the limited selection could have an impact on the load curve analysis if the behavior would look different with different drivers. Furthermore, different drivers could thus change the appearance of the peak loads. Since, the data for the 10 EVs was available for analysis today it is for future studies to analyze data from a larger variety of EVs and their users. Hopefully, this work could contribute to increase the number of FCR performing EVs leading to more data to analyze.

8. Conclusion

This chapter presents the conclusions from the work in this thesis.

This thesis presents data from one of the world's first commercial EV fleet providing frequency control regulation. An analysis of the data was conducted to evaluate the impacts on the grid from the FCR performing EV fleet. Furthermore, the studied system was modeled in Matlab Simulink through which different scenarios were modeled to evaluate grid impacts and system limitations. These scenarios were created through varying the cable length, to simulate weaker grids, and the installed power, to simulate higher penetration of EVs or increased charging capacity. Through the scenarios it was evaluated if the voltage could be controlled through reactive power compensation. In parallel the electrical system limitations were analyzed to find the limits of the studied case. Load profiles were evaluated in terms of thermal impacts as well as impacts on a transformer peak load.

Firstly, it can be concluded that there are no voltage limits violations or severe thermal impacts in the studied system today. However, the shape of the load profile for FF is affected, where the FCR provision is clearly noticeable. In the simulated scenarios, to account for the voltage limits and to not change the load profile severely, the cable length should not be longer than 0.2 km and an installed power should not be higher than 200 kW. However, if only looking at the voltage limits and the maximum capacity for the transformer cases with cables up to 0.2 km and installed power up to 600 kW, all cases are acceptable. Furthermore, the cable length is a crucial factor regarding the electrical system limitations and for 0.4 km or longer voltage limits violations occur for the majority of cases (Fig. 30). Similar voltage issues can be expected for a system with similar cables, transformers and load.

Through implementing a power factor controller (with PF=0.9) the voltage profiles could only be slightly improved. However, if implementing a proportional Q(P) controller (Q_C=- R/X P) improvements for all cases up to 0.4 km cable length and 600 kW installed power are observed, as they managed to keep the voltage within the limits (V=±10% V_{nom}). For the scenarios with cable length 0.8 km and 400 kW or more, and 1.6 km with 200 kW or more installed power, there is no solution to the power flow problem. For the mentioned cases the grid impacts cannot be minimized through reactive power compensation. If cable lengths and installed power of these values are required, the transformer and cables need to be upgraded.

From the load profile analysis it was realized that when the installed power increased a peak appeared in the morning, due to that all vehicles are scheduled to have the battery fully charged at 7 am in the morning. At 400 kW installed power this peak became larger than the initial afternoon peak load and for 600 kW the peak reached values of the rated capacity for the transformer, whereas the capacity was exceeded with 800 kW installed EV power.

From the performed analysis, utilizing the batteries in the EVs for FCR-N provision appears to be a promising candidate for the mentioned ancillary service. However, it should probably be utilized in such manner for which underutilized available grids are utilized to their potential capacity.

If the V2G technology would be implemented to that extend that grid upgrades are necessary, the costs of the grid updates needs to be weighted against the gains from the FCR-N provision. For such analysis it is important to take the whole life cycle of grid upgrades and EV batteries into account.

9. Future Work

This chapter discusses and suggests topics of future work.

In this thesis data from 10 EVs were available, of which all were utilized for utility service. Thus, no private EVs were analyzed nor taken into account for the analysis. Private EVs would presumably give very different results regarding the load profiles and thus affect the thermal impact and peak load analysis. If this V2G technology would be adopted by private users, who could possibly make economical earnings on providing FCR to the system operator, further analysis on private EVs performing FCR would be required to determine the grid impacts. Additionally, economical impacts (including environmental costs) for example in terms of battery life would be interesting for the private user. As aforementioned the analysis only involved 10 EVs which might have limited the variation of user behavior and thereby affected the result and as the technology becomes more adopted research involving a larger variety of EV user behaviors would be possible and could give more reliable results.

The analysis would only be applicable for a system with similar load, cables and transformer. If the system is too different from the studied case a new analysis would be required. However, the methodology could probably be applied. Furthermore, if a system would be comparable to the studied case and cables longer than 0.8 km and larger installed power levels are required, the transformer and cables would need to be upgraded. For such cases it could be beneficial to investigate a Q(V) controller as this might give a more accurately controlled voltage. Additionally, an economical analysis including environmental costs would be required to evaluate the gains of FCR with respect to the costs of transformers and cables.

Regarding how the V2G FCR technology affects the load curves it was seen that a peak load appeared in the morning and the afternoon peak became higher and longer. As previously mentioned, the morning peak could be avoided through 'smarter' scheduling in terms of charging to 'full tank' in the morning. Regarding the peaks created through providing FCR, these could be decreased through only providing upregulating frequency, i.e. discharging. This was however not the aim of this thesis to investigate optimal FCR provision and further research on this topic would be required.

Bibliography

[1] K. B. Roberts. Ud-developed V2G technology launches in Denmark. http://www.udel.edu/udaily/2016/august/vehicle-to-grid-denmark/. Accessed: 2018-04-01.

[2] M. Swierczynski, D. Ioan Stroe, A. Irina Stan, and R. Teodorescu. Primary frequency regulation with li-ion battery energy storage system: A case study for Denmark. pages 487–492. IEEE, 2013.

[3] K. Knezović, M. Marinelli, P. Bach Andersen, and C. Træholt. Concurrent provision of frequency regulation and overvoltage support by electric vehicles in a real Danish low voltage network. pages 1–7. IEEE, 2014.

[4] J. Tan and L. Wang. A game-theoretic framework for vehicle-to-grid frequency regulation considering smart charging mechanism. *IEEE Transactions on Smart Grid*, 8(5):2358–2369, 2017.

[5] E. Yao, V. W. S. Wong, and R. Schober. Robust frequency regulation capacity scheduling algorithm for electric vehicles. *IEEE Transactions on Smart Grid*, 8(2):984–997, 2017.

[6] C. Wu, H. Mohsenian-Rad, J. Huang, and J. Jatskevich. PEV-based combined frequency and voltage regulation for smart grid. pages 1–6. IEEE, 2012.

[7] Parker Project. http://parker-project.com/. Accessed: 2018-04-01.

[8] Technical regulation 3.3.1 for battery plants. Energinet.dk, 2017.

[9] D. M. Kammen A. Jacobson, A. D. Milman. Letting the (energy) gini out of the bottle: Lorentz curves of cumulative electricity consumption and gini coefficients as metrics of energy distribution and equity. *Elsevier*, 2004.

[10] L. Bergman. De svenska energimarknaderna. Statens Offentliga Utredningar, 2014. (in Swedish).

[11] European Union. EU transport policy. https://europa.eu/european-union/topics/transport_en. Accessed: 2018-04-01.

[12] SPBI branschfakta 2017. SPBI, 2017. (in Swedish).

[13] Energiläget. Statens Energimyndighet, 2017. (in Swedish).

[14] Energistyrelsen. Dansk klimapolitik. https://ens.dk/ansvarsomraader/energi-klimapolitik/fakta-om-dansk-energi-klimapolitik/dansk-klimapolitik. Accessed: 2018-04-01.

[15] M. S. Sarma J. D. Glover, T. J. Overbye. *Power System Analysis & Design*. Cengage Learning, sixth edition, si edition, 2017.

[16] M. Alaküla, L. Gertmar, and O. Samuelsson. *Elenergiteknik*. Industriell Elekroteknik och Automation, Lunds Tekniska Högskola, 2013. (in Swedish).

[17] National report Denmark status for 2016. Danish Energy Regulatory Authory, 2016.

[18] K. Gerasimov, K. Gerasimov, and N. Nikolaev. Advanced tools for stability improvement of interconnected electric power systems. International Scientific Symposium 'Electrical Power Engineering 2014', 2014.

[19] Energinet.dk. `https://en.energinet.dk/Electricity/Rules-and-Regulations/Approval-as-supplier-of-ancillary-services---requirements`. Accessed: 2018-04-01.

[20] K. Knezović, M. Marinelli, Y. Perez, and P. Codani. Distribution grid services and flexibility provision by electric vehicles: a review of options. pages 1–6. Power Engineering Conference (UPEC), 2015 50th International Universities, 2015.

[21] Systemutvecklingsplan 2018–2027, mot ett flexibelt kraftsystem i en föränderlig omvärld. Svenska Kraftnät, November 2017. (in Swedish).

[22] O. Samuelsson. Voltage, electric power systems lecture 5. `http://iea.lth.se/eps/L5_17.pdf`, 2017. Accessed: 2018-04-01.

[23] Global EV outlook 2017. OECD/IEA, 2017.

[24] P. A. Gunkel. Optimized market participation of electric vehicles under uncertainties. Master's thesis, Technical University of Denmark, Department of Electrical Engineering, 2018.

[25] NUVVE. `http://nuvve.com/`. Accessed: 2018-04-01.

[26] J. Kristensson. Såska elnatet forsorja 5 miljoner elbilar. *Ny Teknik*, January 2018. (in Swedish).

[27] O. Ingvarsson. Hur dimensionerar vi framtidens elnät? Master's thesis, Lund University Faculty of Engineering, Division of Industrial Electrical Engineering and Automation, 2017. (in Swedish).

[28] A. Philipson and H. Lavin. Future network loading and tariffs with electric vehicles. Master's thesis, Lund University Faculty of Engineering, Division of Industrial Electrical Engineering and Automation, 2017.

[29] Willet kempton. `https://www.ceoe.udel.edu/our-people/profiles/willett`. Accessed:2018-04-01.

[30] K. B. Roberts. Ud-developed V2G technology to be used in California project. `http://www.udel.edu/udaily/2017/july/vehicle-to-grid-technology-california/s`. Accessed: 2018-04-01.

[31] Japan tests virtual power plants with potential capacity on unprecedented scales. `https://www.memoori.com/japan-tests-virtual-power-plants-potential-capacity-unprecedented-scales/`, December 2017. Accessed: 2018-04-01.

[32] S. Han, S. Han, and K. Sezaki. Development of an optimal vehicle-to-grid aggregator for frequency regulation. *IEEE Transactions on Smart Grid*, 1(1):65–72, 2010.

[33] L. S. Berthou. Optimized market participation of electric vehicles under uncertainties. Master's thesis, Technical University of Denmark, Department of Electrical Engineering, 2018.

[34] M. C. Kisacikoglu, M. Kesler, and L. M. Tolbert. Single-phase on-board bidirectional PEV charger for V2G reactive power operation. *IEEE Transactions on Smart Grid*, 6(2):767–775, 2015.

[35] G. Buja, M. Bertoluzzo, and C. Fontana. Reactive power compensation capabilities of V2G-enabled electric vehicles. *IEEE Transactions on Power Electronics*, 32(12):9447–9459, 2017.

[36] K. Knezovic, M. Marinelli, R. Juul Moller, P. Bach Andersen, C. Traholt, and F. Sossan. Analysis of voltage support by electric vehicles and photovoltaic in a real danish low voltage network. pages 1–6. IEEE, 2014.

[37] M. Kesler, M. C. Kisacikoglu, and L. M. Tolbert. Vehicle-to-grid reactive power operation using plug-in electric vehicle bidirectional offboard charger. *IEEE Transactions on Industrial Electronics*, 61(12):6778–6784, 2014.

[38] A. C. Melhorn, K. McKenna, A. Keane, D. Flynn, and A. Dimitrovski. Autonomous plug and play electric vehicle charging scenarios including reactive power provision: a probabilistic load flow analysis. *IET Generation Transmission & Distribution*, 11(3):768–775, 2017.

[39] N. Leemput, F. Geth, J. Van Roy, J. Büscher, and J. Driesen. Reactive power support in residential LV distribution grids through electric vehicle charging. *Sustainable Energy, Grids and Networks*, 3:24–35, Sep 2015.

[40] N. Zou, L. Qian, and H. Li. Auxiliary frequency and voltage regulation in microgrid via intelligent electric vehicle charging. pages 662–667. IEEE, 2014.

[41] M. Restrepo, J. Morris, M. Kazerani, and C. A. Canizares. Modeling and testing of a bidirectional smart charger for distribution system EV integration. *IEEE Transactions on Smart Grid*, 9(1):152–162, 2018.

[42] A. Rabiee, H. Feshki Farahani, M. Khalili, J. Aghaei, and K. M. Muttaqi. Integration of plug-in electric vehicles into microgrids as energy and reactive power providers in market environment. *IEEE Transactions on Industrial Informatics*, 12(4):1312–1320, 2016.

[43] X. Wu, L. Li, J. Zou, and G. Zhang. EV-based voltage regulation in line distribution grid. pages 1–6. IEEE, 2016.

[44] Frederiksbergs Forsyning. About Frederiksberg Forsyning A/S. `http://www.frb-forsyning.dk/Default.aspx?ID=2494`. Accessed: 2018-04-01.

[45] Automotive World. Nissan, Enel and Nuvve operate world's first fully commercial vehicle-to-grid hub in Denmark. `https://www.automotiveworld.com/news-releases/nissan-enel-nuvve-operate-worlds-first-fully-commercial-vehicle-grid-hub-denmark/`, August 2016. Accessed: 2018-04-01.

[46] C. W. Taylor. *Power System Voltage Stability*. McGraw-Hill, Inc., 1994.

Appendices

A. Voltage Analysis Data

The graphs and method presented here was utilized to extract data for the voltage analysis in 4.1.2. The EV feeder load plotted against the total FF feeder load can be seen in Fig. 53.

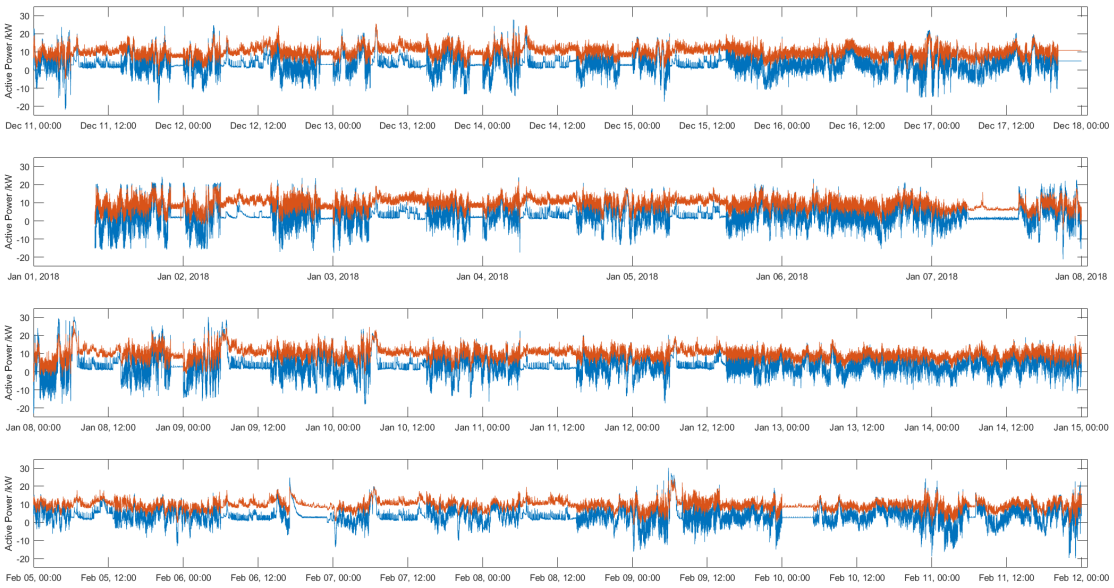

Figure 53: *Shows measured values of active power. Red line represents one out of 6 phases for entire FF feeder, blue represents one out of 3 phases for EV feeder.*

With the conditions in section 4.1.2 and the graphs in Fig. 53 the following time periods look especially interesting for further analysis; morning and daytime Jan 08 2018, morning Jan 09 2018, morning Dec 14 2017, morning Feb 09 2018, night Feb 10-11 2018, evening Feb 08 2018. The method to narrowing the time period down will be described for morning and daytime January 8th.

Morning and Daytime Jan 08 2018
This period contains time frames were the FF load and EV load both follow and not follow the same behavior.

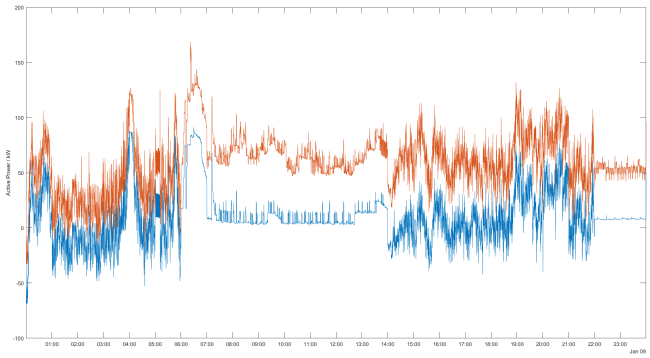

(a) *Active power for FF feeder (red) and EV feeder (blue) for January 8th, assuming that one phase can be multiplied by three to get total power of one cable.*

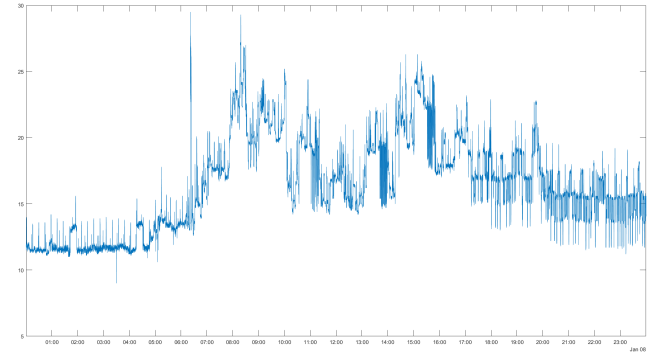

(b) *FF load without load from the EV feeder for one phase (assuming the EV load can be subtracted from the FF load).*

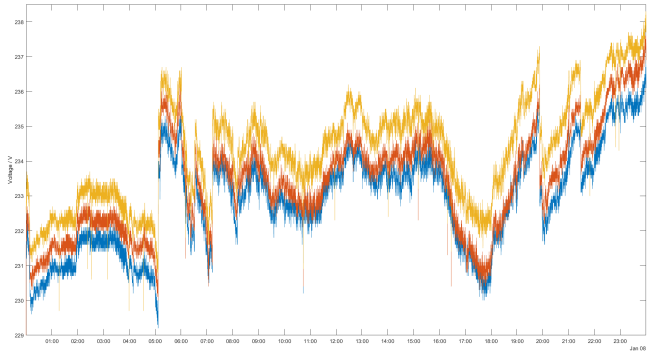

(c) *Shows voltage for January 8th. (blue - phase 1, red - phase 2 and yellow - phase 3)*

Figure 54: *Graphs utilized to pick out time frames for analysis.*

In Fig. 54a it is seen that a period from 00:00 to 06:00 appears interesting to find a time period where FF and EV load follow same behavior. 07:00 to 14:00 looks interesting to find a time period where they do not follow same behavior. As seen in Fig. 54c a tap change occurs at 05:06:52. Thus the time frame needs to be "cut" at this time. In Fig. 54b a load from another feeder seems to be added (possibly a machine starting) around 2:00 and around 4:30. A time frame with little impact from other feeders is thus 01:58:00 to 04:15:00 and a period with intermediate impact is chosen to be 00:00:00 to 05:00:00. To have a time period where the load of the both feeders do not follow the same behavior 08:00:00 to 13:00:00 is chosen.

B. Voltage results - simulation scenarios

Results from the simulated scenarios are found below.

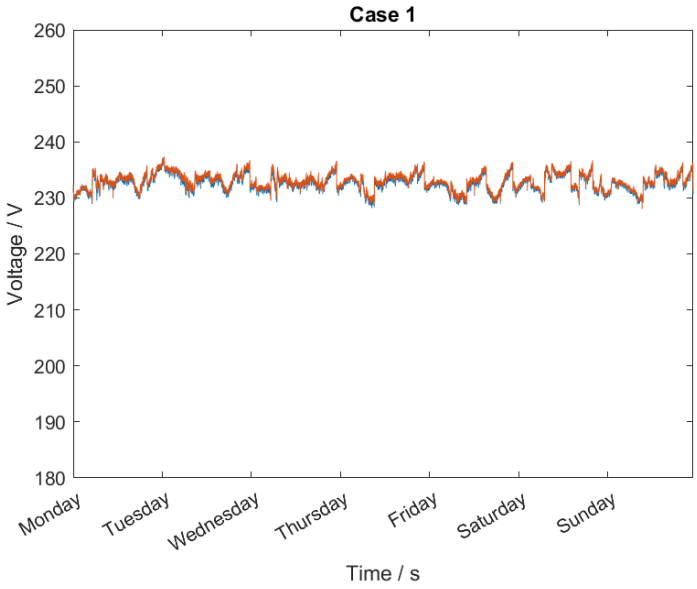

Figure 55: *The red line represent the measured voltage for week 3. The blue line represent the simulated voltage for case 1 for week 3.*

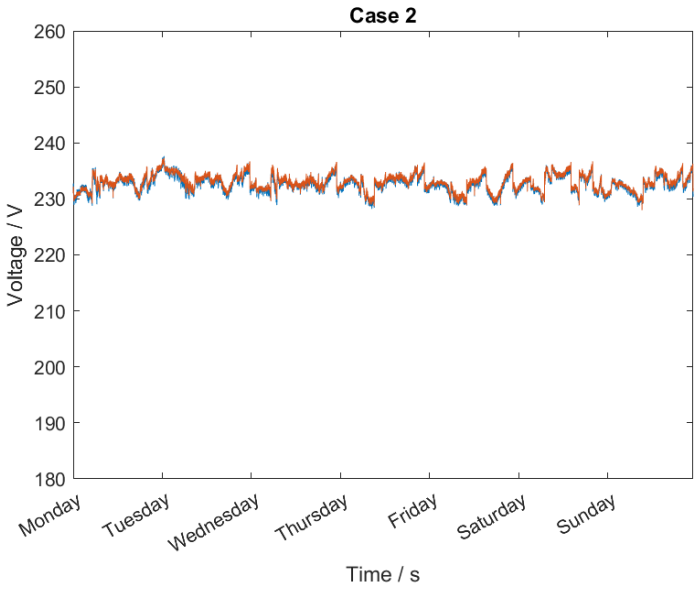

Figure 56: *The red line represent the measured voltage for week 3. The blue line represent the simulated voltage for case 2 for week 3.*

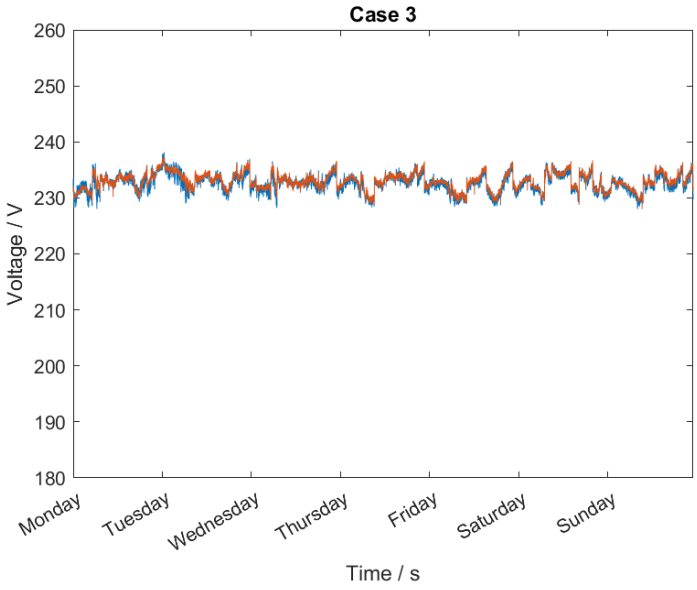

Figure 57: *The red line represent the measured voltage for week 3. The blue line represent the simulated voltage for case 3 for week 3.*

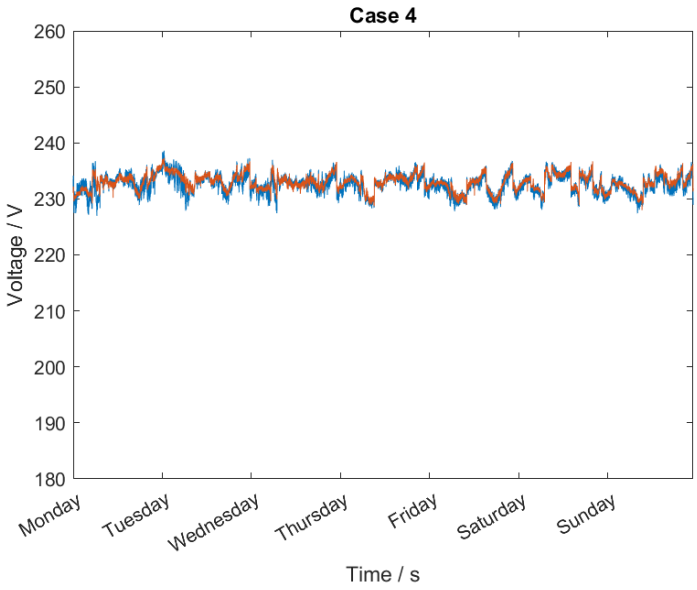

Figure 58: *The red line represent the measured voltage for week 3. The blue line represent the simulated voltage for case 4 for week 3.*

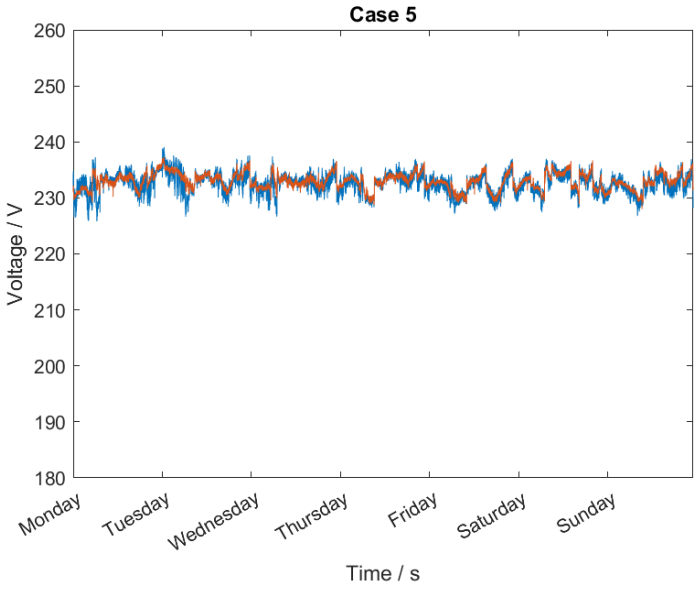

Figure 59: *The red line represent the measured voltage for week 3. The blue line represent the simulated voltage for case 5 for week 3.*

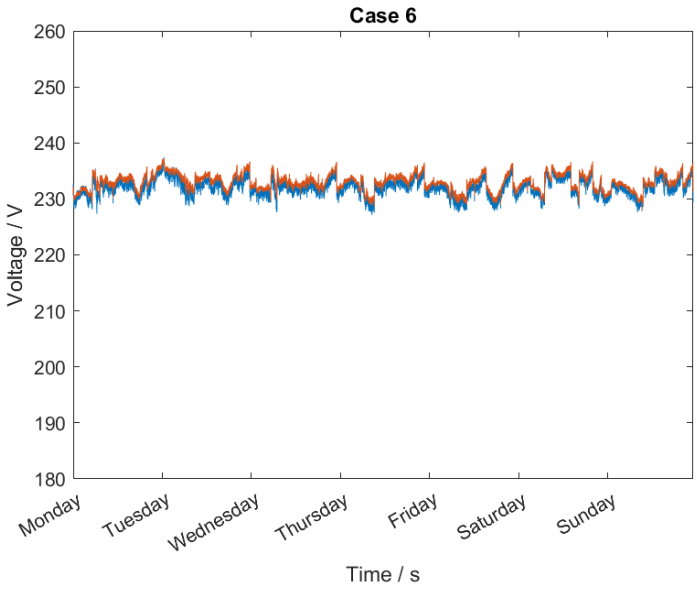

Figure 60: *The red line represent the measured voltage for week 3. The blue line represent the simulated voltage for case 6 for week 3.*

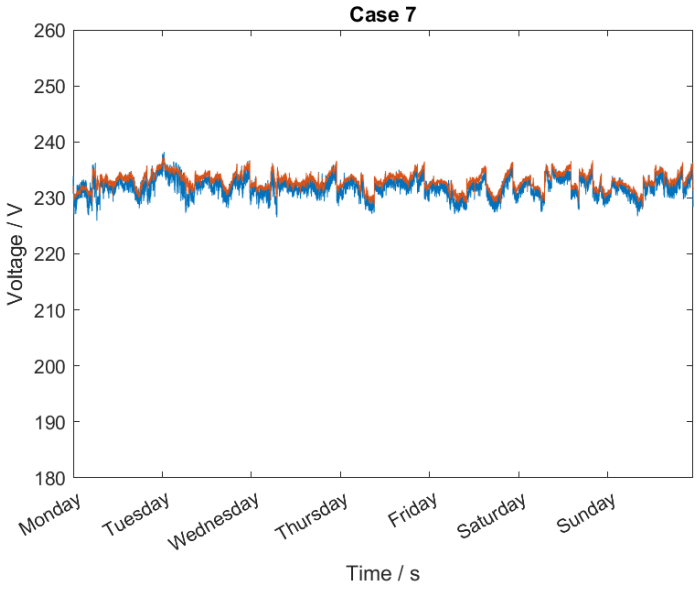

Figure 61: *The red line represent the measured voltage for week 3. The blue line represent the simulated voltage for case 7 for week 3.*

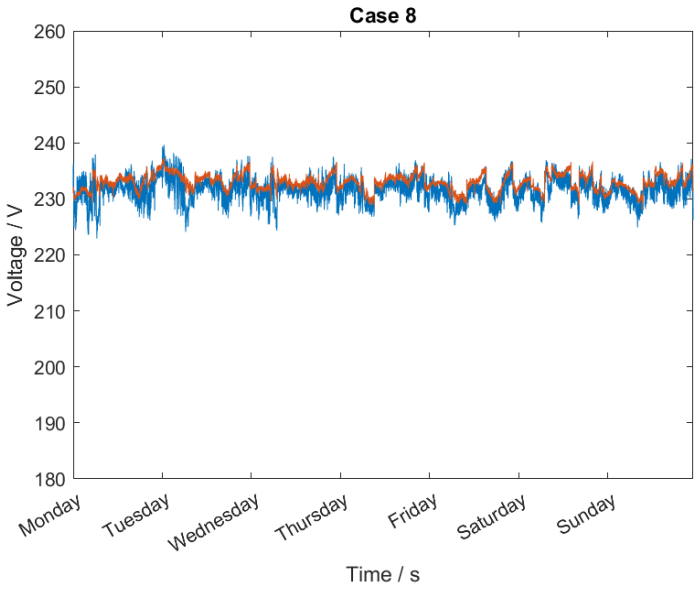

Figure 62: *The red line represent the measured voltage for week 3. The blue line represent the simulated voltage for case 8 for week 3.*

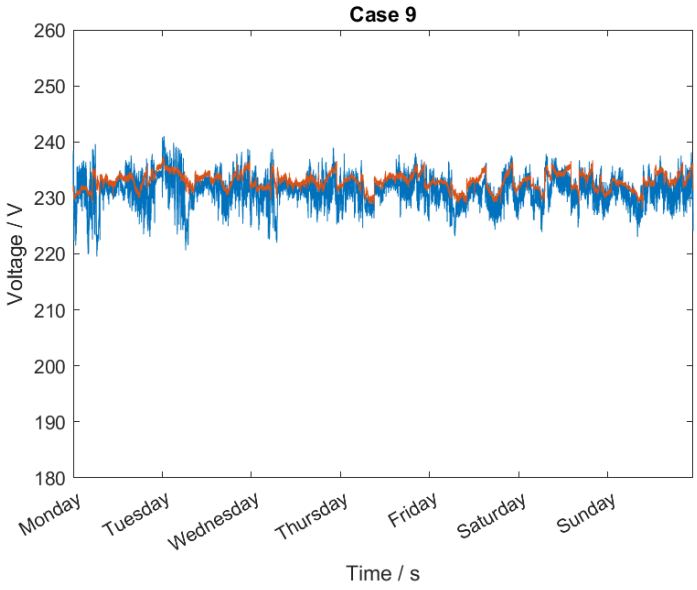

Figure 63: *The red line represent the measured voltage for week 3. The blue line represent the simulated voltage for case 9 for week 3.*

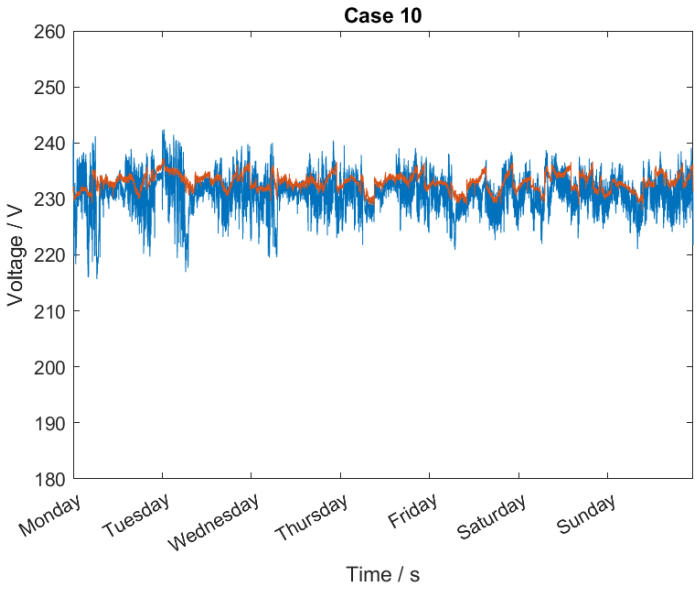

Figure 64: *The red line represent the measured voltage for week 3. The blue line represent the simulated voltage for case 10 for week 3.*

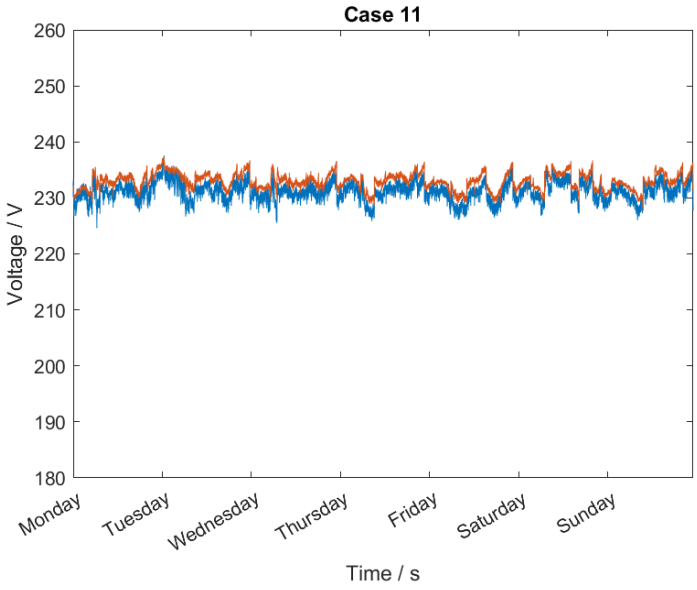

Figure 65: *The red line represent the measured voltage for week 3. The blue line represent the simulated voltage for case 11 for week 3.*

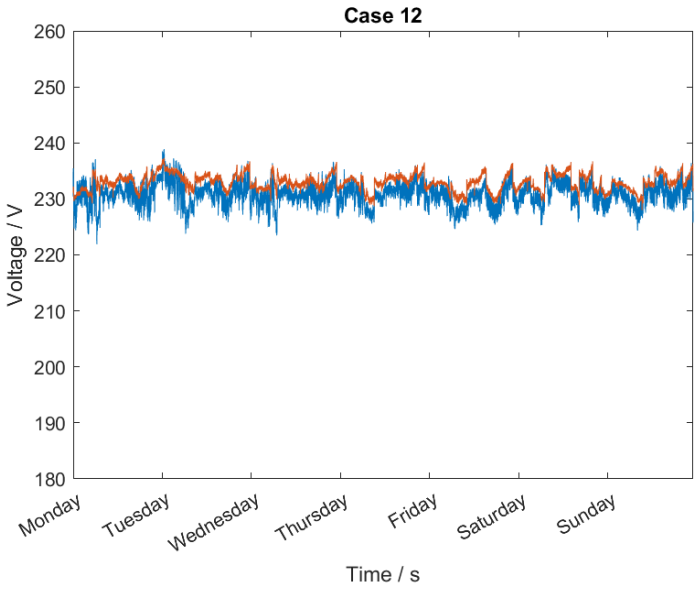

Figure 66: *The red line represent the measured voltage for week 3. The blue line represent the simulated voltage for case 12 for week 3.*

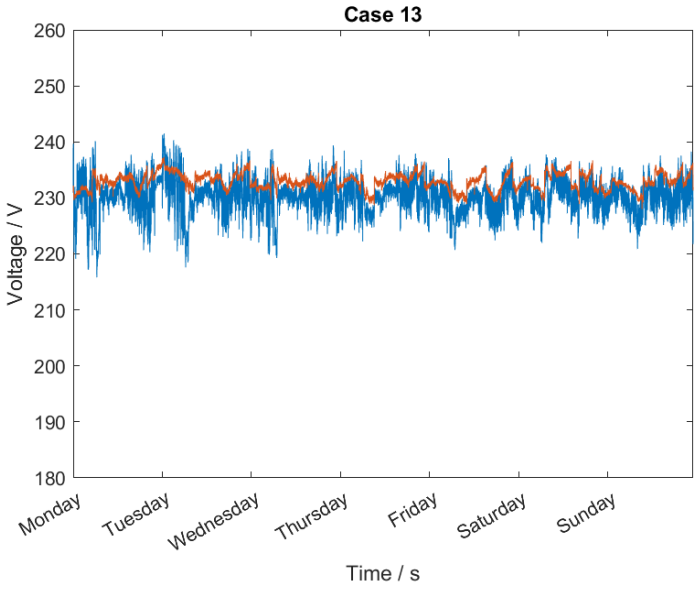

Figure 67: *The red line represent the measured voltage for week 3. The blue line represent the simulated voltage for case 13 for week 3.*

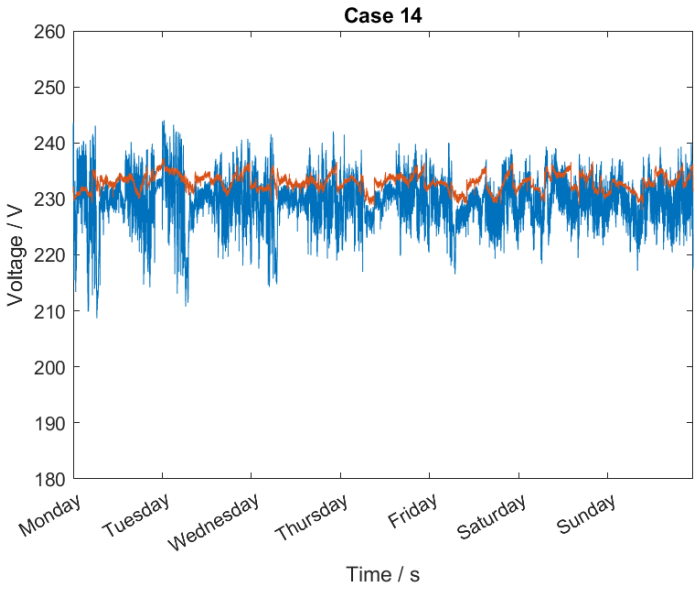

Figure 68: *The red line represent the measured voltage for week 3. The blue line represent the simulated voltage for case 14 for week 3.*

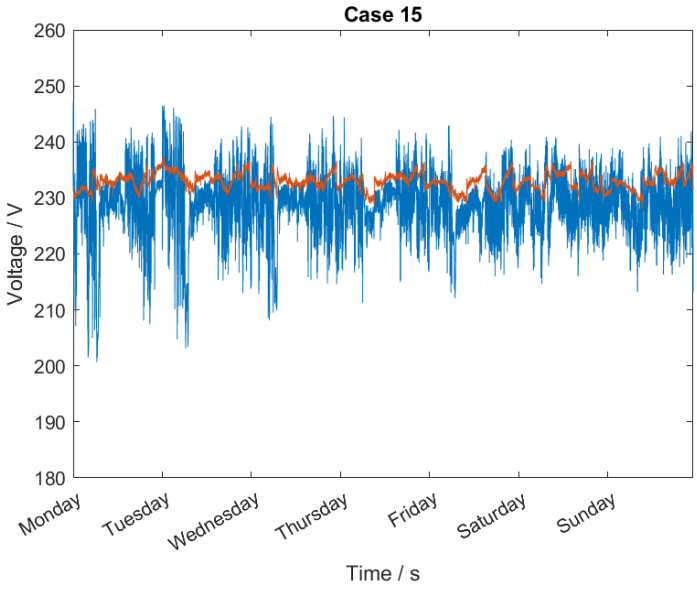

Figure 69: *The red line represent the measured voltage for week 3. The blue line represent the simulated voltage for case 15 for week 3.*

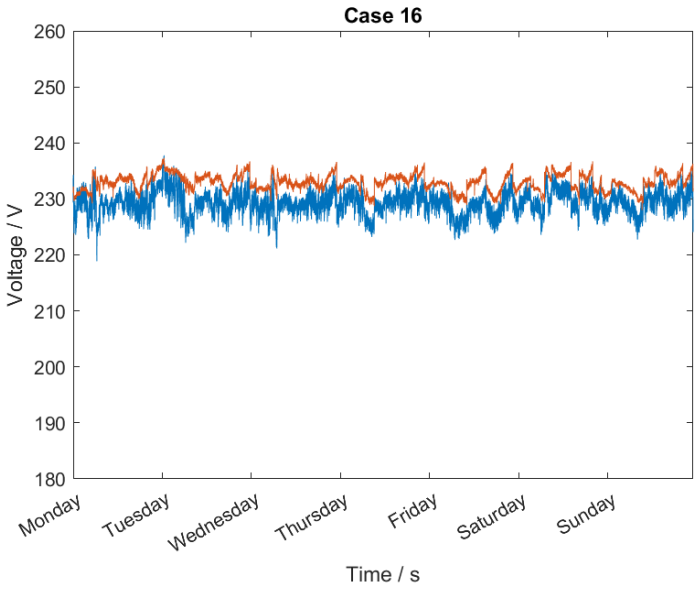

Figure 70: *The red line represent the measured voltage for week 3. The blue line represent the simulated voltage for case 16 for week 3.*

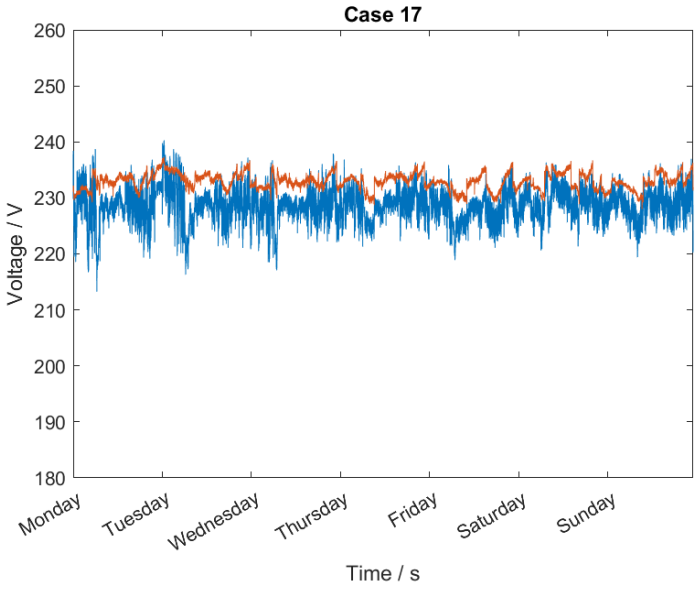

Figure 71: *The red line represent the measured voltage for week 3. The blue line represent the simulated voltage for case 17 for week 3.*

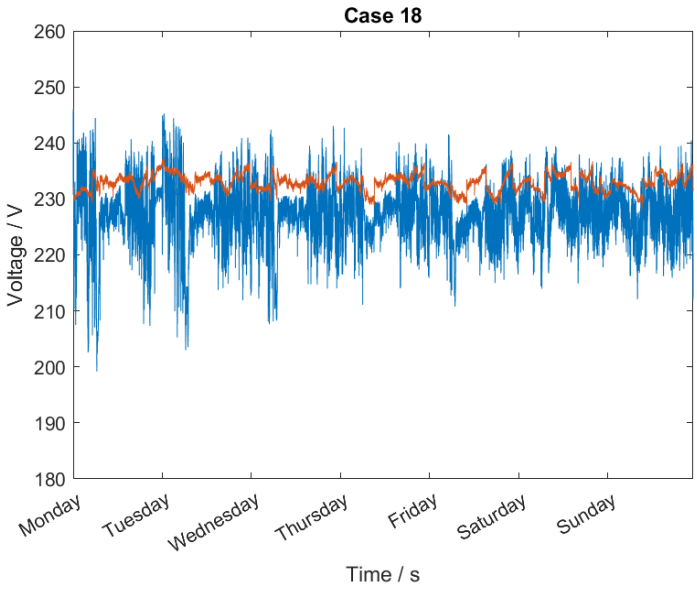

Figure 72: *The red line represent the measured voltage for week 3. The blue line represent the simulated voltage for case 18 for week 3.*

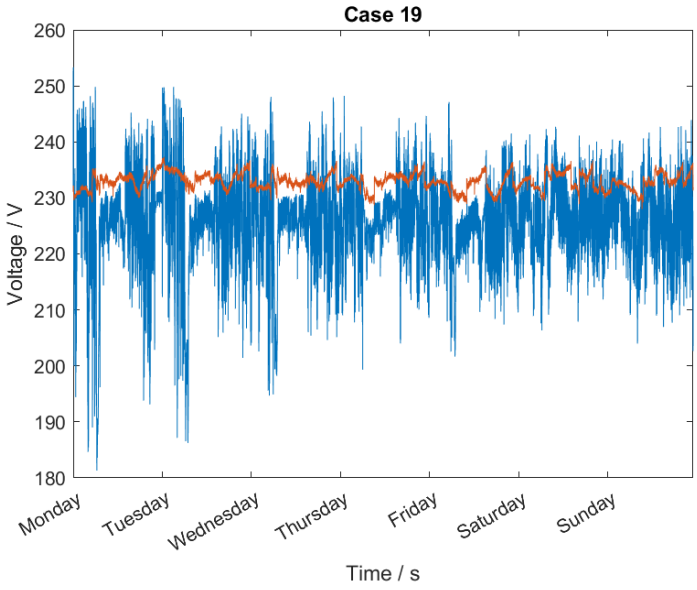

Figure 73: *The red line represent the measured voltage for week 3. The blue line represent the simulated voltage for case 19 for week 3.*

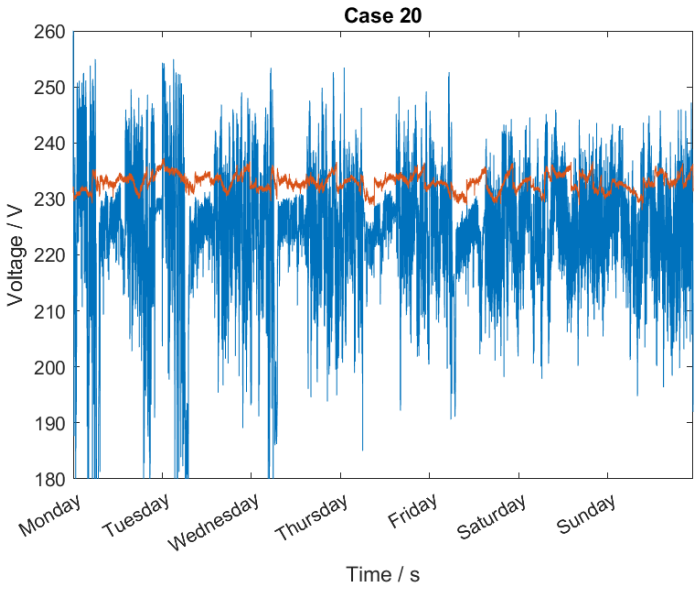

Figure 74: *The red line represent the measured voltage for week 3. The blue line represent the simulated voltage for case 20 for week 3.*

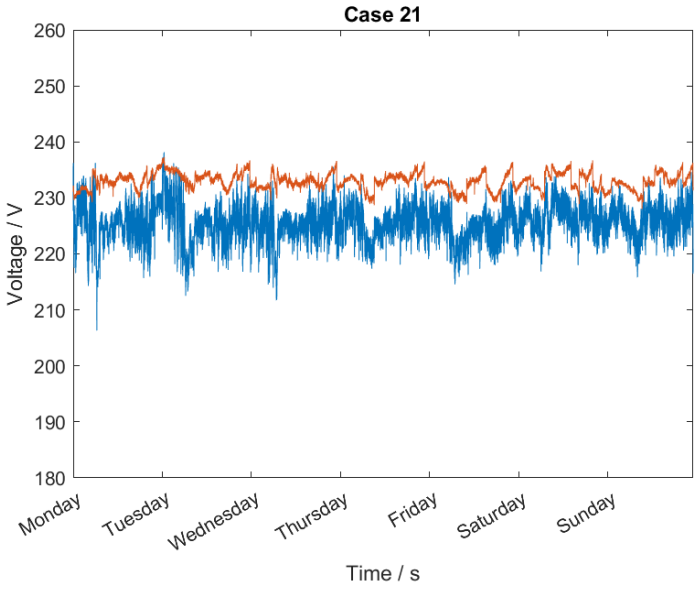

Figure 75: *The red line represent the measured voltage for week 3. The blue line represent the simulated voltage for case 21 for week 3.*

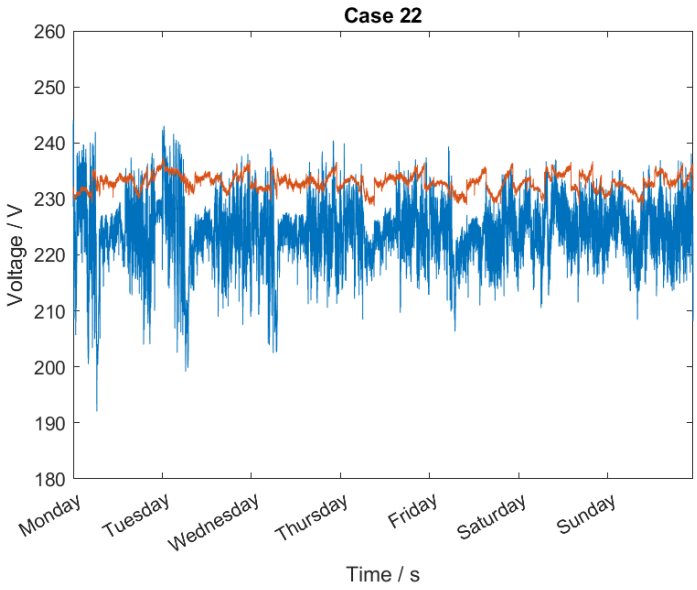

Figure 76: *The red line represent the measured voltage for week 3. The blue line represent the simulated voltage for case 22 for week 3.*

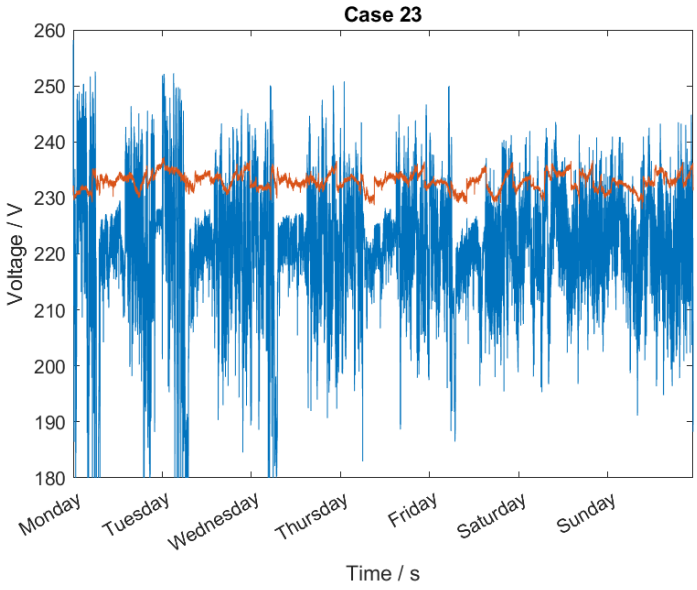

Figure 77: *The red line represent the measured voltage for week 3. The blue line represent the simulated voltage for case 23 for week 3.*

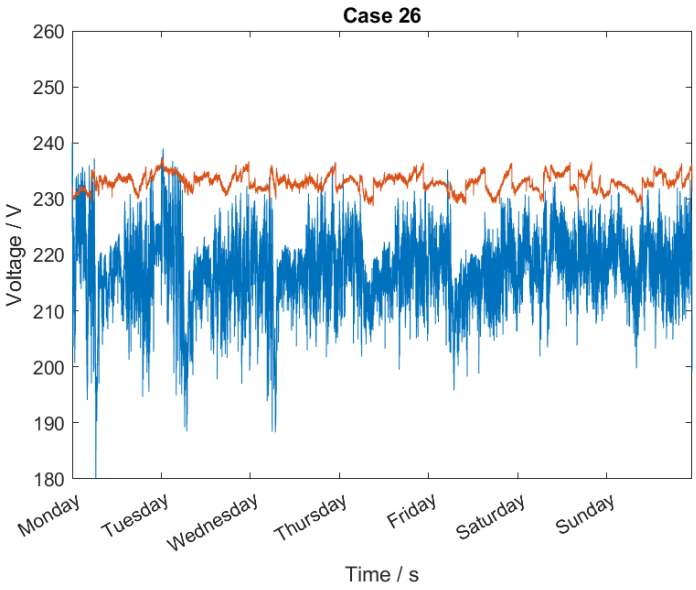

Figure 78: *The red line represent the measured voltage for week 3. The blue line represent the simulated voltage for case 26 for week 3.*

C. Active Power vs. Short Circuit Capacity

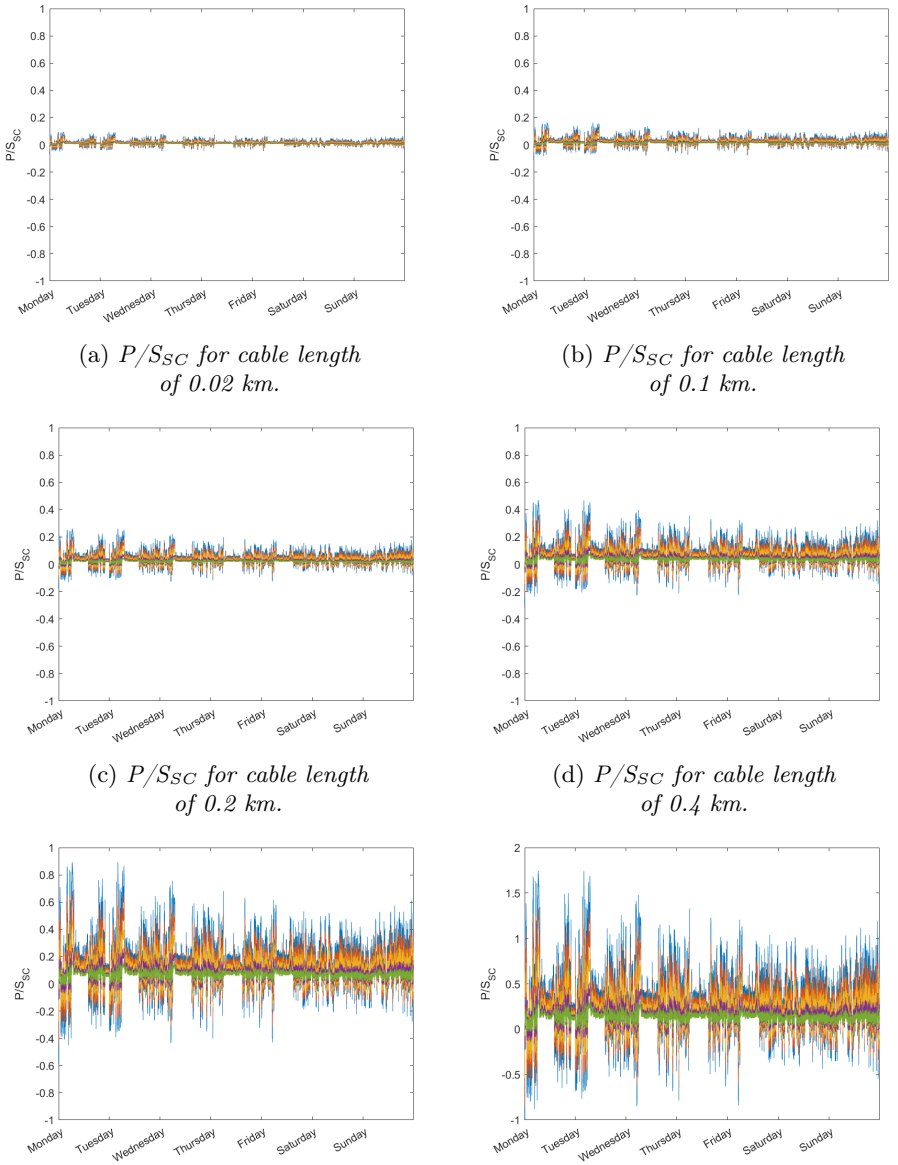

(a) P/S_{SC} *for cable length of 0.02 km.*

(b) P/S_{SC} *for cable length of 0.1 km.*

(c) P/S_{SC} *for cable length of 0.2 km.*

(d) P/S_{SC} *for cable length of 0.4 km.*

(e) P/S_{SC} *for cable length of 0.8 km.*

(f) P/S_{SC} *for cable length of 1.6 km.*

Figure 79: P/S_{SC} *for the different cable lengths. Green - installed P=100 kW, purple - installed P=200 kW, yellow - installed P=400 kW, red - installed P=600 kW, blue - installed P=800 kW.*

D. Load Curves for Bornholm Transformer

In Fig. 80 below the load curve for FF (excluding the EV feeder) is plotted in relation to load curves from different feeders under a 60/10 kV 10 MVA transformer at Bornholm, Denmark. The feeders are connected to a residential area (Kystvejen), an apartment complex (Boligselskabet), a city center (Bymidten), a butcher (Slagteriet), a stadium (Stadion) and a university (Handelsskolen). The measured values from the Bornholm transformer is from 1st to 7th of January 2013 (Tuesday to Monday). Since the data from FF for the same week does not have data for the entire period, week 3 (8th to 14th of January) is analyzed instead. Tuesday January 1st 2013 is a holiday, which explains the deviation in the load curve behavior from a 'normal' weekday.

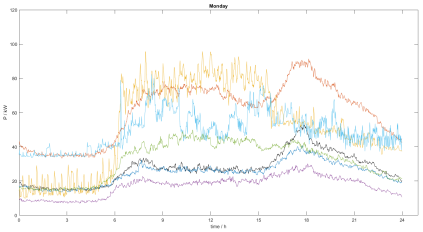

(a) *Load curves for Monday (Jan 7th 2013 and Jan 8th 2018)*

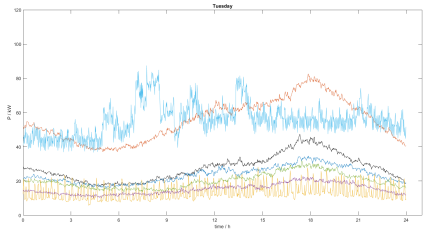

(b) *Load curves for Tuesday (Jan 1rst 2013 and Jan 9th 2018)*

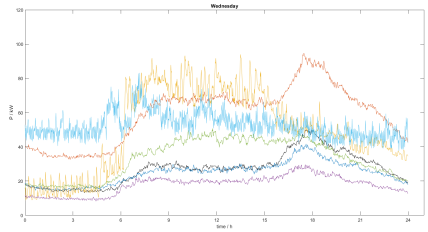

(c) *Load curves for Wednesday (Jan 2nd 2013 and Jan 10th 2018)*

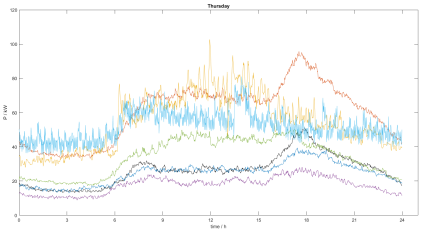

(d) *Load curves for Thursday (Jan 3rd 2013 and Jan 11th 2018)*

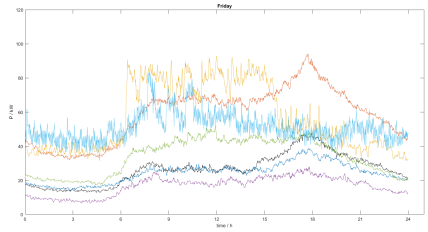

(e) *Load curves for Friday (Jan 4th 2013 and Jan 12th 2018)*

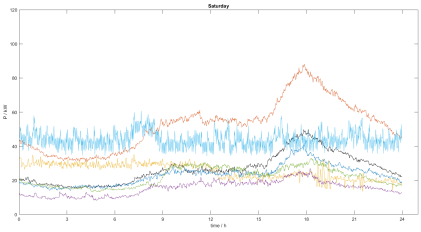

(f) *Load curves for Saturday (Jan 5th 2013 and Jan 13th 2018)*

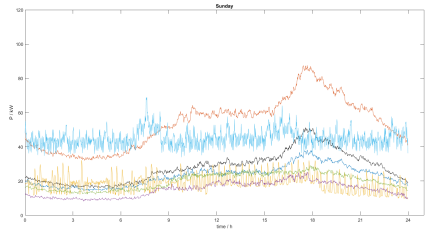

(g) *Load curves for Sunday (Jan 6th 2013 and Jan 14th 2018)*

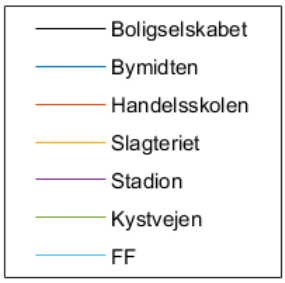

Figure 80: *Load curves for each day of the week. Measurements are from 1st to 7th of January 2013 and 8th to 14th of January 2018.*